

AALBORG UNIVERSITY

STRUCTURAL AND CIVIL ENGINEERING

Safety in nonlinear reinforced concrete design

Structural Engineering Master Thesis

10-06-2020



Author:
Daniel Vestergaard Olesen

Supervisors:
John Dalsgaard Sørensen &
Jannie Sønderkær Nielsen



AALBORG UNIVERSITY
STUDENT REPORT

Second Masters year at Department of
the Built Environment
Civil Engineering
Thomas Manns Vej 23
9220 Aalborg
<http://www.engineering.aau.dk/>

Title:

Safety in nonlinear reinforced concrete design

Project:

Master Thesis - Structural and Civil Engineering

Project period:

September 2019 - June 2020

Project author:

1.203

Authors:

Daniel V. Olesen

Supervisor:

John Dalsgaard Sørensen
Jannie Sønderkær Nielsen

Pages: 123

Appendix: 2

Hand in 10-06-2020

Abstract:

In this report the effects of using different material resistance parameters has on the failure mode of a given structure is examined using two different examples. One simply supported rectangular beam and one simply supported beam with a T shaped cross section. These two examples were then examined using different material resistance input parameters in order to determine whether it is possible to achieve different failure modes in a given example simply by starting with a different material resistance value i.e. mean, characteristic or design values. This was done using ATENA 2D. Thereafter different safety formats using different material resistance starting points were examined. In total four safety formats for each beam example was examined. One of the safety formats examined was the probabilistic method which randomizes material resistance parameters in order to determine the probabilistic distribution function for the given material. This was done using SARA and ATENA 2D. To conclude the report there was some uncertainty around the T-beam example results.

Preface

This master thesis report is made by Daniel Vestergaard Olesen who is a student from the Department of the Built Environment. The report is considers "Safety in nonlinear reinforced concrete design".

Therefore the effects different material resistance parameters has on the failure mode a given concrete structure presents is examined in this report. Furthermore the effects using different safety formats to ensure safety of a given structure has on the failure mode is examined.

The author of this report would like to direct a special thanks to Cervenka Consulting s.r.o for providing the ATENA and SARA licenses needed to conduct nonlinear analysis and reliability assessment. Without the ATENA and SARA licenses this report would have looked much different.

Reading guide

In this report commas are used as decimal seperators while periods are used as thousand seperators as illustrated below.

- 1,500
- 1.500

Figures and tables are numbered by chapter, section and the number of the figure or table, e.g. 1.1.1 would be chapter 1, section 1, figure 1. Figures made by the group itself are presented without a source. Reference to equation are also numbered based on chapter, section and number.

Daniel V. Olesen

Contents

I	Introduction	
1	Summary	3
2	Introduction	5
2.1	Nonlinearity	6
2.2	Safety methods	8
3	Problem Statement	11
4	Nonlinear methods	13
5	Examples	15
5.1	Rectangular beam results	18
5.2	T-beam results	21
5.3	Summary	25
6	Comparison of Safety formats	27
6.1	Partial safety factor	27
6.2	Global resistance factor	28
6.3	ECOV - Estimate of coefficient of variation for resistance	30
6.4	Full probabilistic method	32
6.5	Reliability comparison of safety methods	40

II**Closure**

7	Discussion	45
8	Conclusion	47
	Bibliography	48

III**Appendix**

A	Atena 3D models for Rectangular beam	53
B	SARA LHS results for both beams	63



Introduction

1	Summary	3
2	Introduction	5
2.1	Nonlinearity	
2.2	Safety methods	
3	Problem Statement	11
4	Nonlinear methods	13
5	Examples	15
5.1	Rectangular beam results	
5.2	T-beam results	
5.3	Summary	
6	Comparison of Safety formats	27
6.1	Partial safety factor	
6.2	Global resistance factor	
6.3	ECOV - Estimate of coefficient of variation for resistance	
6.4	Full probabilistic method	
6.5	Reliability comparison of safety methods	

1. Summary

I dette afsnit laves et resume af rapporten på dansk. I denne rapport undersøges hvorvidt forskellige materiale styrke parametre kan lede til forskellige brudformer når der arbejdes med nonlinear beton design. Dette undersøges ved at opsætte to eksempler. Det ene eksempel er en rektangulær simpelt understøtte bjælke med en punkt last i midten. Det andet eksempel er en simpelt understøttet T-bjælke med 4 punkterlaster fordelt symmetrisk omkring midten af bjælken. Begge bjælker er designet med henblik på at et duktilt bøjningsbrud er det dimensionsgivende.

For at undersøge hvorvidt forskellige material styrke parametre kan lede til forskellige brudformer benyttes de to eksempler sammen med tre forskellige beton styrker, C25, C40 og C50. Disse tre betonstyrker benyttes derefter med tre forskellige startpunkter for styrke parametrene, middel, karakteristisk og design styrke, hvilket resulterer i ni eksempler for hver bjælke. Disse ni eksempler for hver bjælke benyttes herefter i FEM programmet ATENA 2D for at foretage nonlinear analyse af eksemplerne. For begge bjælke eksempler viser alle ni scenarier et duktilt bøjningsbrud som brudform. Dette betyder derfor at ved at starte forskellige steder med hensyn til materiale styrke ikke kan præsentere forskellige brudformer for de to eksempler brugt i denne rapport.

Yderligere undersøges det om forskellige foreslåede sikkerhedsmetoder kan forudsagde forskellige brudformer i et givent eksempel. De fire sikkerhedsmetoder der undersøges inkluderer partiel sikkerhedsfaktor metoden, global sikkerhedsfaktor metoden, estimat af varians koefficient metoden og fuld probabilistisk metode. Videnskabelige artikler viser at der ved forskellige sikkerhedsfaktor metoder kan forekomme forskellige brudformer for et givent eksempel derfor undersøges de to eksempler ved brug af alle fire sikkerhedsmetoder.

Efter undersøgelse af de fire sikkerhedsmetoder vises det at den rektangulære bjælke bryder med et duktilt bøjningsbrud for alle fire sikkerhedsmetoder. Yderligere skal det nævnes at alle simuleringer af materale styrke parametre for den fulde probabilistiske metode resulterer i duktile bøjningsbrud. Med hensyn til T-bjælken skal det nævnes at de tre simple sikkerhedsmetoder alle tre viser duktile bøjningsbrud hvilket stemmer overens med videnskabelige artikler. Derudover viser den fulde probabilistiske metode udelukkende duktile bøjningsbrud for T-bjælken. Dette er i strid med [Castaldo and Mancini, 2018] hvilket betyder at endten denne rapport eller [Castaldo and Mancini, 2018] er forkert. For at kunne sammenligne de forskellige sikkerhedsmetoder benyttes sikkerhedsindeks. Sikkerhedsindekset viser at de tre simple metoder er ret lige i sikkerhed. Dette leder til konklusionen at det er problemet med formning af forskellige brudmetoder der er vigtigst med hensyn til at fastsætte en sikkerhedsfaktor metode for nonlinear beton design.

Yderligere kan det konkluderes at der er tale om meget specifikke og delvist komplekse beton konstruktioner hvis disse skal vise mere end en brudmetode. Dette skyldes at den simple rektangulære bjælke ikke viser nogen tegn på forskellige brudmetoder. Derudover er det ikke nogen af de indledende analyser for T-bjælken der viser tegn på mere end en brudmetode.

2. Introduction

In this chapter an introduction to the problems surrounding nonlinear design methods will be presented. This is done to introduce the problems further dealt with throughout the report.

The traditional design methods regarding reinforced concrete structures is a linear design method based around the partial safety factor method in order to achieve a sufficient reliability level. This design method has been used for years and has been proven to be very reliable. However when designing reinforced concrete structures using linear design methods the full potential of the reinforced concrete is not utilized. This leads to the structures being overdimensioned compared to what the strength of the reinforced concrete allows. As FEM design methods have become more and more common nonlinear design methods have gained a lot of attraction due to their better utilization of the reinforced concrete. Additionally the better utilization of the material leads to economic advantages.

As a result of this nonlinear design methods have become increasingly more popular. In the past nonlinear design methods were mostly used to simulate design load conditions in regards to experimentation. However nonlinear design methods offer a way to simulate the concrete structure as a virtual test. This makes the nonlinear methods ideal for reinforced concrete designs that were previously not possible using traditional design methods. The nonlinear methods are ideal for reinforced concrete designs such as high-rise concrete buildings and complicated bridge structures where traditional design methods are not sufficient.

In traditional design methods the distribution of internal forces is carried out using linear analysis tools, there is two main discrepancies in this approach. First the elastic force distribution is one of many different states of equilibrium. This means that redistribution of forces due to an inelastic response is not taken into account. Secondly the partial safety factor used in traditional design only ensures safety locally and is based on assumptions about nonlinear material behaviour such as cracking and yielding.

In order to use nonlinear design methods for reinforced concrete structures safety of the structure has to be ensured. When designing a reinforced concrete structure with nonlinear design methods it has to be determined that the critical failure mode found is in fact the most critical one. Therefore the method developed has to be general enough to be able to determine any failure mode. An example of this could be a bridge pier. A bridge pier will not have the same critical failure mode as a regular simply supported beam. Even though these two examples don't have the same failure mode the nonlinear design methods employed needs to be able to determine the correct failure mode in both

cases.

Furthermore another thing to consider when trying to ensure safety of the nonlinear design methods is whether to use design resistances, mean resistances or characteristic resistances when it comes to the reinforced concrete. The different approaches for the resistance of reinforced concrete structures when using nonlinear analysis is not covered enough in the Eurocodes and therefore an analysis of the different approaches is needed in order to determine the most reliable one.

One critical aspect about the nonlinear methods is the calculation time as mentioned earlier. Nonlinear methods as a design tool is mostly used in numerical models and a result of this is that the safety methods developed needs to be implemented in FEM design methods. Therefore achieving a satisfying reliability for nonlinear design methods should be made possible through methods that can be implemented in FEM design. This makes methods similar to the partial safety factor method ideal since these are easily implemented in FEM design.

2.1 Nonlinearity

In this section the different nonlinear behaviours will be described. Furthermore it will be determined which one is in focus in this report. There are two different types of nonlinear behaviour, geometrical and material. Geometrical nonlinear behaviour is nonlinearity in structural problems that often originate from the effect of large deformations. This means that geometrical nonlinearity comes from the difference between engineering stress/strain and true stress/strain. An example of this is a beam as illustrated on Figure 2.1.1. This beam could illustrate a laundry string set up between two columns.

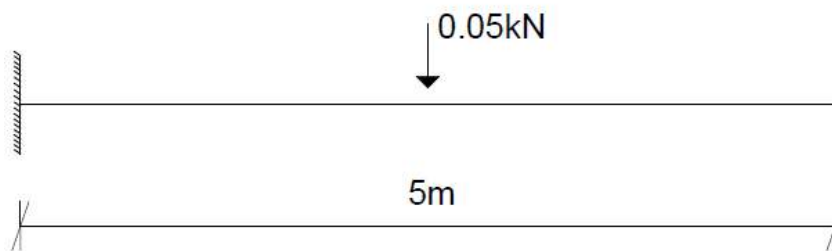


Figure 2.1.1: Example of geometrical nonlinear behaviour using a laundry string with $\text{\O}5$ mm. [Łukasz Skotny, 2020]

The example of a laundry string can be viewed as a fixed steel beam as illustrated on Figure 2.1.1. This would result in a stress in the string of 5081 MPa using a linear approach. A stress of this magnitude results in a deflection of 20.2m. If large deformations and therefore the effects of geometrical nonlinearity is taken into account the deflection of the steel beam is only 57 mm [Łukasz Skotny, 2020]. As illustrated by this example geometrical nonlinear behaviour has a big impact on certain structural scenarios. The important thing to note is that the geometrical nonlinear behaviour depends on the design of the structural element. [Krenk, 2009] [Łukasz Skotny, 2020]

Additionally nonlinear behaviour can originate from the material the structure is made from. In the case of material nonlinearity the nonlinear behaviour stem from the nonlinear relationship between the stress and strain in the material. An example of this is nonlinear material behaviour is soils and concrete. The material nonlinear behaviour can be illustrated from the stress-strain curve of the material as illustrated for concrete on Figure 2.1.2. Material nonlinear behaviour results in all structures constructed from these materials behaving in a nonlinear way regardless of structural design. In this report mainly material nonlinear behaviour will be examined, this is in order to examine the nonlinear material behaviour of concrete and how the nonlinear behaviour can be beneficial in structural design.

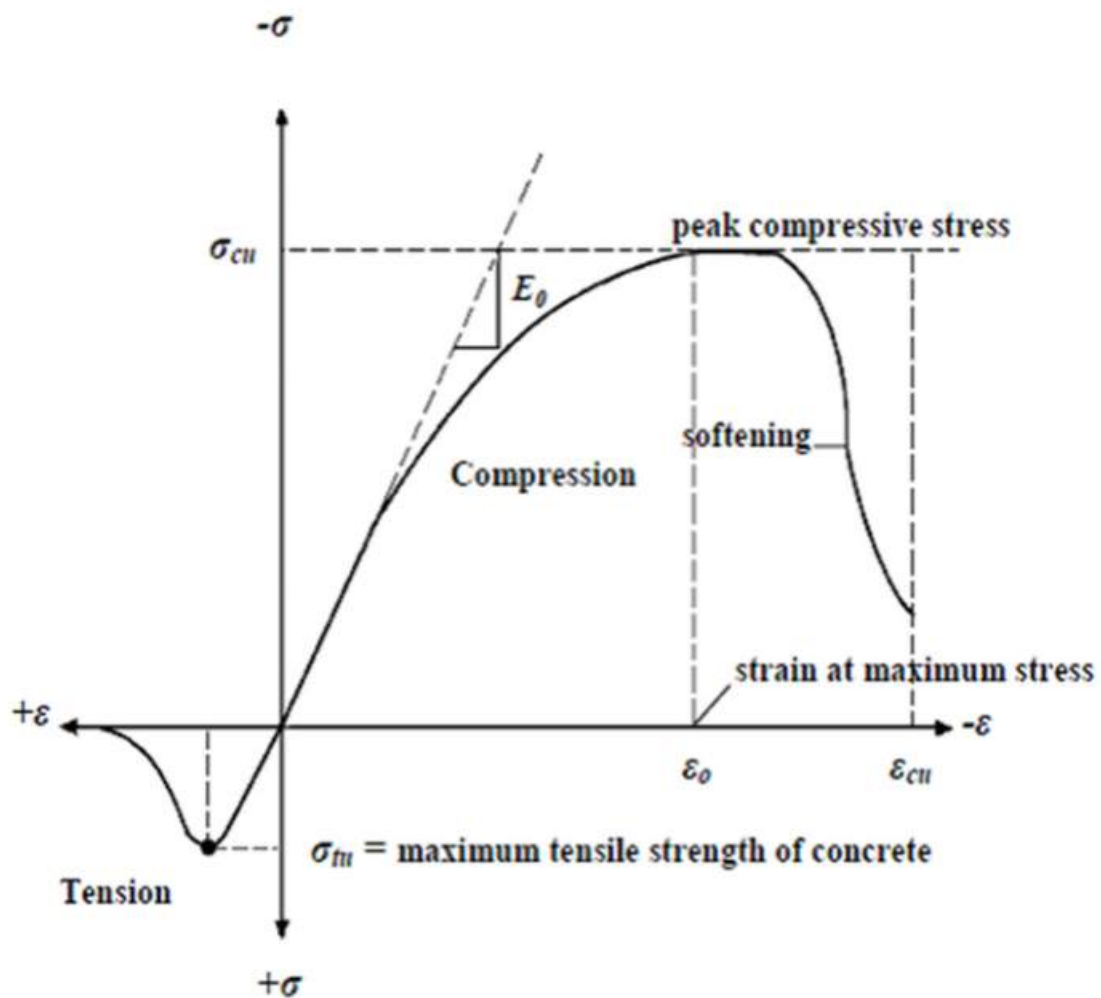


Figure 2.1.2: Stress strain curve for concrete. [Kh, 2020]

As illustrated by Figure 2.1.2 concrete is a highly nonlinear material. This means that nonlinear design of concrete structures could yield great benefits compared to using linear design methods for concrete structures. As illustrated by Figure 2.1.2 concrete material behaviour in compression is linear in the beginning and then gradually flattens until the peak compressive stress. The linearity in the beginning of the stress-strain curve for concrete represents the period of time where no cracks have formed in the material. As cracks start to form the material behaves more nonlinearly. This is due to the internal

redistribution of forces the cracks lead to. Eventually when enough cracks develop and the stress becomes high enough the peak compressive stress is reached. This is the point where further compressive loading will lead to failure in the material. Compressive failure in concrete is characterised by compression softening. Compression softening of concrete signifies a gradual decrease in mechanical resistance due to a continuous increase in deformation. A continuous increase in deformation is also known as cracks forming in the concrete structure. [Vonk, 1992]

Furthermore from Figure 2.1.2 the tensile strength of concrete is illustrated and as it is clear from the figure the tensile strength of concrete is far lower than the compression strength of concrete. Therefore reinforcement is often used in concrete structures where tension forces are expected. However the tension strength of concrete being so much lower than the compression strength results in the Eurocodes prohibiting concrete structural design from including the concrete tensile strength as a resistance parameter. It should be noted that for this project the tension strength of concrete is included due to restrictions in the FEM program used, ATENA 2D. Additionally the tension strength of concrete does exist even if it is small and since the nonlinear design methods used are simulations of reality the tension strength being included is the most correct representation of reality. [Standard, 1992]

2.2 Safety methods

As mentioned earlier there is a wide range of safety methods that can be used to ensure a sufficient level of reliability when designing structures using nonlinear design methods. The safety methods considered here are the ones that relate to assessment of reliability of reinforced concrete structures exposed to permanent and variable loads. When traditionally determining the structural resistance of a structure the partial safety factor is used. When applying safety methods to any structure it is important to determine what material parameters are being used as a starting point. For the partial safety factor method traditionally the Eurocodes allow starting with design values of material resistance and starting with characteristic values of material resistance is allowed. However when using nonlinear design methods it is possible to use the mean values of material resistance as a starting point when using the global safety factor method or the Estimate of Coefficient of Variation method (ECOV) these two methods are however not covered by the Eurocodes and therefore not allowed in traditional design.

Additionally [Castaldo and Mancini, 2018] illustrated that depending on what material resistance is used as a starting point different failure modes can present themselves. This of course presents a problem regarding what material resistance to use as a starting point. The problem with this discovery is that the safety methods aim to ensure reliability of the structure by ensuring a specific failure mode is presented for all cases of the given structure. However with the discovery of [Castaldo and Mancini, 2018] it is not guaranteed that the failure mode for all the possible safety methods regardless of starting point will be the same. This presents additional issues with regards to the inherent randomness of material strength when producing concrete since the material parameters of concrete follows a log-normal distribution the material parameters will vary from concrete structure

to concrete structure even in the same structural scenarios. When two structural concrete parts does not have the same failure mode even in the same design scenario this leads to problems regarding structural reliability as there is essentially no way to know which structural part will have which failure mode without individually assessing all structural parts using samples and experiments. As a result of this discovery a few different options present themselves. Either the traditional design methods need to be altered to be able to take into account the possibility of different failure modes or a new safety method has to be adopted that is currently not covered by the Eurocodes such as the global safety factor method or the Estimate of Coefficient of Variation method (ECOV).

The Partial Safety Factor method obtains the design resistance through applying local safety factors to characteristic values of material strength and loading. For material strength parameters typically 5% quantiles are used as characteristic values. This method is the safety method primarily used for linear design methods. This is due to the simplicity of the method while ensuring structural reliability regardless of structural design. However when using nonlinear design methods the partial safety factor method can present different failure modes based on which characteristic strength value is used. [Standard, 1990]

Another safety method is the Global Safety Factor method this method seeks to obtain a representative design resistance by estimating global resistance through mean values of steel and concrete material parameters in order to apply a single safety factor to the entire structure. While this method provides a simpler way of ensuring structural reliability through one global resistance factor the issue with this method when using nonlinear analysis is that the nonlinear analysis in some cases will be conducted using material parameters much smaller than the mean values. This is due to lower values being more critical in some cases and therefore the mean material parameters used when estimating the global resistance factor won't be the most critical in all cases when using nonlinear analysis. This method is traditionally not covered by the Eurocodes as the starting point being mean material parameters is not traditionally covered by the Eurocodes.

A different approach to a global safety factor is the Estimate of Coefficient of Variation method (ECOV). This method obtains the global resistance factor through estimation based on two Nonlinear Finite Element Analysis (NLFEA) with mean and characteristic material properties respectively. The advantage to the ECOV method compared to the global safety factor method is that it estimates the global safety factor through simplifications based on NLFEA. However the problem is that the mean strength and characteristic strength is assumed to have the same failure mode. Furthermore the material strengths are assumed lognormal distributed which might not always be the case.

The last safety method considered in this report is the Full probabilistic method. This method consists of running several NLFEA adopting a sampling technique such as Monte Carlo simulation or Latin hypercube sampling to define the input data for material strength parameters. Through this sampling technique and multiple NLFEA the full probabilistic method can accurately assess design resistance according to a specific reliability index for a given structural case. This method provides a very accurate assessment of design resistance to a specific structural case. However since the method requires several NLFEA it can be time consuming as several NLFEA has to be set up for each specific case within a structure. Traditionally this method is allowed by the Eurocodes as it is viewed as the

highest level of reliability for a given structure. However as mentioned it is very time consuming and it has to be done on a specific structural member basis making it a non viable design option for big concrete structures. [Standard, 1990]

3. Problem Statement

This report is based on the following problem statement:

How can nonlinear design methods be used to design reinforced concrete structures while maintaining a satisfying level of reliability?

To determine a nonlinear design approach that achieves a satisfying level of reliability the following points will be examined during the report.

- Compare different methods for the resistance of reinforced concrete when using nonlinear analysis using nonlinear FEM
- Methods to estimate the reliability of reinforced concrete structures using non-linear FEM methods
- Methods to verify sufficient reliability of reinforced concrete structures using non-linear FEM by the 'partial safety factor' (semi-probabilistic) approach

4. Nonlinear methods

In this chapter the nonlinear solution methods used in this report will be described alongside the program used for those methods. Traditionally when using linear analysis the solution comes down to a solution of a system of linear equations. However when using nonlinear analysis the solution is often an iteration of a series of nonlinear equations storing force and displacement for each time step. In this project the nonlinear method used is a special instance of the Newton-Rhapson method. The nonlinear analysis is illustrated on Figure 4.0.1. [Krenk, 2009]

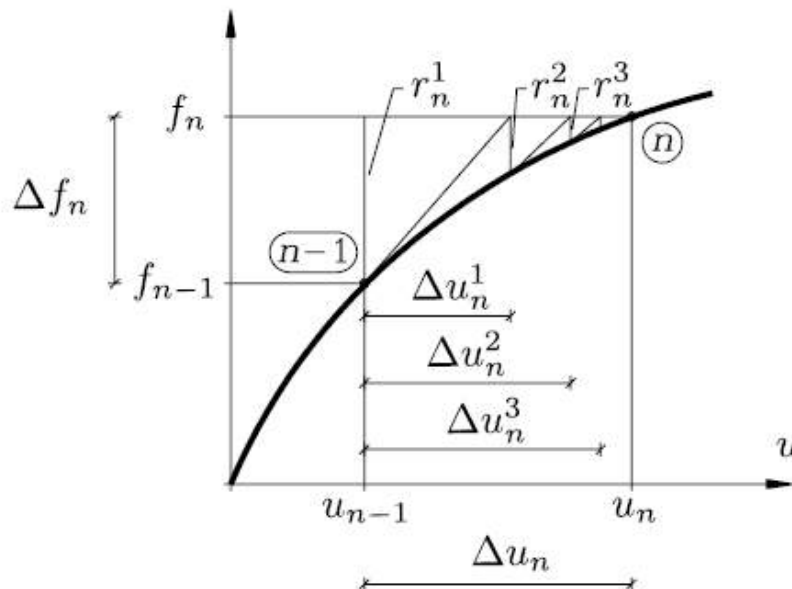


Figure 4.0.1: Newton-Rhapson method. [Krenk, 2009]

As illustrated on Figure 4.0.1 the method is used to compute displacement for each time step while making sure that equilibrium in the system is fulfilled. It should be noted that in practice equilibrium is not ensured in the beginning of each time step due to the load being increased without new displacement being developed yet. As illustrated by Figure 4.0.1 for each time step the load is increased Δf_n which leads to an increase in the residual force, r_n which then over time converts to an increase in displacement, Δu_n [Krenk, 2009]. To conduct nonlinear analysis the nonlinear finite element software ATENA 2D from Cervenka Consulting is used in this project.

When using ATENA 2D for NLFE modelling the ATENA manual [Cervenka and Červenka, 2015] is followed with regards to recommendation for model setup. The recommendations

include using steel plates as load and support points in order to avoid singularities by applying these directly to the structure as illustrated on Figure 4.0.2.

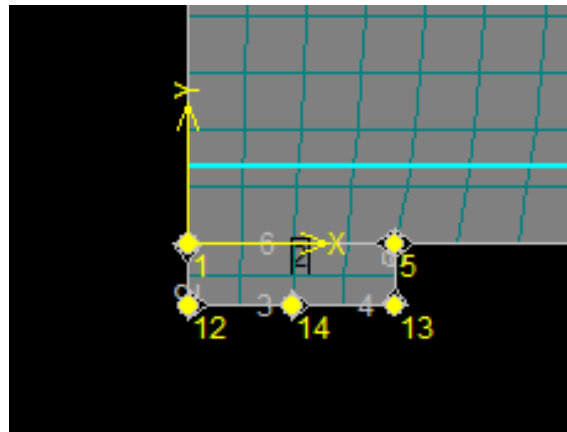


Figure 4.0.2: Steel support plates used in ATENA.

Furthermore NLFE advice with regards to FEM mesh is followed. Meaning that 4-6 elements per structure thickness is used in order to ensure a sufficient level of accuracy. Therefore the FEM mesh used is designed to have 4-6 mesh elements per thickness. This is done in order to ensure accurate results when using NLFEA. The mesh elements used are quadratic elements. An example of a mesh used in this report is given on Figure 4.0.3.

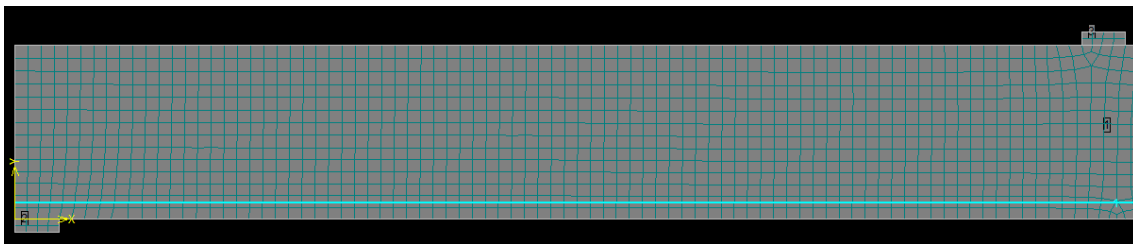


Figure 4.0.3: An example of a FEM mesh used for the given example.

In the beginning of the project all models were set up using ATENA 3D. However since ATENA 3D proved to have some issues project had to be swapped over to using ATENA 2D instead. The issues with ATENA 3D included not being able to perform proper analysis on the T-beam example presented in Chapter 5 as the simulation would show the beam breaking before any bending or shear failure modes had developed. The initial 3D models for the bending beam are presented in Appendix A. This sudden swap from 3D to 2D models resulted in a rather big time loss with regards to simulation time and project work.

5. Examples

In this chapter two examples will be presented in order to examine the effects of using characteristic, mean or design values of the material parameters with regards to a NLFEA of a reinforced concrete structure. As previously described the NLFEA in this project will be conducted using a Newton-Rhapson approach in the NLFE software ATENA 2D from Cervenka Consulting. The two examples used are presented in Figure 5.0.1 and 5.0.2. In this chapter C25-M means the concrete characteristic compressive strength is 25 MPa and that the mean value is used in that case. This naming system is used throughout the report.

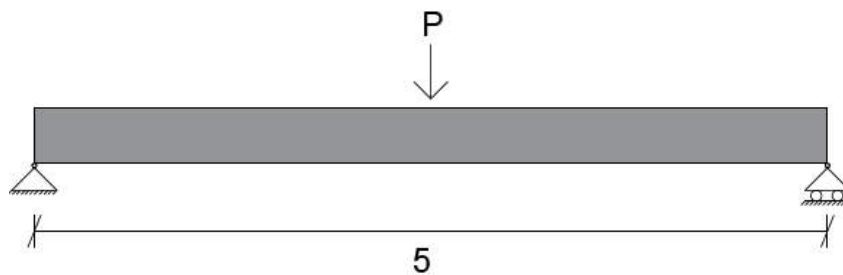


Figure 5.0.1: Principle sketch of the simple supported rectangular beam. Dimensions are not to scale.

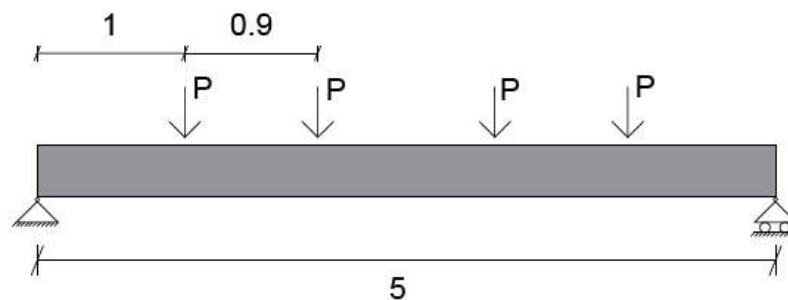


Figure 5.0.2: Principle sketch of the T-Beam. Dimensions are not to scale.

Example one is a simply supported rectangular beam affected by one point load in the middle of the beam as illustrated on Figure 5.0.1. The beam is expected to fail in bending as it is essentially a 3-point bending beam. The cross section of the simply supported rectangular beam is illustrated on Figure 5.0.3. $\text{Ø}24$ reinforcement is used in the bottom

part.

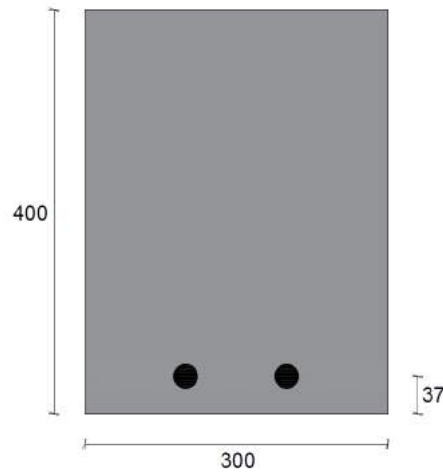


Figure 5.0.3: Principle sketch of cross section for the simply supported rectangular beam. All dimensions are in mm.

Example two is a simply supported T-beam affected by four point loads as illustrated on Figure 5.0.2. The beam is designed according to the T-beam from [Castaldo and Mancini, 2018]. The beam is designed for bending failure. The cross section of the simply supported T-beam is illustrated on Figure 5.0.4. $\text{Ø}24$ reinforcement is used for tension, $\text{Ø}14$ reinforcement is used for compression and $\text{Ø}8$ is used for the stirrups placed every 200 mm.

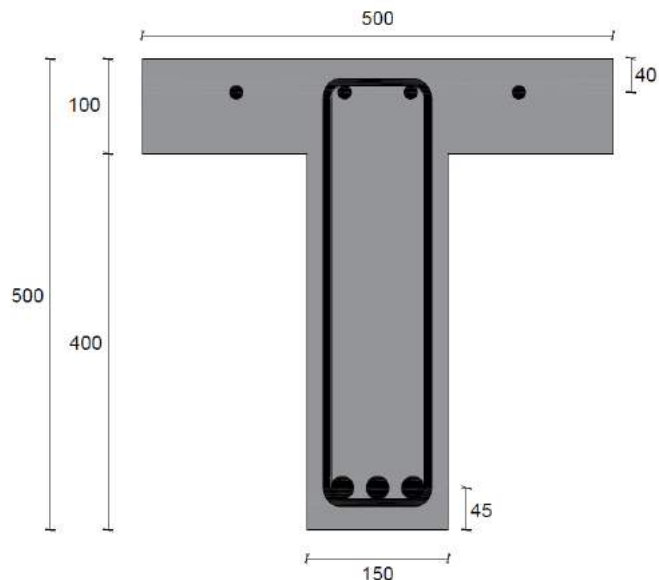


Figure 5.0.4: Principle sketch of cross section for the T-Beam. All dimensions are in mm.

In accordance with [Castaldo and Mancini, 2018] different design values of material strength parameters can lead to inconsistencies in the failure mode of a given structural

example. Therefore the effects different resistance levels have on a given structural example is examined by using characteristic, design or mean values of material strength parameters for three different base concrete types. The three base concrete types are C25, C40 and C50. Furthermore the reinforcement used for the examples are chosen such that each example has a bending failure mode according to traditional design methods. The mean strength of each concrete type is achieved by adding 8MPa to the characteristic strength, while the design strength of each concrete is achieved by using a partial safety factor of 1,5. For reinforcement the mean strength is achieved by multiplying a factor of 1,1 while the design strength is achieved by dividing with a safety factor of 1,2. Both design strengths are determined in accordance with DS/EN-1992 [Standard, 1992]. The characteristic, design and mean strength levels used are presented in Table 5.0.1 for both concrete and reinforcement.

Table 5.0.1: The three different resistance levels used for the examples with regards to concrete and reinforcement strength. [Standard, 1992]

	Mean f_{cm} / f_{ym}	Characteristic, f_{ck} / f_{yk}	Design f_{cd} / f_{yd}
C25	33MPa	25MPa	16.67MPa
C40	48MPa	40MPa	26.67MPa
C50	58MPa	50MPa	33.33MPa
Rectangular Beam	550MPa	500MPa	416.667MPa
Reinforcement T-Beam	495MPa	450MPa	375MPa

For each concrete strength presented in Table 5.0.1 the corresponding reinforcement strength is used i.e. if a characteristic concrete strength is used the reinforcement strength used is also characteristic. Additionally in order to evaluate whether the failure mode is a ductile bending failure mode or a brittle shear failure mode a few criteria is used. These criteria are presented below.

- Ductile Bending failure
 - Concrete crushing occurs in the top middle part of the beams.
 - Reinforcement is yielding in the bottom middle part of the beam.
 - Largest displacement is in the bottom middle of the beam.
- Shear Failure
 - Concrete crushing occurs above the supports in the beam.
 - Reinforcement is not yielding.
 - Largest displacement is near the supports in the bottom part of the beam.

The two examples illustrated on Figure 5.0.1 and 5.0.2 are examined using Atena 2D as previously described and the criteria above is used to determine the failure for each strength scenario. The NLFE models are set up as previously described in section 4. The amount of concrete strengths used for each model results in a total of 18 different results (9 for each example).

5.1 Rectangular beam results

In this section the results for the rectangular beam are presented in terms of stress in concrete and reinforcement alongside where cracks are formed in the rectangular beam. Furthermore the Load-displacement graphs for all nine cases are presented. The results for concrete and reinforcement stress alongside the cracks are presented in Figure 5.1.1-5.1.9, only cracks wider than 0.1 mm are shown on the Figures. On all the 9 Figures 5.1.1-5.1.9 red indicates concrete crushing, green indicates concrete in compression and blue indicates concrete in tension. Values for stresses and loading is presented in Table 5.3.1.

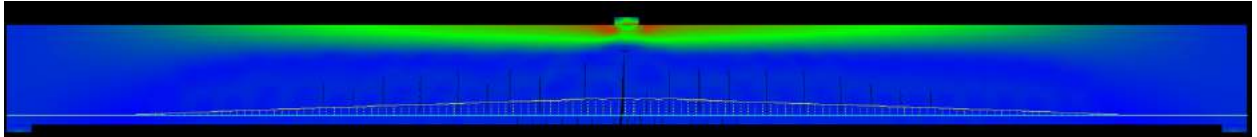


Figure 5.1.1: Concrete and Reinforcement stress for the rectangular beam example C25 Mean.

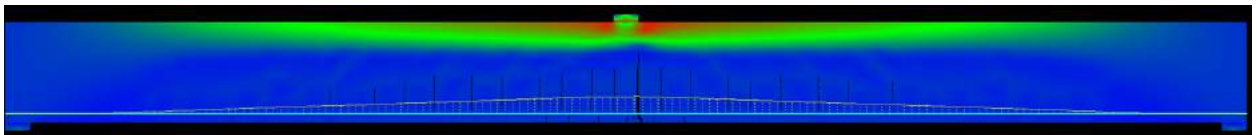


Figure 5.1.2: Concrete and Reinforcement stress for the rectangular beam example C25 Characteristic.

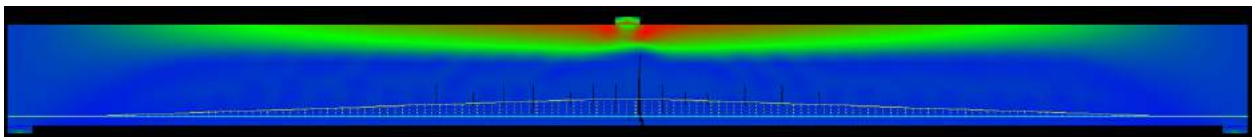


Figure 5.1.3: Concrete and Reinforcement stress for the rectangular beam example C25 Design.

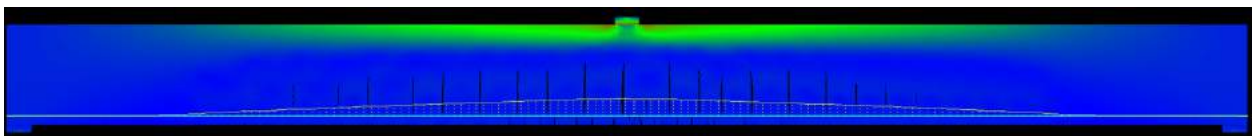


Figure 5.1.4: Concrete and Reinforcement stress for the rectangular beam example C40 Mean.

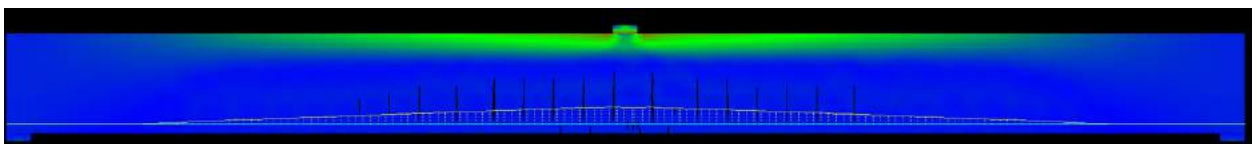


Figure 5.1.5: Concrete and Reinforcement stress for the rectangular beam example C40 Characteristic.

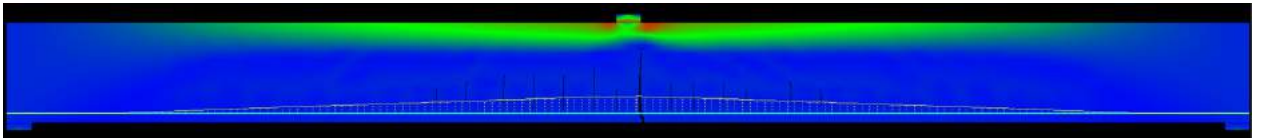


Figure 5.1.6: Concrete and Reinforcement stress for the rectangular beam example C40 Design.

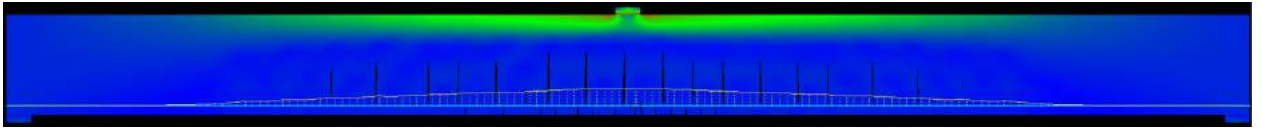


Figure 5.1.7: Concrete and Reinforcement stress for the rectangular beam example C50 Mean.

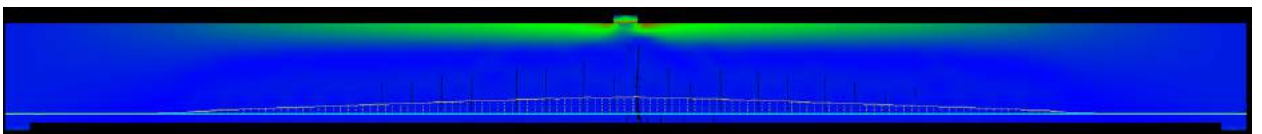


Figure 5.1.8: Concrete and Reinforcement stress for the rectangular beam example C50 Characteristic.

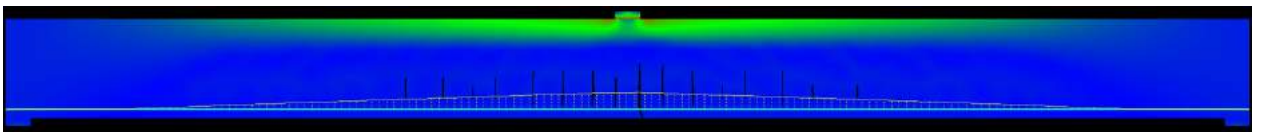


Figure 5.1.9: Concrete and Reinforcement stress for the rectangular beam example C50 Design.

From the Figures 5.1.1-5.1.9 it is clear that all the rectangular beams present a ductile bending failure mode. This is apparent by the reinforcement yielding, and concrete crushing that occurs in the top middle of the beams. However it should be noted that the higher the concrete strength the smaller an area is in crushing. This means that the reinforcement strength is the limiting factor in the high concrete strength cases, namely the C50-M and C50-C case on Figure 5.1.7 and 5.1.8. Additionally the Figures all present cracks in the lower middle part of the beam. This corresponds to a bending failure as well.

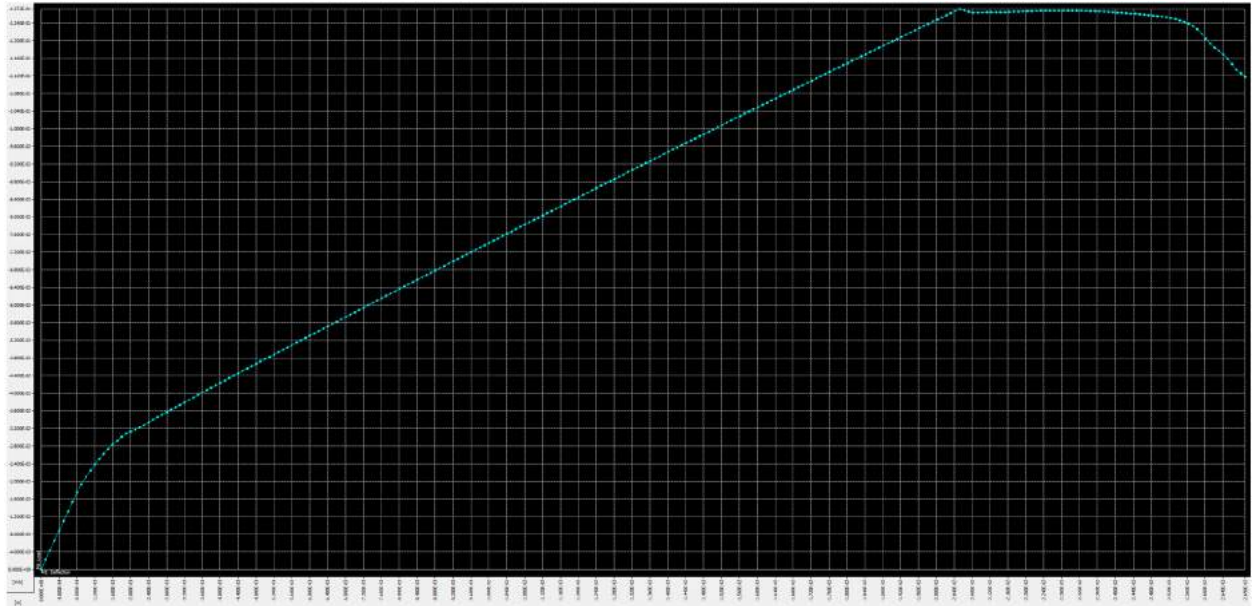


Figure 5.1.10: Load displacement for the C25C rectangular beam used as an example.

All load displacement graphs for the Rectangular beam follow the same path. Therefore only one is used as an example. From Figure 5.1.10 it is clear that the nonlinear behaviour of the T-beam has three parts to it. The first linear part is before cracks are formed. A stress distribution from that section is illustrated on Figure 5.1.11.

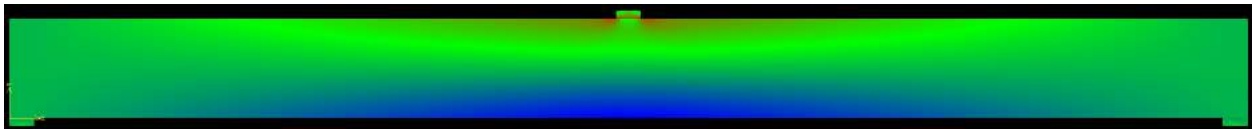


Figure 5.1.11: Stress distribution for first part of the load displacement graph.

The second part of the graph is when cracks start to form. The cracks forming is what causes the sudden change in incline of the load displacement graph.

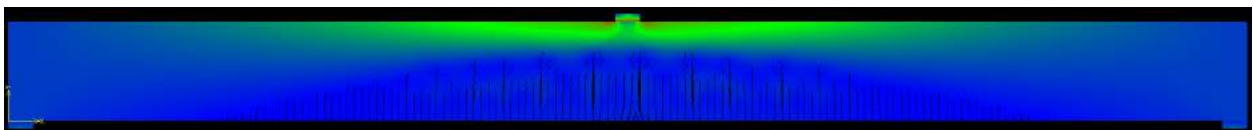


Figure 5.1.12: Stress distribution for first part of the load displacement graph.

The last part of the graph is after the maximum load is reached and the beam keeps on deforming until failure occurs. This clearly illustrates the big impact cracks and crack growth has on the loading of the structure and more specifically on the stress development within a structure.

5.2 T-beam results

In this section the results for the T-beam are presented in terms of stress in concrete and reinforcement alongside where cracks are formed in the rectangular beam. Furthermore the Load-displacement graphs for all 9 cases are presented. The results for concrete and reinforcement stress alongside the cracks are presented in Figure 5.2.1-5.2.9, only cracks wider than 0.1 mm are shown on the Figures. For all T-beams only half the beam is modelled due to beam symmetry. For all T-beams red indicates concrete crushing, bright green indicates concrete in compression and dark green/blue indicates concrete in tension. Values for stresses and loading is presented in Table 5.3.2.

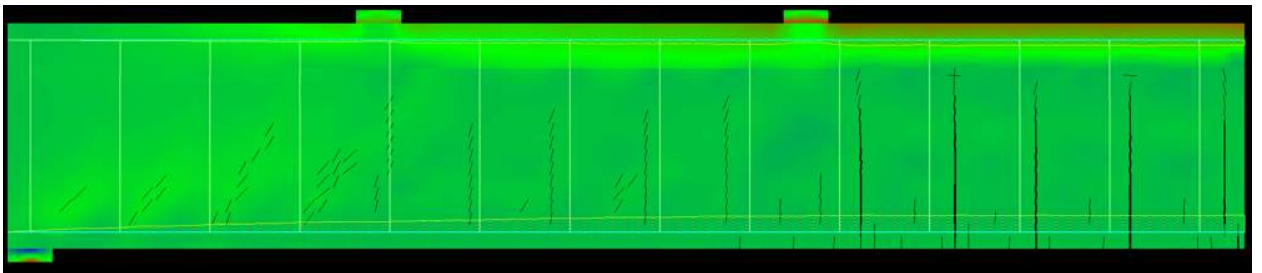


Figure 5.2.1: Concrete and Reinforcement stress for the T-beam example C25 Mean.

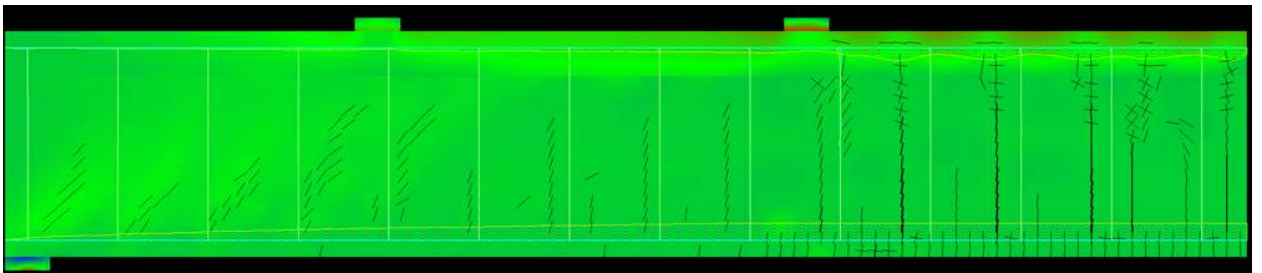


Figure 5.2.2: Concrete and Reinforcement stress for the T-beam example C25 Characteristic.

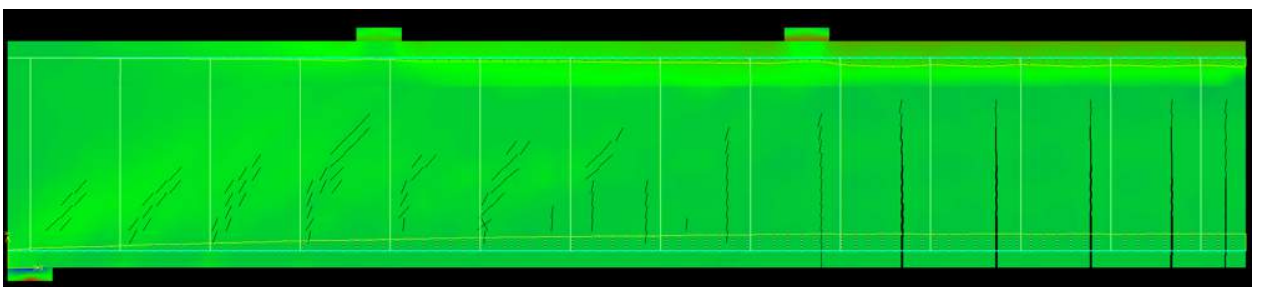


Figure 5.2.3: Concrete and Reinforcement stress for the T-beam example C25 Design.

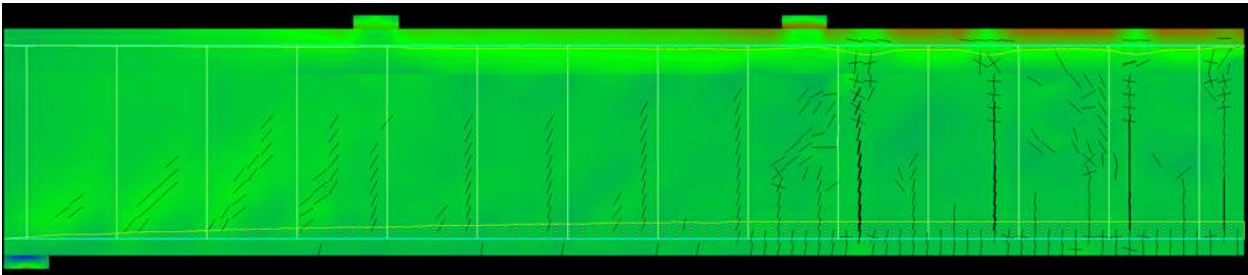


Figure 5.2.4: Concrete and Reinforcement stress for the T-beam example C40 Mean.

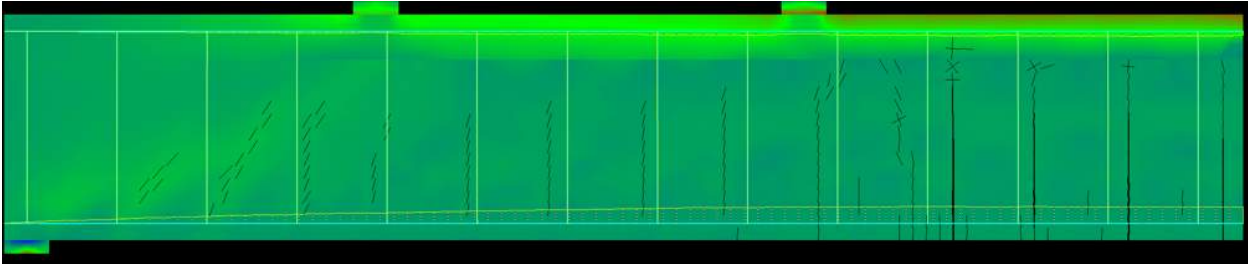


Figure 5.2.5: Concrete and Reinforcement stress for the T-beam example C40 Characteristic.

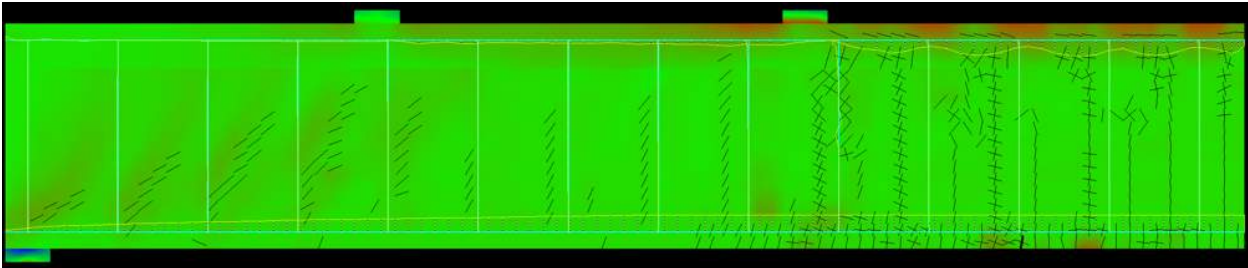


Figure 5.2.6: Concrete and Reinforcement stress for the T-beam example C40 Design.

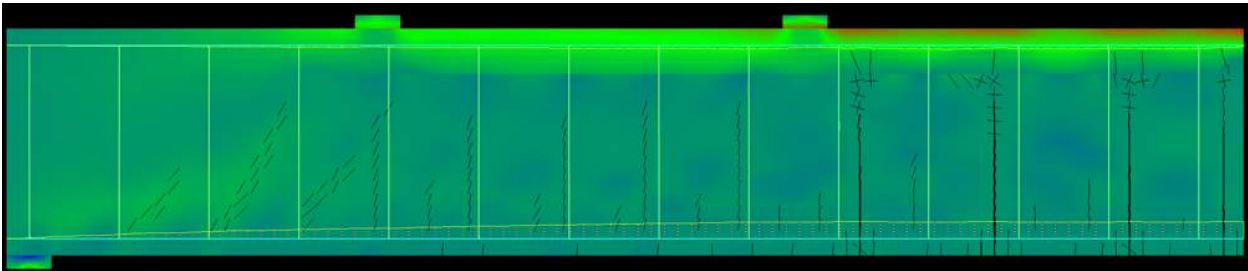


Figure 5.2.7: Concrete and Reinforcement stress for the T-beam example C50 Mean.

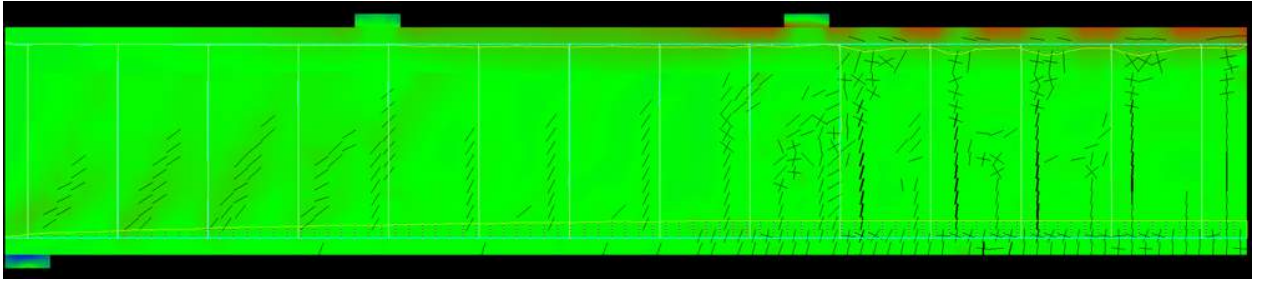


Figure 5.2.8: Concrete and Reinforcement stress for the T-beam example C50 Characteristic.

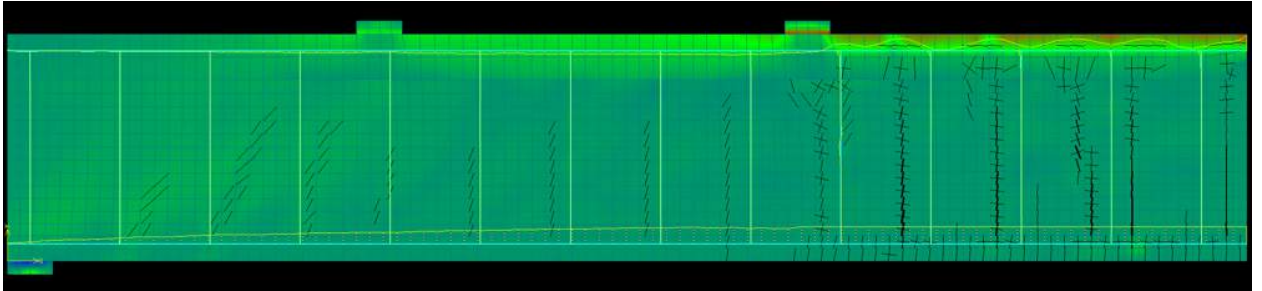


Figure 5.2.9: Concrete and Reinforcement stress for the T-beam example C50 Design.

From the Figures 5.2.1-5.2.9 it is clear that all the T-beams present a ductile bending failure mode. This is apparent by the reinforcement yielding, and concrete crushing that occurs in the top middle of the beams. However it should be noted that the higher the concrete strength the smaller an area is in crushing. This means that the reinforcement strength is the limiting factor in the high concrete strength cases, namely the C50-M and C50-C case on Figure 5.2.7 and 5.2.8. Additionally the Figures all present cracks in the lower middle part of the beam. This corresponds to a bending failure as well. However it should be noted that the C40-D beam is showing signs of being close to a brittle shear failure. This is presented as concrete crushing being close to happening above the support on Figure 5.2.6 alongside diagonal cracks leading from the support to the first load position. All load displacement graphs for the T-beam follow the same path. Therefore only one is used as an example. The load displacement graph is illustrated on Figure 5.2.10. Furthermore the T-beam load displacement graphs follow the same path as the rectangular beam example illustrated on Figure 5.1.11 and 5.1.12.

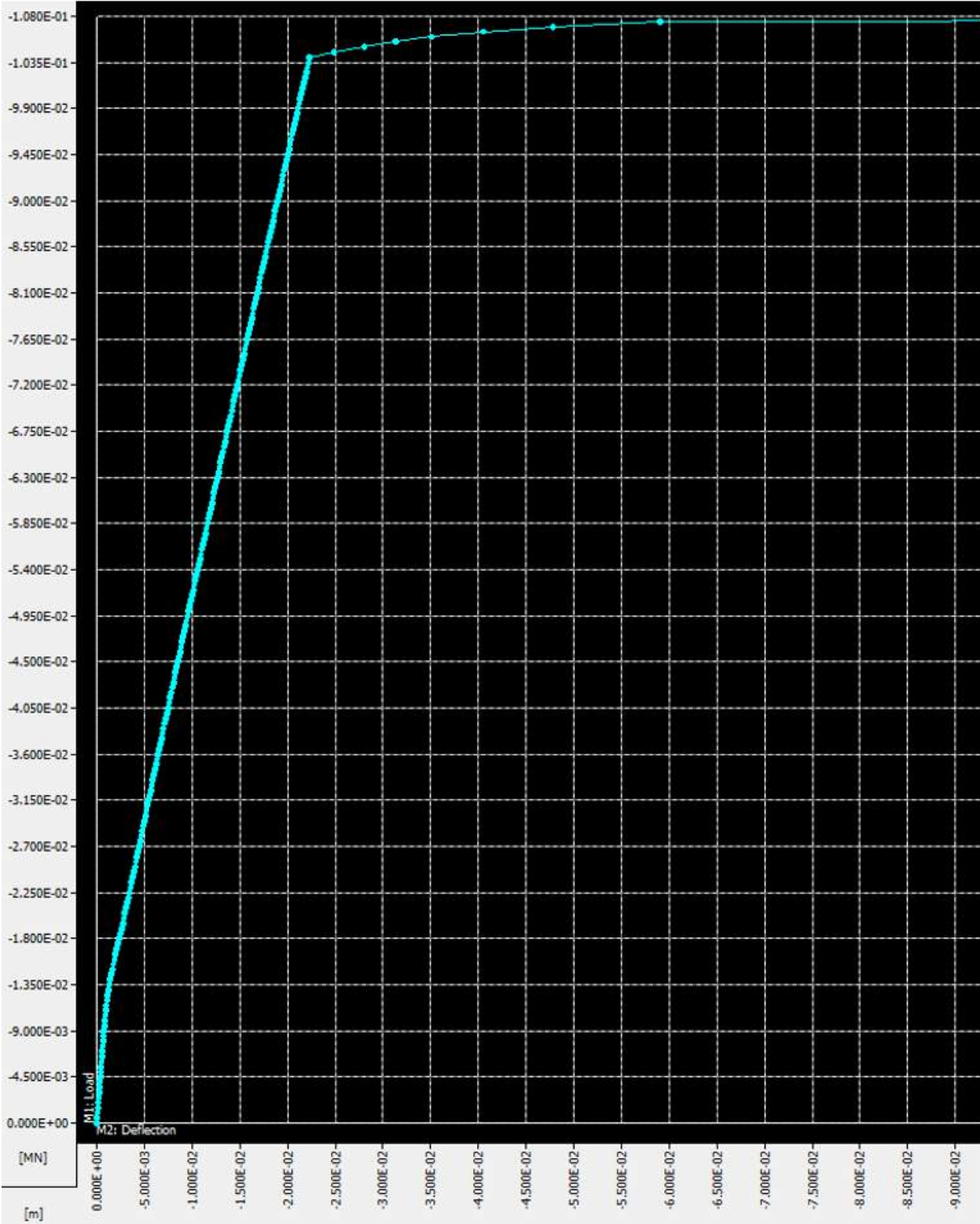


Figure 5.2.10: Load displacement for the C25C rectangular beam used as an example.

5.3 Summary

The maximum load and the resulting failure mode for each example scenario is presented in Table 5.3.1 and 5.3.2. In Table 5.3.1 and 5.3.2 the case names such as C25-M mean a Concrete with a characteristic compressive strength of 25 MPa and in the C25-M case the mean material values are used.

Table 5.3.1: Results of each case regarding the failure mode of simply supported rectangular beam example

Case	Maximum stress		Maximum load	Failure mode
	Concrete	Reinforcement		
C25-M	33.9MPa	543.6MPa	141.6kN	Bending
C25-C	24.6MPa	498.0MPa	126.8kN	Bending
C25-D	16.3MPa	415.6MPa	102.9kN	Bending
C40-M	48.7MPa	549.6MPa	150.2kN	Bending
C40-C	40.9MPa	492.2MPa	132.6kN	Bending
C40-D	26.7MPa	415.3MPa	107.9kN	Bending
C50-M	51.1MPa	550MPa	152.3kN	Bending
C50-C	45.6MPa	496.4MPa	133kN	Bending
C50-D	28.2MPa	415.7MPa	110.9kN	Bending

Table 5.3.2: Results of each case regarding the failure mode of simply supported T-beam example

Case	Maximum stress		Maximum load	Failure mode
	Concrete	Reinforcement		
C25-M	33.6MPa	495MPa	119kN	Bending
C25-C	27.6MPa	450MPa	108kN	Bending
C25-D	16.2MPa	374MPa	89kN	Bending
C40-M	47.3MPa	495MPa	121.5kN	Bending
C40-C	40.2MPa	449.5MPa	110kN	Bending
C40-D	26.3MPa	375MPa	91.5kN	Bending
C50-M	51.6MPa	495MPa	124kN	Bending
C50-C	41.4MPa	450MPa	114kN	Bending
C50-D	38.4MPa	375MPa	95kN	Bending

As it is clear from Table 5.3.1 and 5.3.2 all strength scenarios chosen for the examples result in a bending failure mode. Furthermore it can be concluded that the limiting factor for the high strength concrete scenarios (C50) is the strength of the reinforcement, as previously mentioned, since crushing does not occur as much at the high strength as at the low ones. However it should be noted that several T-beam examples are close to having a shear failure mode as previously mentioned. This include Figure 5.2.6 and 5.2.8. Therefore it is expected that several T-beams will show shear failure modes when the probabilistic method is used to examine the T-beam example.

6. Comparison of Safety formats

In this chapter the safety formats previously presented in Chapter ?? are applied to the rectangular and T-beam examples. To compare the safety methods stated in Chapter ?? NLFE models for each safety format is made. For each example all four safety methods are examined using the same base concrete material strength for each example, C25 for the Rectangular beam and C20 for the T-beam. The reason for lowering the T-beam concrete strength is the results from [Castaldo and Mancini, 2018] showing that a low concrete strength and a high reinforcement strength can lead to different failure modes presenting themselves. Furthermore to compare the different safety methods the reliability index is used alongside the ultimate load and the failure mode the given safety format presents.

As previously described the safety formats examined are the partial safety factor method, global resistance factor method, the ECOV method and the full probabilistic method. For comparison between safety methods the full probabilistic method is considered the correct method and is therefore used as a comparison to the more simplified methods.

6.1 Partial safety factor

The partial safety factor method obtains the design resistance by means of simplified assumptions. The partial safety factor method is presented in equation 6.1.1 [Castaldo and Mancini, 2018].

$$R_d = R_{NLFEA}(f_d) \quad (6.1.1)$$

Where:

R_d	Design resistance
$R_{NLFEA}(f_d)$	Global load bearing capacity
f_d	Design values of material resistance

This method ensures safety through applying local safety factors. This approach is defined as local as it ensures sufficient resistance on a sectional level instead of on a global structural level. This method is used in many model codes for linear as well as nonlinear design problems. This safety format covers both linear and nonlinear analysis in accordance with EN1990 [Standard, 1990].

As previously described the partial safety factor method (PSFM) is covered by EN1990 [Standard, 1990] and traditionally used in linear design methods.

The partial safety factor method results, with regards to stress distribution, for the Rectangular beam example and the T-beam example are illustrated on Figure 6.1.1 for the Rectangular beam of strength C25-D. Additionally the T-beam results are illustrated on Figure 6.1.2 for the strength C20-D. Partial safety factor used for concrete compressive strength is 1,5 while the partial safety factor for reinforcement strength is 1,2.

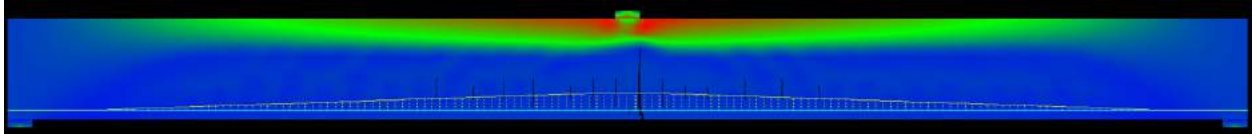


Figure 6.1.1: Concrete and Reinforcement stress for the rectangular beam example C25 Design.

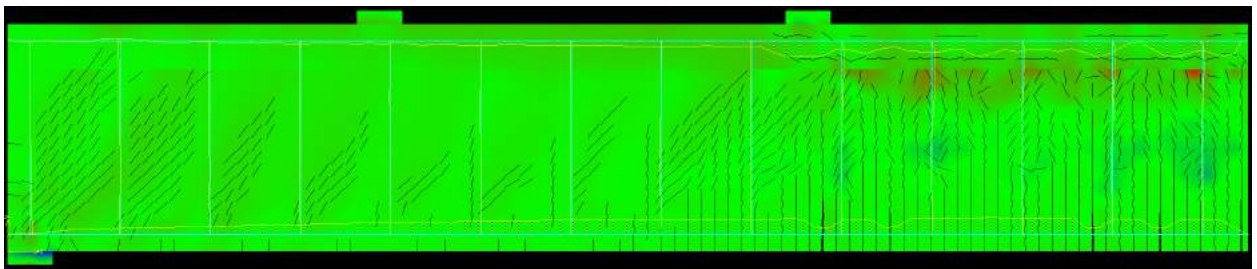


Figure 6.1.2: Concrete and Reinforcement stress for the T-beam example C20 Design.

As it is clear from Figure 6.1.1 and 6.1.2 the two beam examples both present a ductile bending failure mode. The ultimate load, failure mode, Coefficient of variation, Global safety factor and design load is presented in Table 6.1.1.

Table 6.1.1: Results for the partial safety factor method for both examples.

Case	Ultimate load [kN]	Failure mode [-]	COV [-]	Global Safety factor [-]	Design load [kN]
Rectangular beam	102,9	Bending	-	-	102,9
T-Beam	100	Bending	-	-	100

6.2 Global resistance factor

The global resistance factor method obtains design resistance by applying a global safety factor to the resistance as presented in equation 6.2.1 [Castaldo and Mancini, 2018].

$$R_d = \frac{R_{rep}(f_{cmd}, f_{ym})}{\gamma_{GL}} \quad (6.2.1)$$

Where:

R_d		Design resistance
R_{rep}		Global structural resistance
f_{cmd}		Mean yield stress for concrete
f_{ym}		Mean yield stress for reinforcing steel
γ_{GL}		Safety factor

The applicability of the global resistance factor method depends highly on the case it is used. To estimate the representative value of global resistance the mean value of the yield stress has to be considered for steel and concrete as presented in equation 6.2.2 and 6.2.3 [Castaldo and Mancini, 2018].

$$f_{ym} = 1.1f_{yk} \quad (6.2.2)$$

Where:

f_{ym}		Mean yield stress for reinforcing steel
f_{yk}		Characteristic yield stress for reinforcing steel

$$f_{cmd} = 0,85f_{ck} \quad (6.2.3)$$

Where:

f_{cmd}		Mean yield stress for concrete
f_{ck}		Characteristic yield stress for concrete

The global resistance factor method is not covered by EN1990 [Standard, 1990] as the starting point being mean material values is not covered for either linear or nonlinear design methods. The global resistance factor method (GRF) results, with regards to stress distribution, for the Rectangular beam example and the T-beam example are illustrated on Figure 6.2.1 for the Rectangular beam of strength C25-M. Additionally the T-beam results are illustrated on Figure 6.2.2 for the strength C20-M. For the global resistance factor 1,27 is used in accordance with [Castaldo and Mancini, 2018].

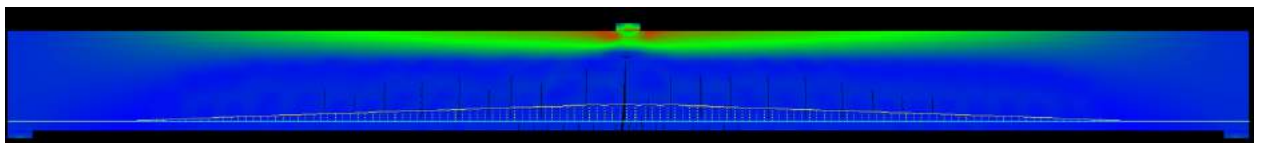


Figure 6.2.1: Concrete and Reinforcement stress for the rectangular beam example C25 Mean.

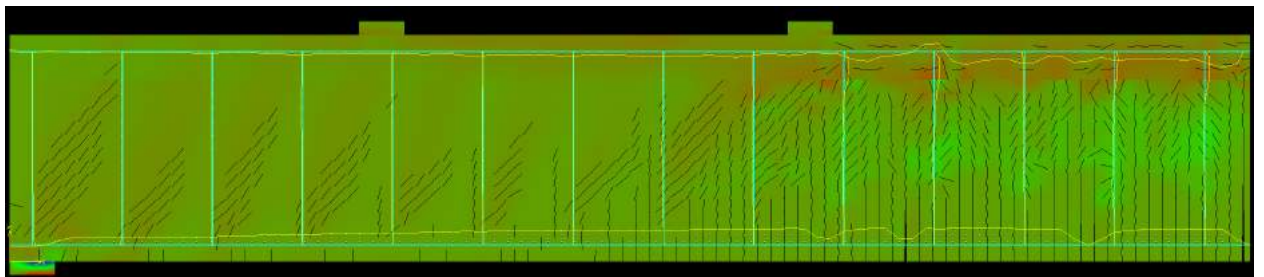


Figure 6.2.2: Concrete and Reinforcement stress for the T-beam example C20 Mean.

As it is clear from Figure 6.2.1 and 6.2.2 the two beam examples both present a ductile bending failure mode. The ultimate load, failure mode, Coefficient of variation, Global safety factor and design load is presented in Table 6.2.1.

Table 6.2.1: Results for the global resistance factor method for both examples.

Case	Ultimate load [kN]	Failure mode [-]	COV [-]	Global Safety factor [-]	Design load [kN]
Rectangular beam	141,6	Bending	-	1,27	111,5
T-Beam	131	Bending	-	1,27	103,2

From using the global resistance factor method it is clear that the design loads presented in Table 6.2.1 are approximately the same as the design loads from the partial safety factor method presented in Table 6.1.1.

6.3 ECOV - Estimate of coefficient of variation for resistance

The estimate of coefficient of variation for resistance, ECOV, method obtains the global design resistance through equation 6.3.1 [Castaldo and Mancini, 2018] [Cervenka, 2013]. This method is an alternative adaptation of the global

$$R_d = \frac{R_m}{\gamma_R} \quad (6.3.1)$$

Where:

R_d	Design resistance
R_m	Structural resistance using mean values
γ_R	Global resistance safety factor

In equation 6.3.1 R_m denotes the structural resistance predicted by a nonlinear finite element analysis, NLFEA, based on mean resistances. γ_R from equation 6.3.1 denotes the global resistance factor accounting for uncertainties related to the material properties while γ_{Rd} accounts for model uncertainties related to the resistance being based on a NLFEA. Using equation 6.3.2 the global resistance factor γ_R can be estimated assuming a lognormal distribution for the global load bearing capacity of the structure [Castaldo and Mancini, 2018] [Cervenka, 2013].

$$\gamma_R = \exp(\alpha_R \cdot \beta \cdot V_R) \quad (6.3.2)$$

Where:

γ_R	Global resistance factor
V_R	Coefficient of variation of global structural resistance

In equation 6.3.2 V_R is the coefficient of variation of the distribution of the global structural resistance. The ECOV method estimates V_R with a simplified approach using a lognormal

distribution for global structural resistances. The ECOV method is presented in equation 6.3.3 [Castaldo and Mancini, 2018] [Cervenka, 2013].

$$V_R = \frac{1}{1.65} \ln \left(\frac{R_m}{R_k} \right) \quad (6.3.3)$$

Where:

V_R	Coefficient of variation of global structural resistance
R_m	Structural resistance using mean values
R_k	Structural resistance using characteristic values

Using equation 6.3.3 in the ECOV method the value of V_R can be estimated using the two different NLFEA for mean and characteristic resistances respectively. The ECOV method is not covered by EN1990 [Standard, 1990] for linear or nonlinear design methods. It is presented as an alternative method to the global resistance factor method. The ECOV method aims to provide a more accurate estimate of the global resistance factor than the global resistance factor does. The ECOV method results, with regards to stress distribution, for the Rectangular beam example and the T-beam example are illustrated on Figure 6.3.1 and 6.3.3 for the Rectangular beam of strength C25-M/C. Additionally the T-beam results are illustrated on Figures 6.3.2 and 6.3.4 for the strength C20-M/C. For the global resistance factor 1,27 is used in accordance with [Castaldo and Mancini, 2018].

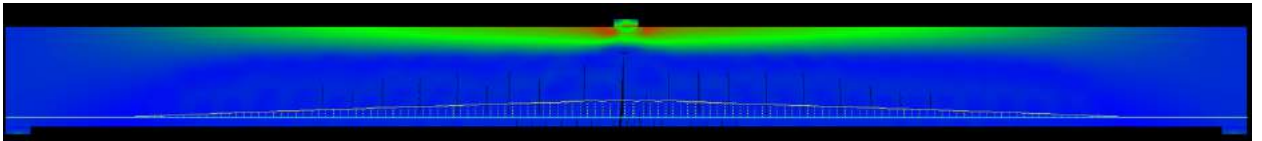


Figure 6.3.1: Concrete and Reinforcement stress for the rectangular beam example C25 Mean.

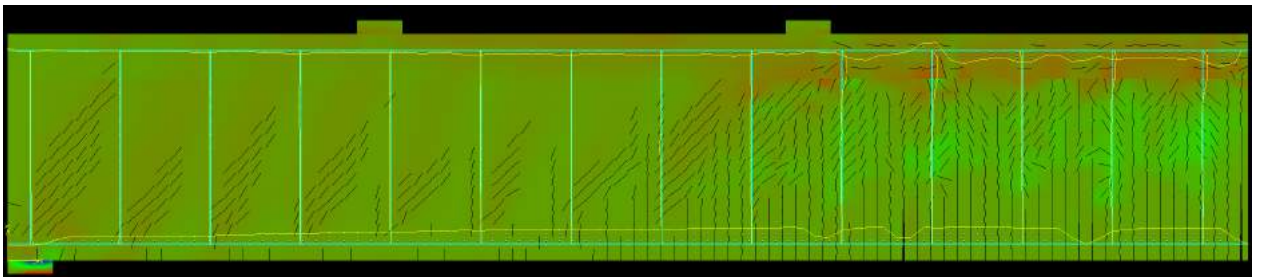


Figure 6.3.2: Concrete and Reinforcement stress for the T-beam example C20 Mean.

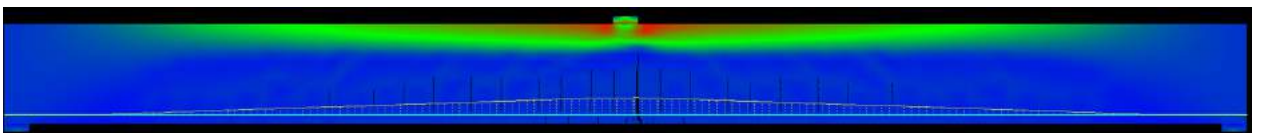


Figure 6.3.3: Concrete and Reinforcement stress for the rectangular beam example C25 Characteristic.

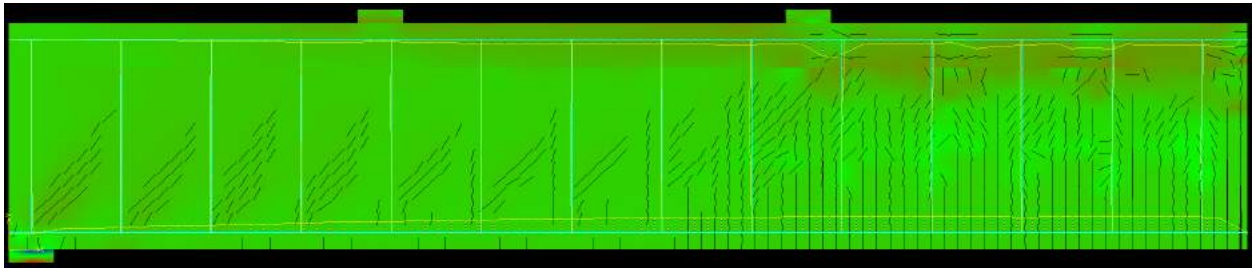


Figure 6.3.4: Concrete and Reinforcement stress for the T-beam example C20 Characteristic.

As it is clear from Figure 6.3.1, 6.3.2, 6.3.3 and 6.3.4 the four beam examples both present a ductile bending failure mode. The ultimate load, failure mode, Coefficient of variation, Global safety factor and design load is presented in Table 6.3.1. The reliability index β used for ECOV calculation is equivalent to 3,8 for ordinary structures with moderate consequences in the case of failure with a lifetime of 50 years. The FORM sensitivity factor α_R used is considered equal to 0,8.

Table 6.3.1: Results for the ECOV method for both examples.

Case	Ultimate load [kN]	Failure mode [-]	COV [-]	Global Safety factor [-]	Design load [kN]
Rectangular beam	141,6 – 126,8	Bending	0,067	1,23	115,5
T-Beam	131 – 118	Bending	0,063	1,21	108,2

The two ultimate loads signify mean and characteristic model loads

From using the global resistance factor method it is clear that the design loads presented in Table 6.2.1 are approximately the same as the design loads from the partial safety factor method presented in Table 6.1.1.

6.4 Full probabilistic method

The full probabilistic method consists of running several NLFEMs adopting a sampling technique such as Monte Carlo simulation or latin hypercube sampling to define the input data. The results of the simulation are then fitted to an appropriate probabilistic model. This probabilistic model may differ from the lognormal one further highlighting the issue with always assuming a lognormal distribution as described in the ECOV method. Using the appropriate probabilistic method the statistical parameters can be described. From the probabilistic distribution it is possible to directly assess the design value of resistance according to a specific reliability index [Castaldo and Mancini, 2018].

The full probabilistic method can very accurately assess design resistance values to a specific design case. However the disadvantage is the method being time consuming as a probabilistic model needs to be set up for all the different design resistance scenarios in a structure.

The Full probabilistic method is carried out using multiple NLFEM models. These differ-

ent models are set up using randomized material strength parameters for concrete and reinforcement. In order to set up the randomized input models are set up using SARA. SARA is a program developed by Cervenka Consulting in order to make full probabilistic analysis of ATENA models possible. Using SARA the randomization technique Latin Hypercube Sampling is used in order to determine the random input parameters. In this report 30 different random input parameter ATENA models per example are set up using SARA. The relatively low number of samples are used due to the sampling technique actively trying to fit the given probabilistic distribution instead of being completely random as a Monte-Carlo simulation would have been.

The random input parameters for material strengths are determined based on their probability density function, standard deviation and coefficient of variation. The probability density function and standard deviation and coefficient of variation used for generation of random input parameters are presented in Table 6.4.1.

It should be noted that the concrete tensile strength, f_t and Youngs modulus, E , are determined based on their relation to the concrete compressive strength, f_c . This relation is input in SARA using a pearson statistical correlation matrix. This statistical correlation matrix is defined based on the recommended values from the SARA user manual. [Havlásek and Pukl, 2017]

Table 6.4.1: The input parameters for SARA random value generation. The two material strengths represent the rectangular and T-beam respectively. [Castaldo and Mancini, 2018]

Random Variable	PDF	Mean Value	Std	COV
Concrete compressive strength, f_c	Log-normal	33 MPa/28 MPa		0,15
Reinforcement yield strength, f_y	Log-normal	550 MPa/495 MPa		0,05
Reinforcement young modulus, E_s	Log-normal	200 000 MPa		0,03

Using these parameters random input parameters are defined for concrete and reinforcement. The 30 material scenarios for the Rectangular beam and the T-beam are presented in Table 6.4.2 and 6.4.3. For the T-beam steel hardening of the reinforcement is taken into account by adding 15% to the yield strength. This is done in accordance with [Castaldo and Mancini, 2018]. The hardening of the reinforcement is taken into account in order to illustrate the same issues regarding failure mode that [Castaldo and Mancini, 2018] found. These issues are as previously mentioned that different failure modes can present themselves within the same material strength. As previously mentioned this is of course an issue when it comes to structural design due to the inability to ensure structural reliability when the failure mode is not certain.

Table 6.4.2: Material input parameters for the Rectangular beam example.

	Concrete			Reinforcement	
	f_c [MPa]	f_t [MPa]	E_c [MPa]	f_y [MPa]	E_s [MPa]
1	-26,6	1,56	24.947	531,1	190.287
2	-28,5	1,52	26.178	533,8	201.697
3	-23,8	1,45	26.871	574,7	199.660
4	-25,5	1,67	27.389	550,5	200.161
5	-27,3	1,69	27.816	517,6	208.377
6	-27,9	1,61	28.190	525,1	195.906
7	-29,5	1,59	28.527	555,1	210.020
8	-31,6	1,95	28.839	545,9	197.613
9	-30,4	1,93	29.133	538,8	207.185
10	-32,4	1,71	29.413	610,9	187.549
11	-29,0	1,88	29.683	548,2	200.665
12	-33,3	1,75	29.946	571,3	199.158
13	-32,8	1,81	30.205	588,6	204.664
14	-32,0	1,85	30.462	559,9	198.652
15	-29,9	1,74	30.718	583,0	205.397
16	-30,1	1,72	30.980	562,6	195.269
17	-30,8	1,72	30.975	562,6	195.267
18	-31,2	1,78	31.235	506,5	202.234
19	-36,1	1,80	31.500	493,9	213.086
20	-34,6	2,05	31.773	505,9	196.504
21	-35,6	1,86	32.055	521,6	197.070
22	-34,1	1,90	32.660	557,5	203.995
23	-37,3	1,98	32.349	552,8	198.139
24	-44,1	1,90	32.660	596,4	203.995
25	-35,0	1,77	32.993	543,6	191.787
26	-40,1	2,21	33.354	596,4	202.791
27	-38,9	1,66	33.753	512,6	192.890
28	-33,9	2,11	35.410	528,2	193.792
29	-41,7	2,02	36.350	536,4	194.569
30	-44,8	1,92	38.140	565,3	206.220

Table 6.4.3: Material input parameters for the T-beam example.

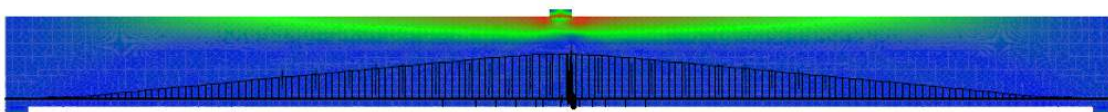
	Concrete			Reinforcement		
	f_c [MPa]	f_t [MPa]	E_c [MPa]	f_y [MPa]	f_{y2} [MPa]	E_s [MPa]
1	-21,7	1,65	22.581	499,6	574,6	205.397
2	-25,0	1,81	23.696	487,1	560,2	202.791
3	-20,2	2,03	24.323	465,8	535,7	207.185
4	-22,5	1,91	24.791	508,7	585,1	200.665
5	-23,7	1,78	25.178	495,4	569,7	206.222
6	-23,2	2,05	25.516	517,2	594,8	200.161
7	-26,1	1,73	25.822	480,4	552,5	195.267
8	-29,4	2,02	26.104	520,7	598,8	199.660
9	-22,4	1,99	26.370	549,9	632,3	202.234
10	-27,5	1,96	26.623	469,4	539,8	194.570
11	-27,2	2,08	26.868	444,5	511,2	193.791
12	-24,2	2,10	27.106	506,3	582,3	192.890
13	-24,6	1,89	27.341	484,9	557,7	198.652
14	-25,8	2,12	27.573	461,4	530,6	191.787
15	-28,2	1,87	27.805	478,0	549,7	199.158
16	-28,6	2,18	28.037	482,7	555,1	195.906
17	-29,7	2,26	28.273	514,1	591,2	210.020
18	-27,9	2,23	28.513	501,8	577,0	204.664
19	-26,5	1,84	28.760	475,4	546,7	203.995
20	-30,6	2,21	29.015	489,2	562,6	187.549
21	-30,2	1,98	29.281	536,7	617,2	198.139
22	-28,9	2,34	29.563	529,8	609,2	201.697
23	-26,8	1,94	29.864	497,5	572,1	203.375
24	-32,3	2,41	30.190	503,9	579,6	190.287
25	-33,1	2,52	30.552	472,6	543,5	208.377
26	-34,0	2,06	30.962	491,3	564,9	201.176
27	-31,1	1,92	31.445	511,3	588,0	196.504
28	-31,6	2,16	32.051	493,4	567,4	197.070
29	-35,4	2,14	32.899	524,7	603,4	197.613
30	-38,0	2,29	34.524	455,4	523,7	213.086

NLFEA is then carried out for all 30 samples for both the rectangular and the T-beam examples. This is done by letting SARA control inputs for the two ATENA models. The results for the 30 input parameter scenarios for the Rectangular beam and the T-beam are presented in Table 6.4.4 and 6.4.5. Table 6.4.4 shows the results for the 30 samples for the Rectangular beam example.

Table 6.4.4: Results of the 30 input cases and the failure mode of the Rectangular beam example

	Maximum stress		Maximum load	Failure mode
	Concrete	Reinforcement		
	[MPa]	[MPa]	[kN]	-
1	-26,4	529,1	134,4	Bending
2	-29,0	528,7	135,8	Bending
3	-23,2	573,0	142,6	Bending
4	-27,1	545,5	138,4	Bending
5	-28,8	512,1	131,8	Bending
6	-28,5	520,1	133,7	Bending
7	-29,4	553,5	141,3	Bending
8	-33,2	541,4	139,7	Bending
9	-31,7	533,2	137,7	Bending
10	-32,8	607,0	154,8	Bending
11	-29,4	543,3	139,2	Bending
12	-32,7	569,9	146,3	Bending
13	-34,3	584,3	149,9	Bending
14	-33,8	555,8	143,2	Bending
15	-31,0	581,5	147,9	Bending
16	-31,6	558,2	143,2	Bending
17	-31,3	562,2	147,2	Bending
18	-35,9	500,6	131,6	Bending
19	-37,4	488,2	128,4	Bending
20	-33,8	502,3	135,6	Bending
21	-34,6	518,4	143,2	Bending
22	-35,3	556,1	143,5	Bending
23	-38,1	547,2	140,6	Bending
24	-45,1	592,0	154,4	Bending
25	-37,8	538,3	133,9	Bending
26	-42,1	591,4	146,9	Bending
27	-38,0	512,6	140,3	Bending
28	-34,1	522,9	136,5	Bending
29	-44,1	531,9	140,6	Bending
30	-43,5	565,3	148,2	Bending

As presented by Table 6.4.4 all 30 material parameter scenarios result in a bending failure mode for the rectangular beam example. The stress distribution for all 30 samples follow the same overall pattern. This overall pattern is illustrated by Figure 6.4.1.

**Figure 6.4.1:** Concrete and Reinforcement stress for sample 1 of the Rectangular beam.

As illustrated by Figure 6.4.1. The rectangular beam samples presents a stress distribution that includes concrete crushing in the top middle part of the beam alongside yielding in the reinforcement in the middle of the beam. These two traits are indication of ductile bending being the failure mode for all 30 rectangular beam examples. The load-displacements for all the rectangular beam samples are illustrated on Figure 6.4.2.

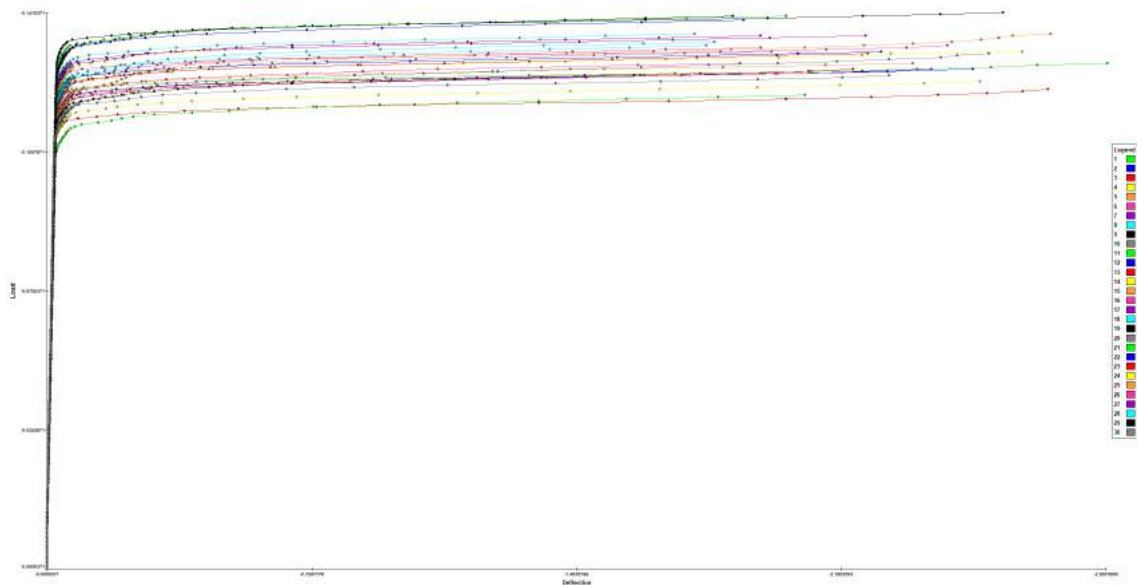


Figure 6.4.2: Load-Displacement graphs for all 30 samples for the Rectangular beam.

As it is clear from Figure 6.4.2 all the samples for the rectangular beam example follow the same load-displacement path as described in Chapter 5 on Figure 5.1.11 and 5.1.12. Table 6.4.5 shows the results for the 30 samples for the T-beam example.

Table 6.4.5: Results of the 30 input cases and the failure mode of the T-beam example

	Maximum stress		Maximum load	Failure mode
	Concrete	Reinforcement		
	[MPa]	[MPa]	[kN]	-
1	-23,0	570,2	128,5	Bending
2	-30,6	557,7	127,0	Bending
3	-26,9	530,2	122,0	Bending
4	-23,6	574,1	131,5	Bending
5	-29,6	564,4	128,5	Bending
6	-24,8	592,9	133,0	Bending
7	-28,8	549,7	127,0	Bending
8	-32,0	588,6	136,0	Bending
9	-23,5	623,1	141,5	Bending
10	-29,4	536,5	125,5	Bending
11	-29,1	503,7	120,5	Bending
12	-28,1	576,0	131,5	Bending
13	-25,5	554,6	127,0	Bending
14	-26,9	524,1	124,0	Bending
15	-31,8	544,1	126,5	Bending
16	-29,6	543,6	128,5	Bending
17	-36,9	576,0	135,5	Bending
18	-34,5	573,3	134,0	Bending
19	-26,8	544,0	125,5	Bending
20	-30,8	558,8	131,5	Bending
21	-32,3	613,7	140,5	Bending
22	-35,1	605,3	139,5	Bending
23	-34,3	569,1	131,0	Bending
24	-29,2	569,1	134,5	Bending
25	-28,8	538,7	136,0	Bending
26	-36,0	559,6	132,5	Bending
27	-28,4	576,1	135,5	Bending
28	-37,2	559,4	133,0	Bending
29	-34,1	597,2	140,5	Bending
30	-39,3	517,6	131,0	Bending

As presented by Table 6.4.4 all 30 material parameter scenarios result in a bending failure mode for the T-beam example. The stress distribution for all 30 samples follow the same overall pattern. This overall pattern is illustrated by Figures 6.4.3, 6.4.4 and 6.4.5.

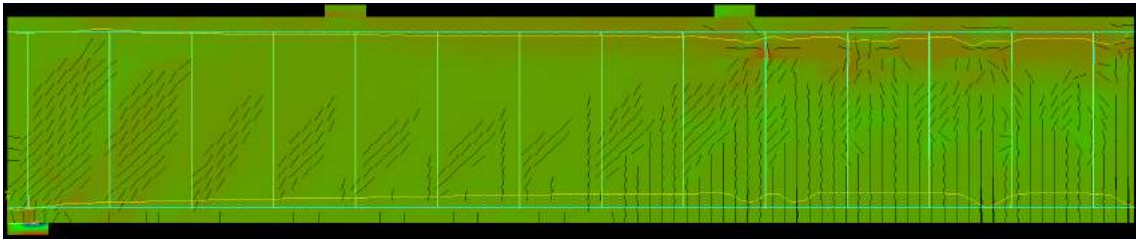


Figure 6.4.3: Concrete and Reinforcement stress for sample 1 of the T-beam.

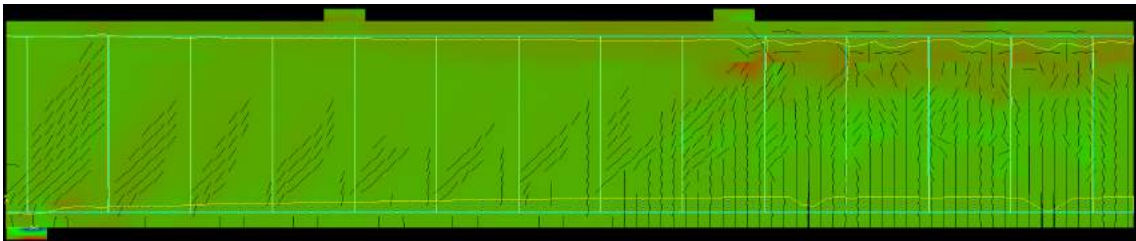


Figure 6.4.4: Concrete and Reinforcement stress for sample 3 of the T-beam.

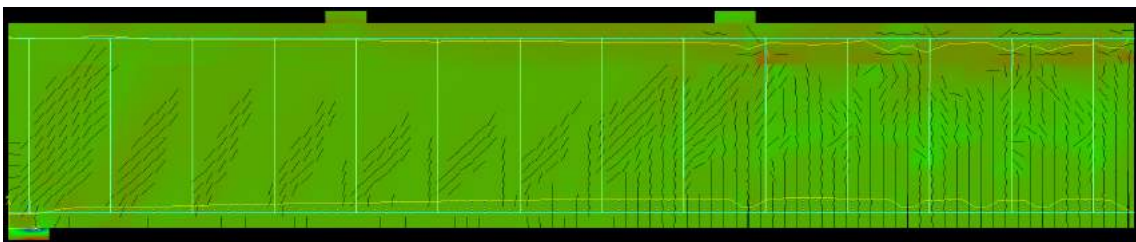


Figure 6.4.5: Concrete and Reinforcement stress for sample 9 of the T-beam.

As illustrated by Figure 6.4.3-6.4.5. The T-beam samples presents a stress distribution that includes concrete crushing in the top middle part of the beam alongside yielding in the reinforcement in the middle of the beam. These two traits are indication of ductile bending being the failure mode for all 30 T-beam examples. However most of the T-beam samples also show crack development and beginning concrete crushing near the support which suggests a ductile shear failure mode. The reason the samples are evaluated as having a ductile bending failure mode is due to the reinforcement being in yielding for all 30 samples. Furthermore this is clearly illustrated by Figure 6.4.3-6.4.5. The load-displacements for all the T-beam samples are illustrated on Figure 6.4.6.

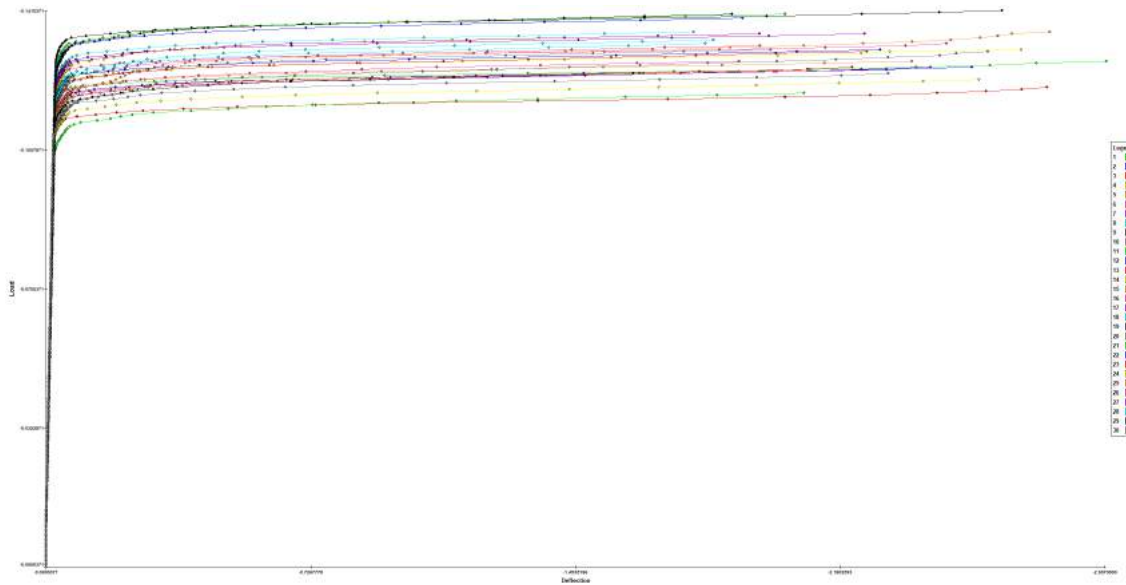


Figure 6.4.6: Load-Displacement graphs for all 30 samples for the T-beam.

As it is clear from Figure 6.4.6 all the samples for the T-beam example follow the same load-displacement path as the examples described in Chapter 5 on Figure 5.1.11 and 5.1.12.

As mentioned earlier the T-beam should according to [Castaldo and Mancini, 2018] present different failure modes when using LH Sampling as input parameters. This is not the case for this report which leads to the conclusion that either [Castaldo and Mancini, 2018] is wrong in their result for the T-beam or the T-beam example of this report is wrong. It should be noted however that the material parameters used are not exactly the same. This is due to [Castaldo and Mancini, 2018] using experimental results to determine material parameters.

Additionally these results illustrate that the issue with one structural beam presenting multiple different failure modes for different material resistance parameters only occurs in very specific scenarios.

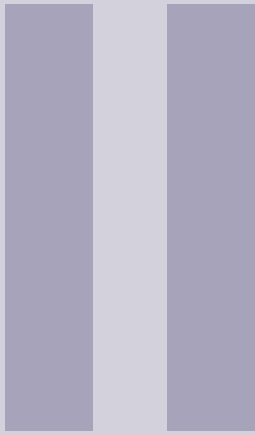
6.5 Reliability comparison of safety methods

In this Section the reliability of the different safety methods is compared using the reliability index for each method. The reliability index is determined using SARA. The reliability index is presented in Table 6.5.1.

Table 6.5.1: Reliability results for all safety methods for both examples.

	β	
	Rectangular beam	T-Beam
Partial Safety Factor	3,8	3,8
Global Resistance Factor	3,1	3,5
ECOV	2,8	2,9
Probabilistic	5,3	4,6

As presented by Table 6.5.1 the reliability index for each safety method has been determined. In conclusion it can be said that the probabilistic method is too safe to consider as a viable option when it comes to determining a viable broadterm safety method to use. The other three safety methods, partial safety factor, global safety factor and the ECOV method can all be considered as viable options for a nonlinear safety method to use in design of any nonlinear reinforced concrete structure. Additionally the ECOV method is in general less reliable then the partial safety factor and the global resistance factor. In this report the results regarding the failure modes each method presents and especially the failure modes the probabilistic method presents makes it impossible to determine whether these reliability indexes are correct or not as it can not be known whether the probabilistic distribution used to determine them is correct or not. This uncertainty is due to the inconsistency between the T-beam in this report and the T-beam in [Castaldo and Mancini, 2018].



Closure

7	Discussion	45
8	Conclusion	47
	Bibliography	48

7. Discussion

In this chapter the results of the report are discussed in order to determine their validity. For starters the results of the initial examples are considered. The initial Rectangular beam example illustrates a bending failure mode, as expected, for all nine material resistance scenarios. Therefore the initial rectangular beam results are considered a valid result. With regards to the initial T-beam examples. All nine material resistance scenarios result in a bending failure mode therefore this result does not show more than one failure mode as it is expected from the T-beam example. However it should be noted that the same T-beam in [Castaldo and Mancini, 2018] only presents different failure modes when subjected to random sampling during the probabilistic method. Therefore when using only Mean, Characteristic or Design material input parameters instead of a mix of the parameters a bending failure mode is expected and proven due to that being the failure mode the T-beam is designed to fail in.

In order to assess the effect of using different safety methods has on the failure mode four different safety methods was presented in Chapter 6. The four safety methods presented include, the partial safety factor method, the global resistance factor method, the ECOV method and the probabilistic method with the probabilistic method being viewed as the most reliable method. This is due to the probabilistic method being on a specific example level while the other safety methods are more generally applicable. Furthermore the probabilistic method is the only one of the presented failure modes that randomize material input parameters in order to ensure safety.

The partial safety method, global resistance factor method, the ECOV method and the probabilistic method all present a bending failure mode for the Rectangular beam. This is in accordance with the expected failure mode for the Rectangular beam and therefore these results are viewed as viable.

With regards to the T-beam result the partial safety factor method, global resistance factor method and the ECOV method all present a bending failure mode. This is in correspondence with the results presented for the same beam example in [Castaldo and Mancini, 2018] meaning that the T-beam does not show different failure modes for the initial safety methods. Since this is the case for both this report and [Castaldo and Mancini, 2018] these results are deemed as a viable representation of reality. However when comparing the results of the probabilistic method from [Castaldo and Mancini, 2018] to the probabilistic method for the T-beam in this report it is clear that the results in [Castaldo and Mancini, 2018] show a nearly 50/50 split between a bending failure mode and a shear failure mode. On the contrary when the probabilistic method is used to assess the T-beam in this report all 30 samples present a bending failure mode. This disparity presents two possible explanations. The first explanation is that there is an error in the material models

used for the T-beam in this report making the results misleading. The second possible explanation is that the [Castaldo and Mancini, 2018] assessment of the T-beam is wrong.

The argument for the first explanation is that the [Castaldo and Mancini, 2018] material models are set up based on experiments. This means that the material models used by [Castaldo and Mancini, 2018] are more accurate as they are directly based on a real concrete sample. The argument for the second explanation is that the three other safety methods all present a bending failure mode. Furthermore all the other examples used in [Castaldo and Mancini, 2018] also present only one failure mode for all safety methods except the probabilistic method. It should be noted that the results of this report in cooperation with [Castaldo and Mancini, 2018] indicates that in order for a concrete structure to present more than one failure mode very specific examples are needed, even the smallest of changes in a given example can result in there only being one failure mode presented.

With regards to the reliability indexes found for the different safety methods it can be concluded that they correspond with the reliability indexes in [Castaldo and Mancini, 2018] except for the probabilistic method which differs between this report and [Castaldo and Mancini, 2018]. The reason for that is as [Castaldo and Mancini, 2018] states that the reliability index is affected by the different failure modes presenting themselves in the T-beam from [Castaldo and Mancini, 2018] making the reliability index much lower than it would be if there was only one failure mode. Furthermore it is hard to determine whether the probabilistic distribution is correct within this report as it does not show the same failure modes as [Castaldo and Mancini, 2018] for the same T-beam on the other hand the T-beam within this report shows the same failure mode as the rest of the safety methods.

If this project was given more time more examples would have to be made in order to determine how common or uncommon more than one failure mode for a given example is. In this report it was chosen to model the T-beam example after [Castaldo and Mancini, 2018] in order to prove that the T-beam example would yield different failure modes for different random input parameters. However since this was not proven the project would have to find additional examples that could yield the same result of presenting more than one failure mode. Furthermore in order to make the project more accurate experiments should be conducted for multiple reasons. Firstly in order to determine the failure mode presented by a given example in reality. Secondly conducting experiments would allow the ATENA models to be more accurate as the material input parameters can be based on the concrete and reinforcement used for the experiments conducted. With more time given another possibility is to make many experiments on the same example. This would be done in order to see if the inherent randomness when producing concrete would have a similar effect in reality as it has in [Castaldo and Mancini, 2018]. This way it would be possible to determine whether the two different failure modes scenario is just a theoretical issue or an issue presenting itself at random in reality as well.

8. Conclusion

In this Chapter the results and findings of the report will be concluded on. Furthermore the problem statement will be concluded on. The problem statement is presented below.

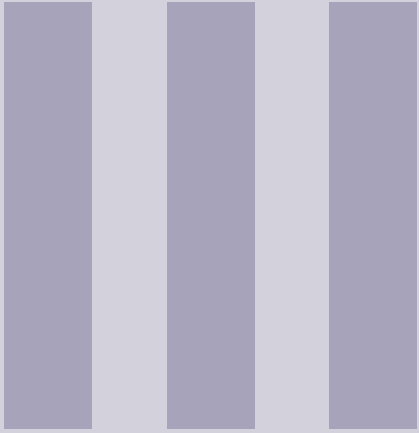
How can nonlinear design methods be used to design reinforced concrete structures while maintaining a satisfying level of reliability?

Firstly based on this report it can be concluded that as long as the same type of material resistance i.e. mean, characteristic or design is used for both concrete and reinforcement strength only one failure mode will present itself.

Secondly based on this report it can be concluded that it is possible to design reinforced concrete structures while maintaining a satisfying level of reliability using a number of different safety methods. However it can also be concluded that the issue with nonlinear reinforced concrete design is not in the level of reliability achieved but instead the problem lies in the failure modes different safety methods present. Therefore the safety method chosen for nonlinear reinforced concrete design has to be able to determine the correct failure mode in a vast number of scenarios. Based on this report and [Castaldo and Mancini, 2018] it can be concluded that the partial safety factor method, global resistance factor method and the ECOV method all provide a sufficient level of reliability while presenting the correct failure mode for a given example. However it can also be concluded that specific concrete examples can present more than one failure mode making it hard to ensure structural reliability. This is especially true when using randomization to generate material input parameters for a given example. In conclusion it can be said about the nonlinear design methods that as long as the reinforced concrete structures are simple any of the presented failure modes will present the correct failure mode. Furthermore it can also be concluded that only very specific reinforced concrete examples present more than one failure mode. This is clear due to the T-beam in this report and the T-beam in [Castaldo and Mancini, 2018] being designed to have the same material and model inputs. Nonetheless the outcomes with regard to failure modes are different.

Bibliography

- Castaldo and Mancini, 2018.** Diego Gino Castaldo and Giuseppe Mancini. *Safety formats for non-linear finite element analysis of reinforced concrete structures: Discussion, Comparison and Proposals*. Department of Structural, Geotechnical and Building Engineering (Diseg), Politecnico di Torino, 2018.
- Cervenka, 2013.** Vladimir Cervenka. *Reliability-based non-linear analysis according to fib Model Code 2010*. Ernst & Sohn Verlag für Architektur und technische Wissenschaften GmbH & co, 14(1), 19–28, 2013.
- Cervenka and Červenka, 2015.** Vladimír Cervenka and Jan Červenka. *ATENA Program documentation Part 2-1 - User's Manual for ATENA 2D*, 2015. URL <https://www.cervenka.cz>.
- Havlásek and Pukl, 2017.** Petr Havlásek and Radomír Pukl. *Sara Documentation - Sara Engineering - Sara Studio - User's Manual*, 2017. URL <https://www.www.cervenka.cz>.
- Kh, 2020.** Hind M. Kh. *A Review on Nonlinear Finite Element Analysis of Reinforced Concrete Beams Retrofitted with Fiber Reinforced Polymers*, 2020. URL https://www.researchgate.net/figure/Typical-stress-strain-curve-for-concrete-45_fig4_315716360.
- Krenk, 2009.** Steen Krenk. *Non-linear Modeling and Analysis of Solids and Structures*. ISBN: 978-0-511-60151-4, eBook. Cambridge University Press, 1. udgave edition, 2009.
- Standard, 1990.** Dansk Standard. *DS/EN1990-2002: Eurocode - Basis of structural design*, 1990.
- Standard, 1992.** Dansk Standard. *DS/EN1990-2: Eurocode - Design of concrete structures*, 1992.
- Vonk, 1992.** René Alfred Vonk. *Softening of concrete loaded in compression*. Technische Universiteit Eindhoven, 1st edition, 1992. ISBN 90-386-Q062-3.
- Łukasz Skotny, 2020.** Łukasz Skotny. *Geometrically nonlinear analysis – how does it work?*, 2020. URL <https://enterfea.com/geometrically-nonlinear-analysis-introduction/>.

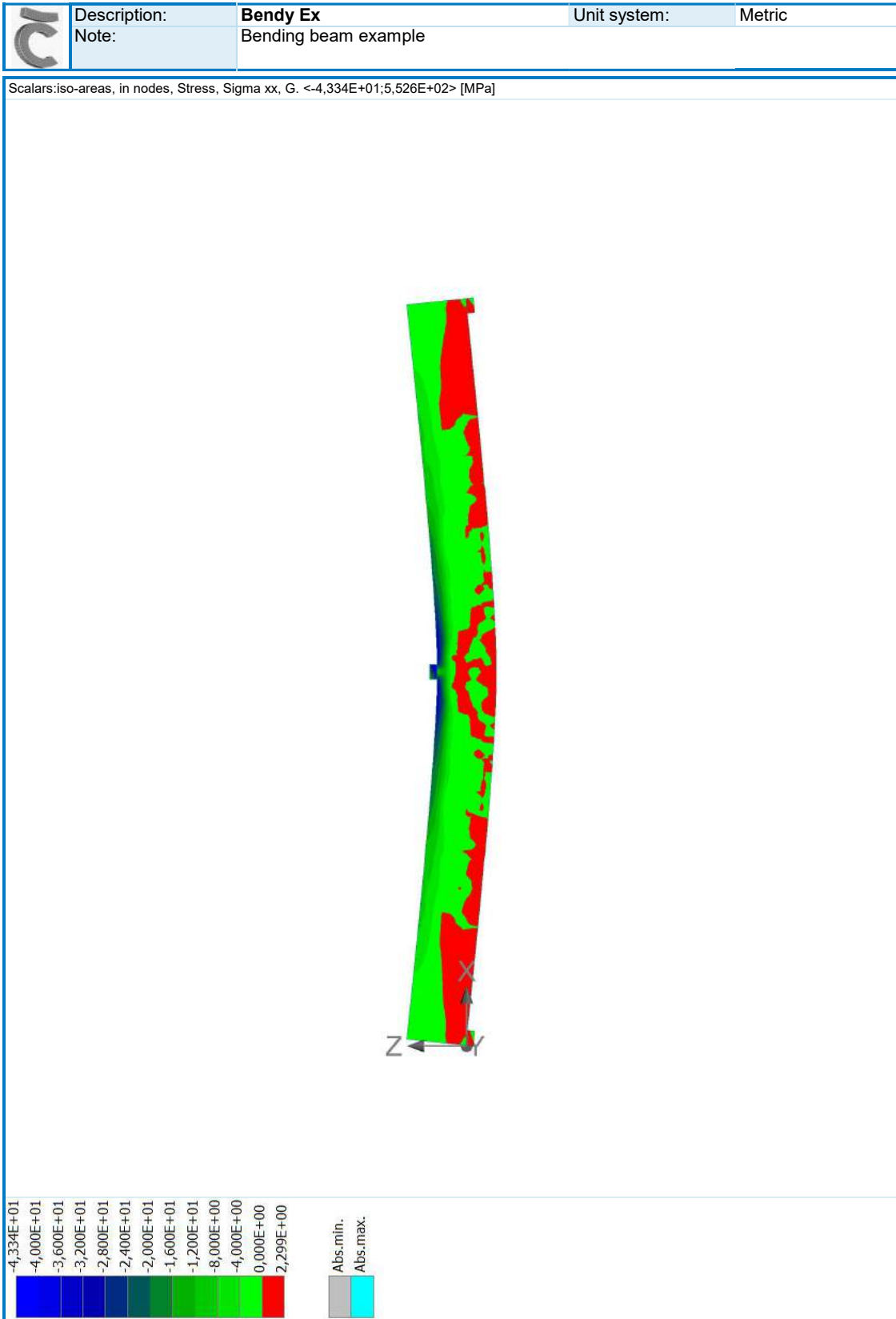


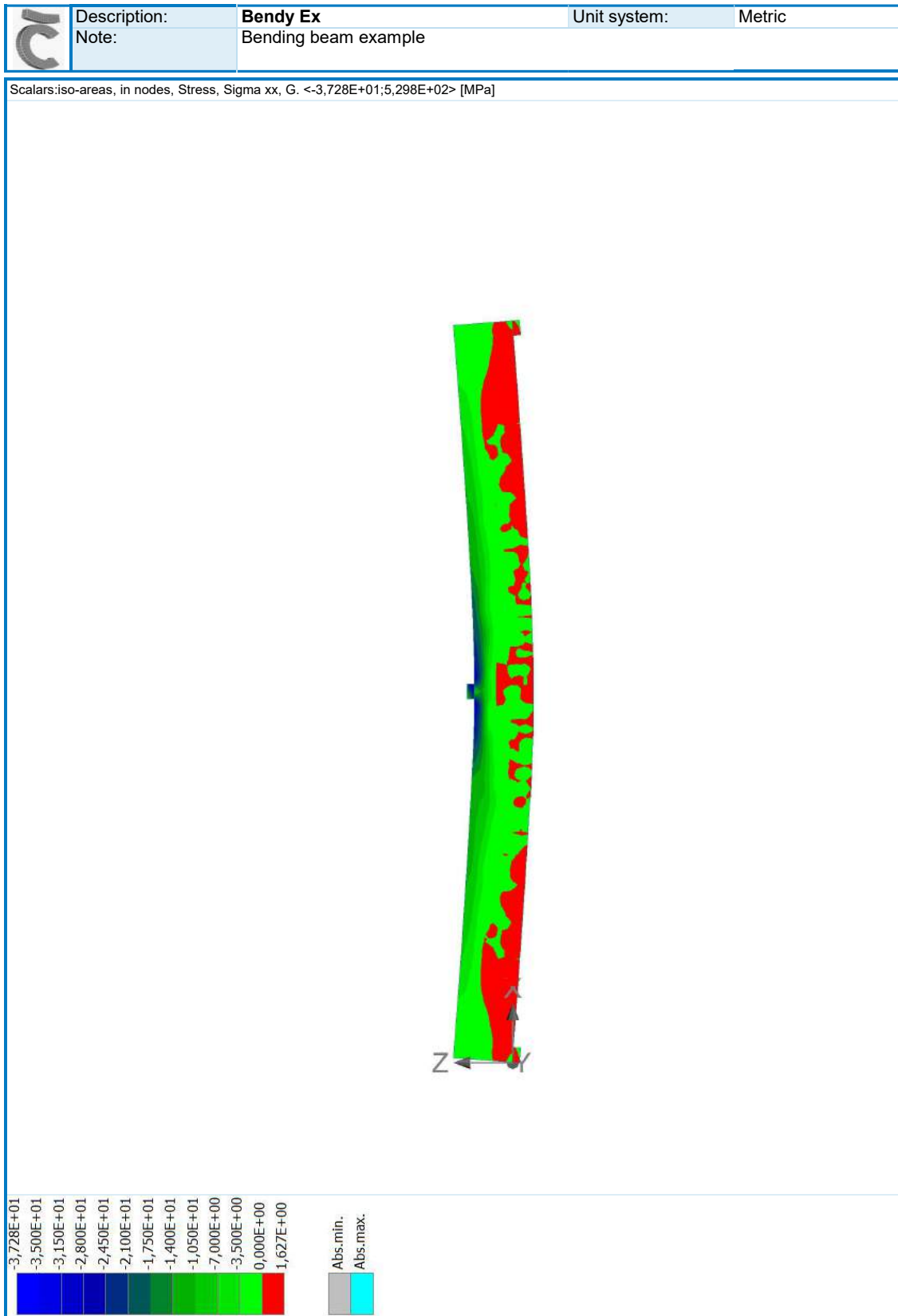
Appendix

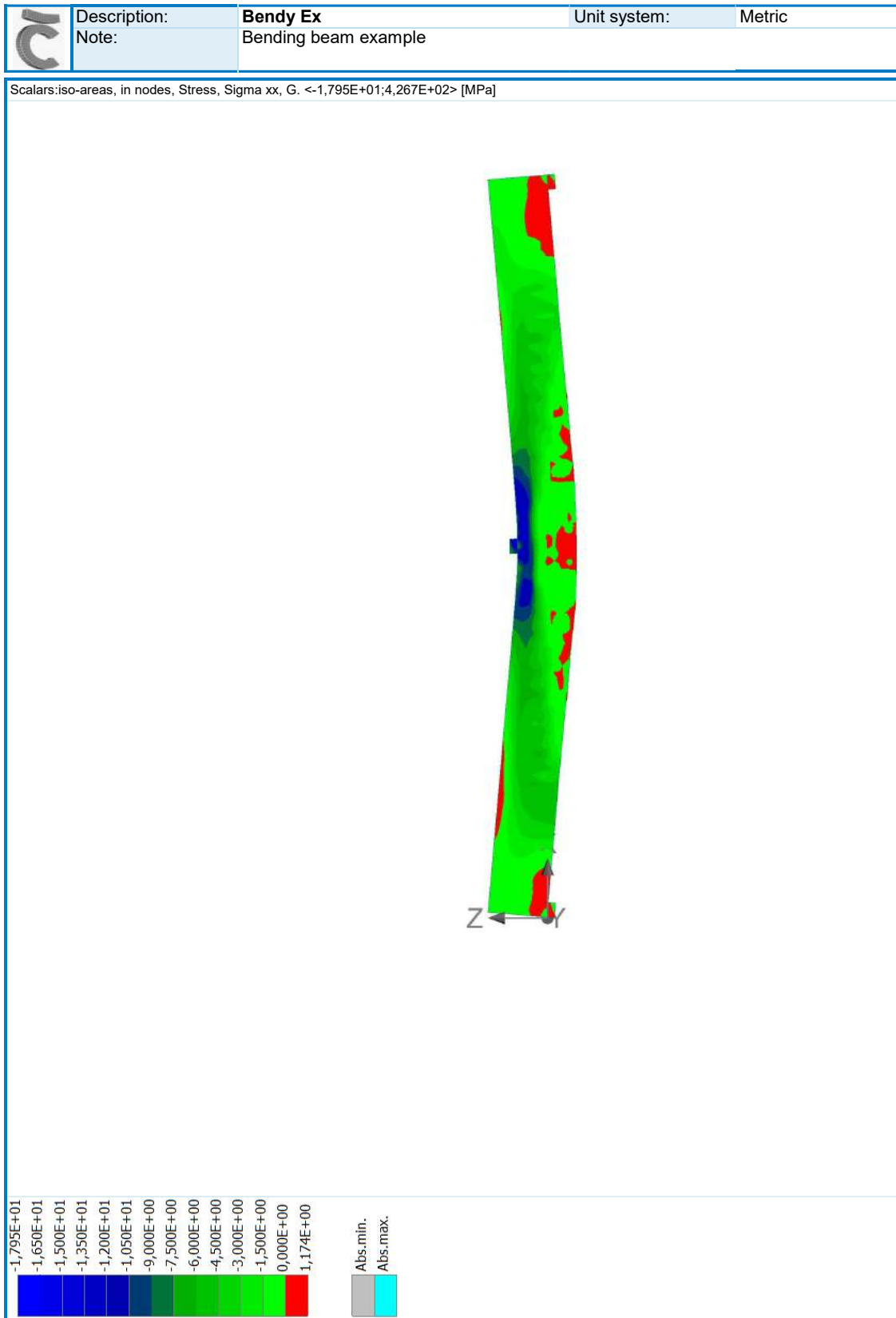
- A** **Atena 3D models for Rectangular beam** 53
- B** **SARA LHS results for both beams** 63

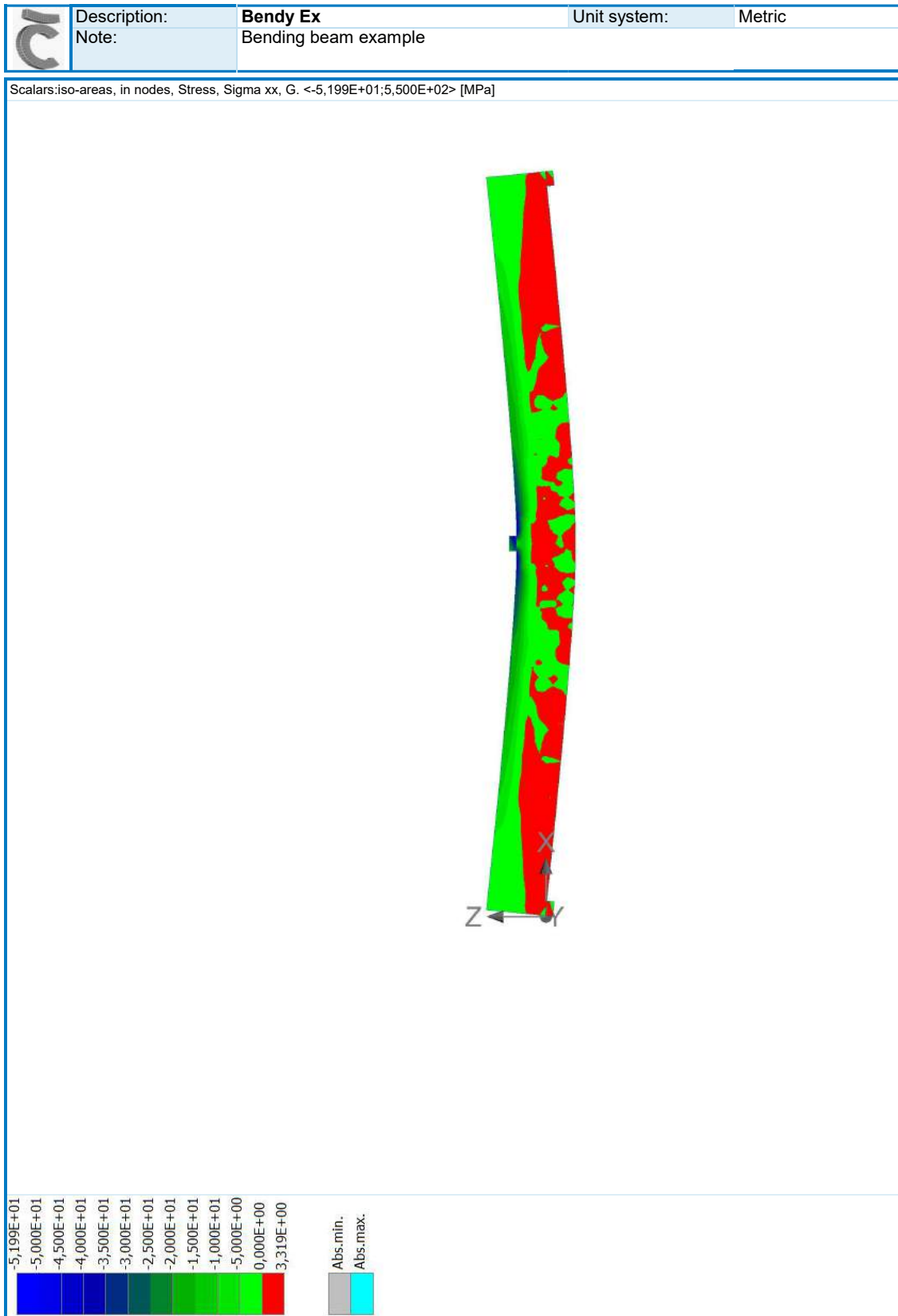
A. Atena 3D models for Rectangular beam

As explained in Chapter 4 the initial models from ATENA 3D are presented below. These models include C25-C40-C50 using Mean, Characteristic and Design values for material resistance parameters. All models are on the Rectangular beam example. It should be noted that the ATENA 3D models illustrate compression as blue/green and tension as red.



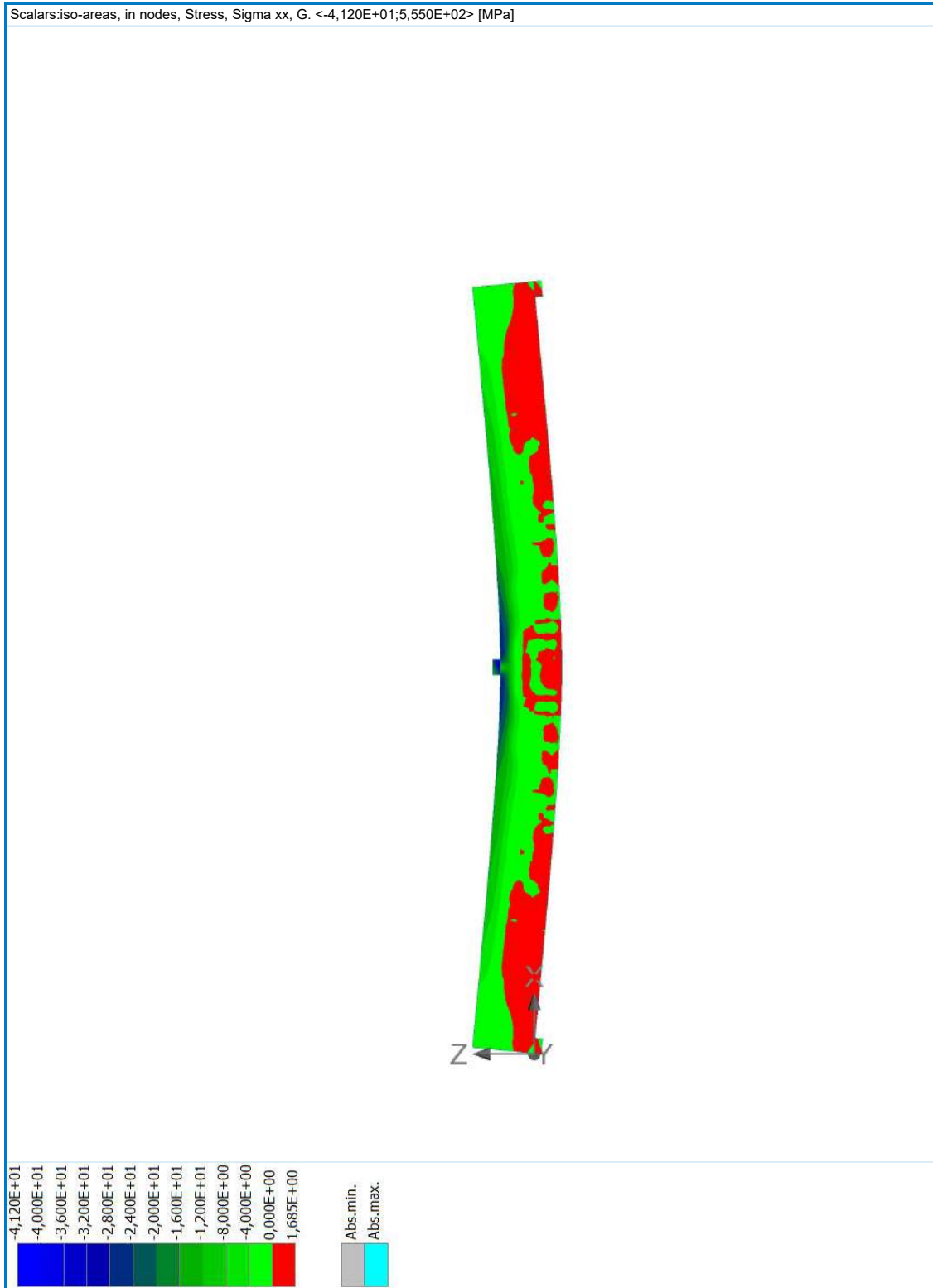




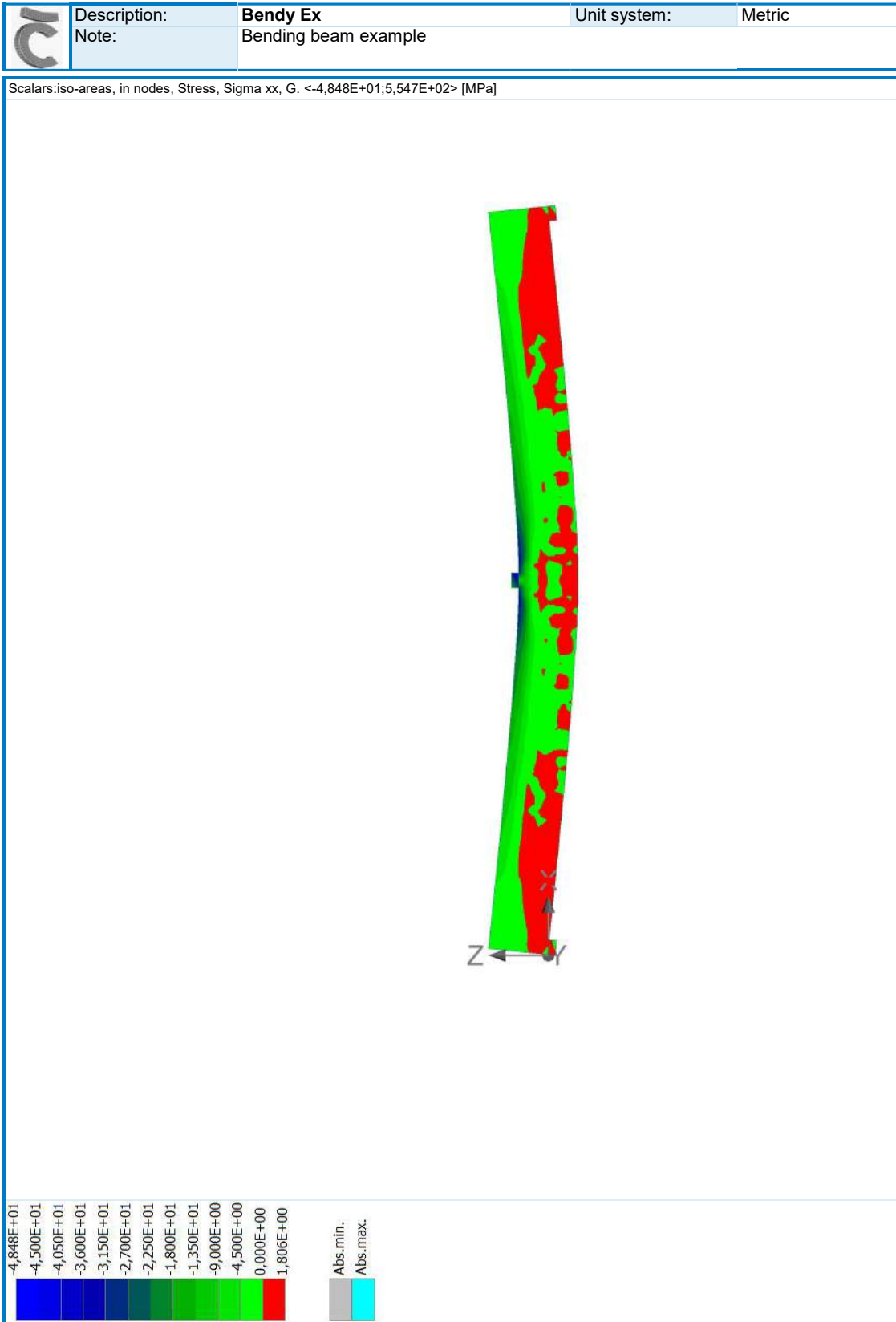




	Description:	Bendy Ex	Unit system:	Metric
	Note:	Bending beam example		



[Atena - ATENA 3D | version 5.6.1.0 | Copyright (c) 2017 Cervenka Consulting All Rights Reserved | www.cervenka.cz]



	Description:	Bendy Ex	Unit system:	Metric
	Note:	Bending beam example		



[Atena - ATENA 3D | version 5.6.1.0 | Copyright (c) 2017 Cervenka Consulting All Rights Reserved | www.cervenka.cz]

B. SARA LHS results for both beams

In this appendix all of the results for the probabilistic method performed in SARA are illustrated. This results in 30 results for each beam which are all numbered by sample number 1-30 and illustrated below. Figures B.0.1-B.0.30 are for the Rectangular beam while Figures B.0.31-B.0.60 are for the T-beam.



Figure B.0.1: Rectangular beam Sample no. 1.



Figure B.0.2: Rectangular beam Sample no. 2.



Figure B.0.3: Rectangular beam Sample no. 3.

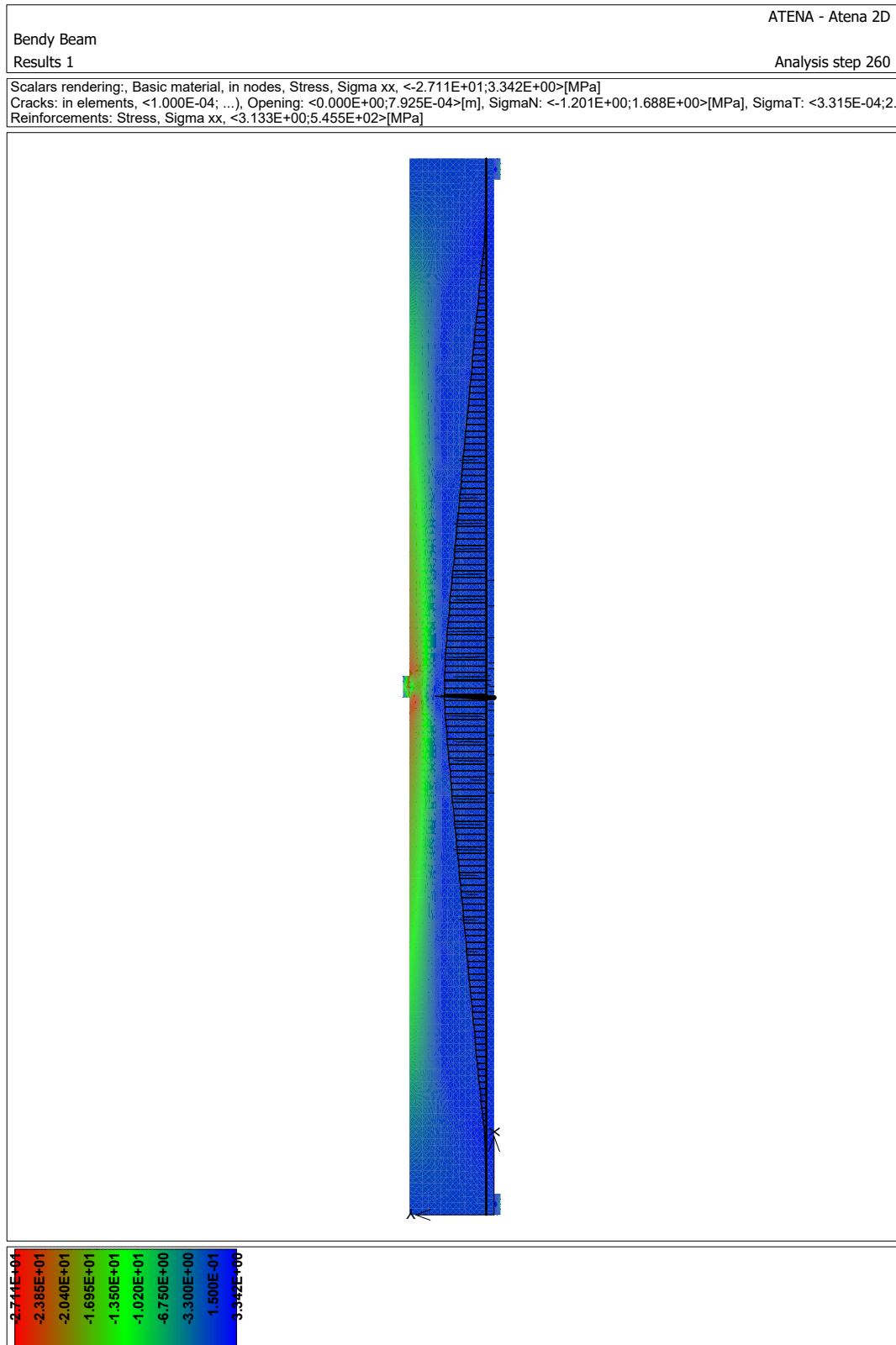


Figure B.0.4: Rectangular beam Sample no. 4.

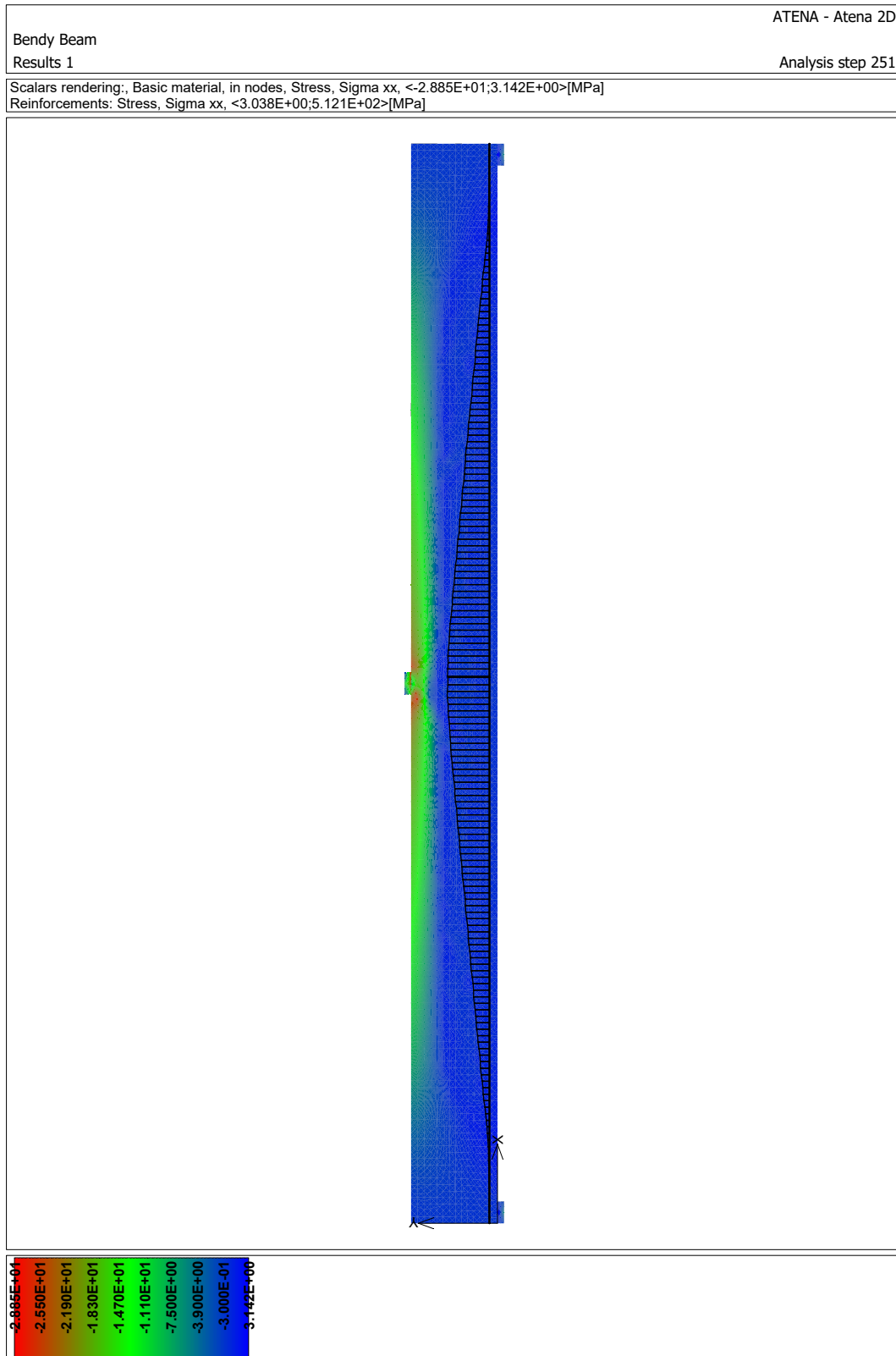


Figure B.0.5: Rectangular beam Sample no. 5.

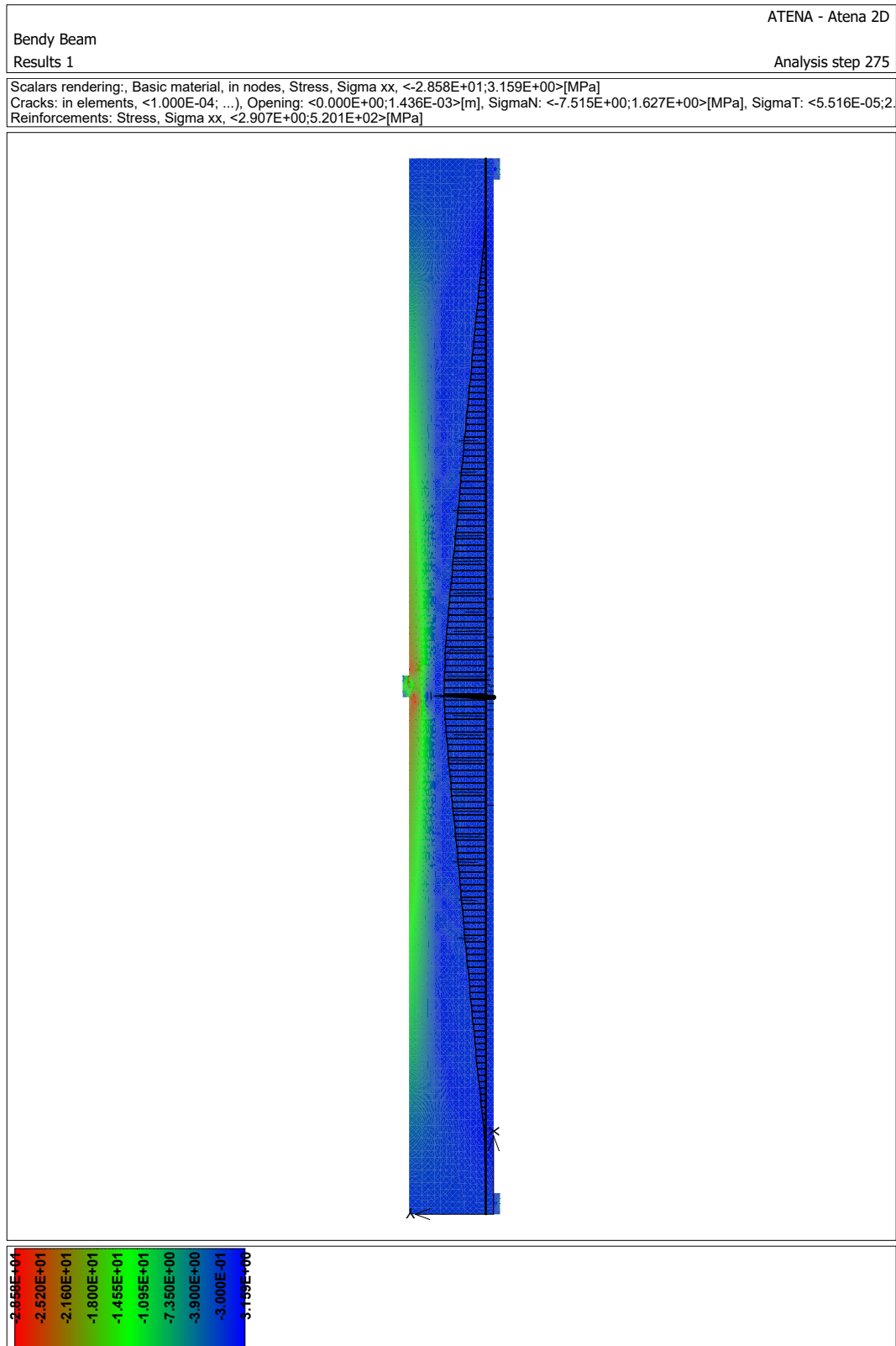


Figure B.0.6: Rectangular beam Sample no. 6.

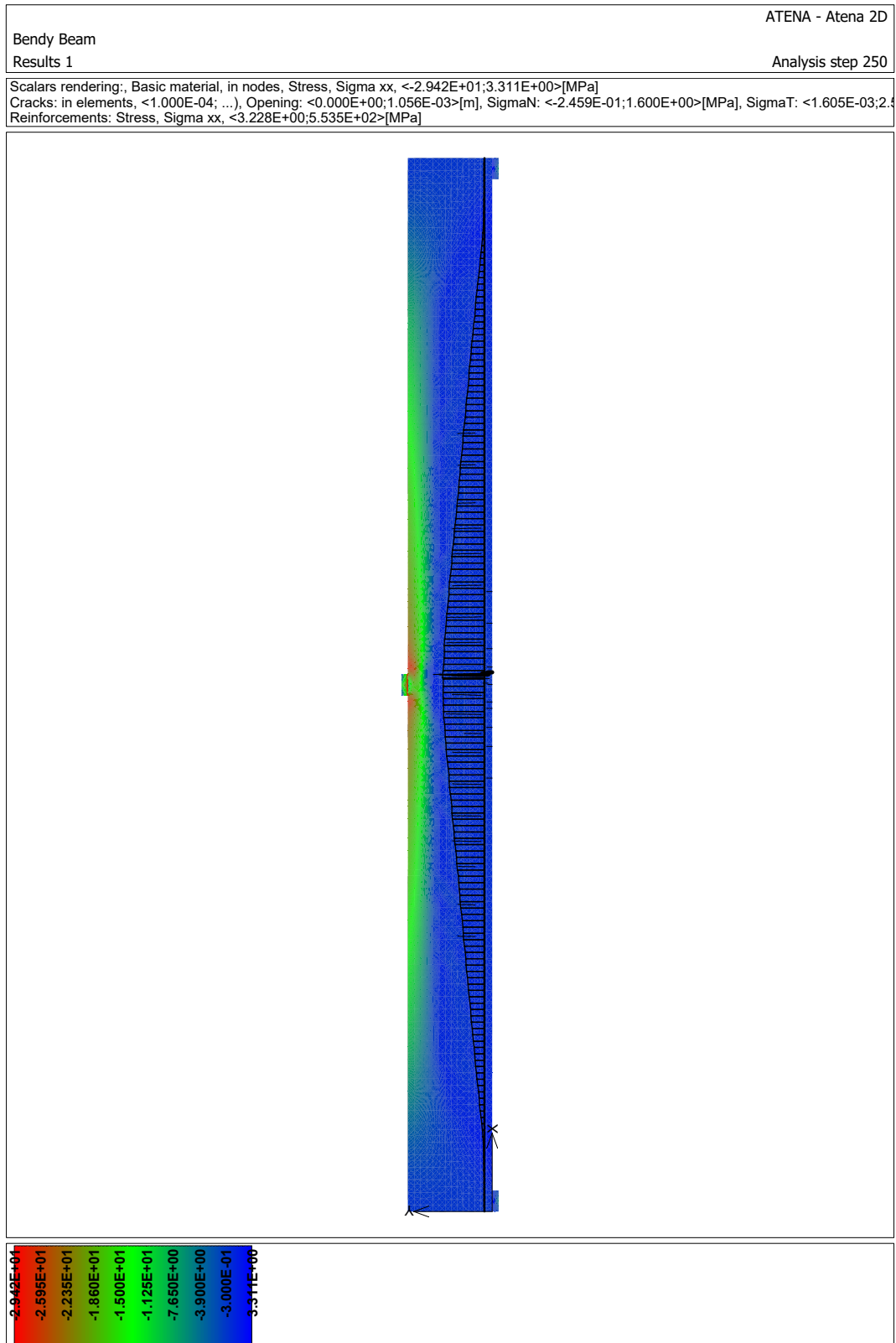


Figure B.0.7: Rectangular beam Sample no. 7.

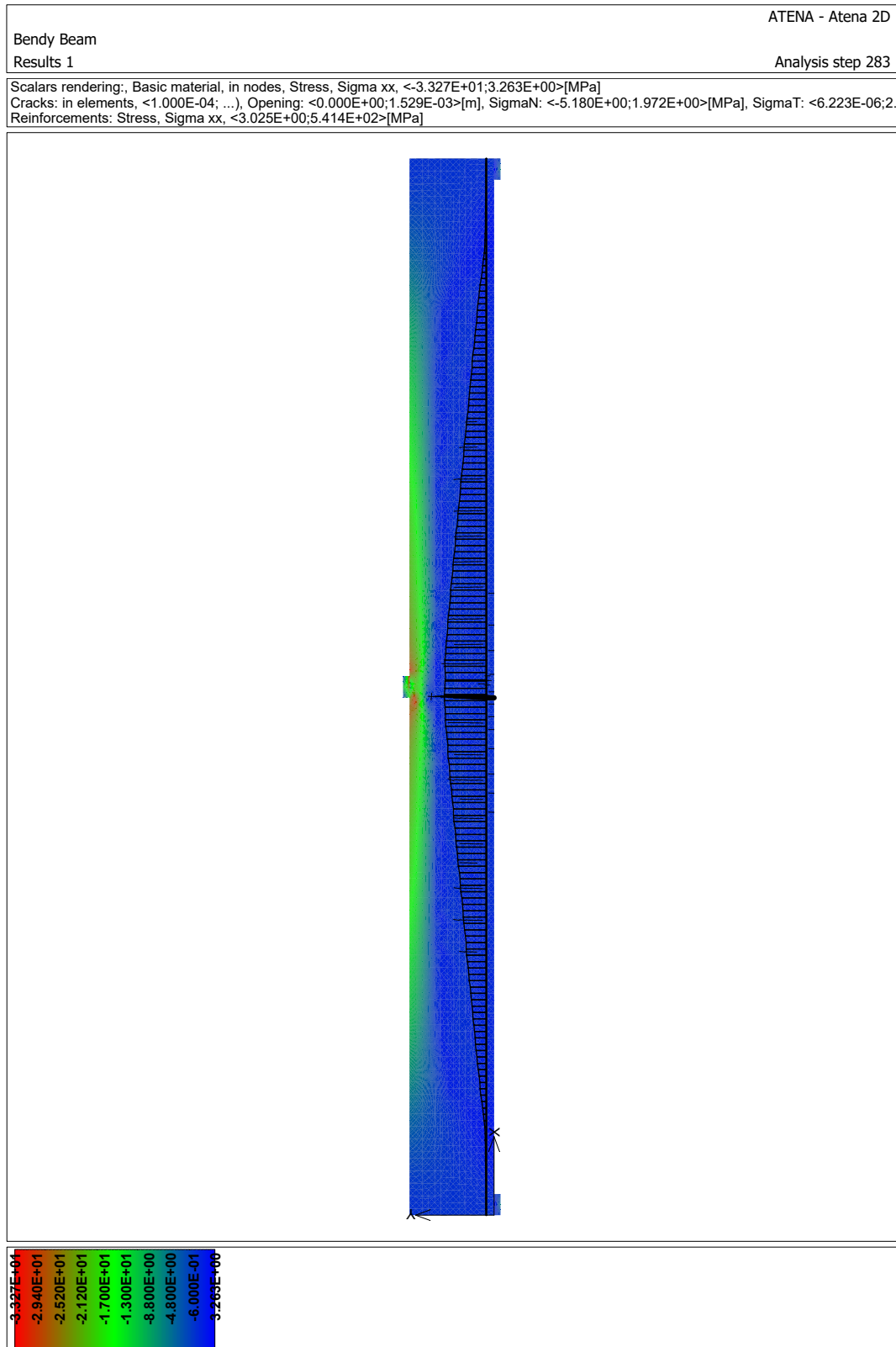


Figure B.0.8: Rectangular beam Sample no. 8.

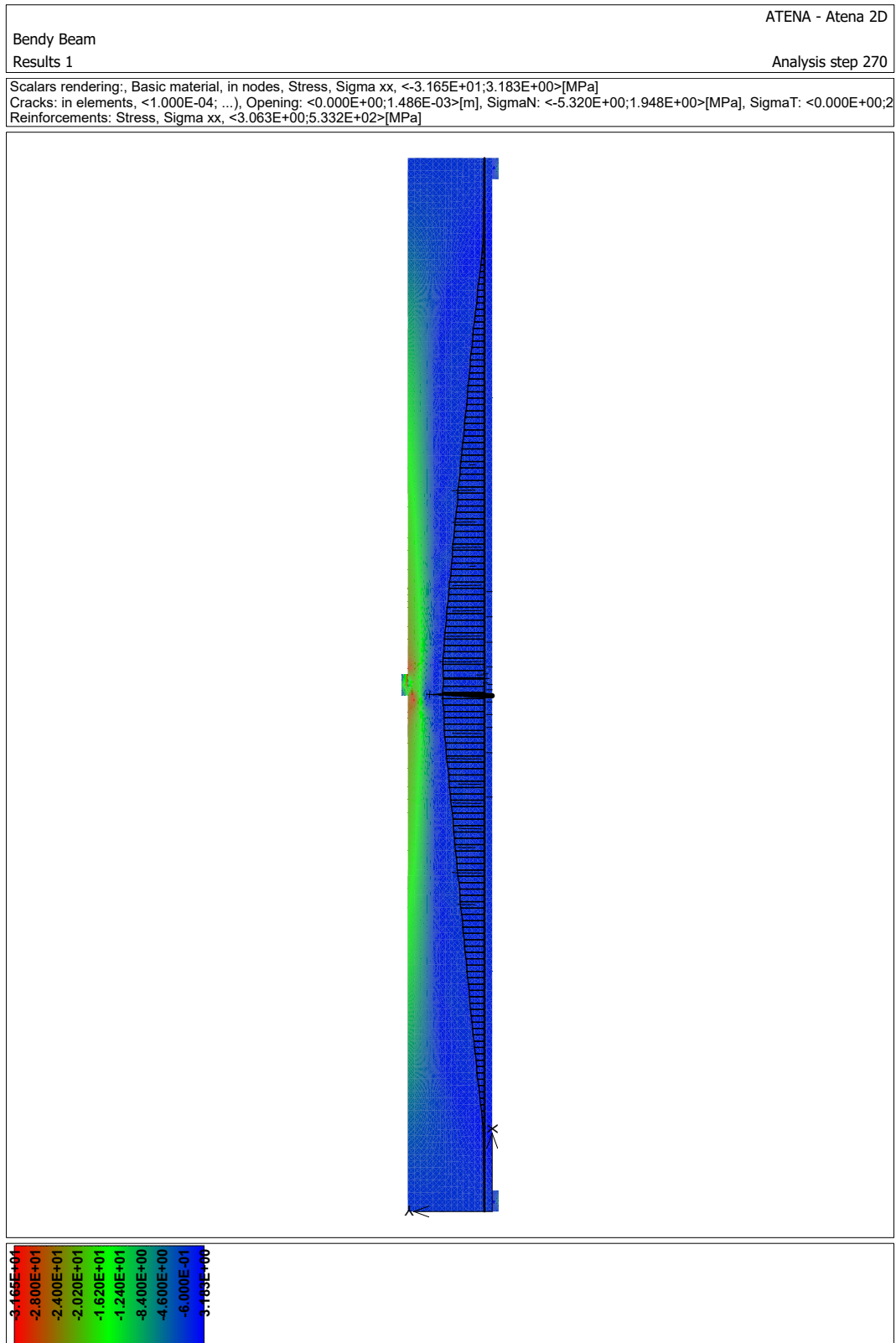


Figure B.0.9: Rectangular beam Sample no. 9.

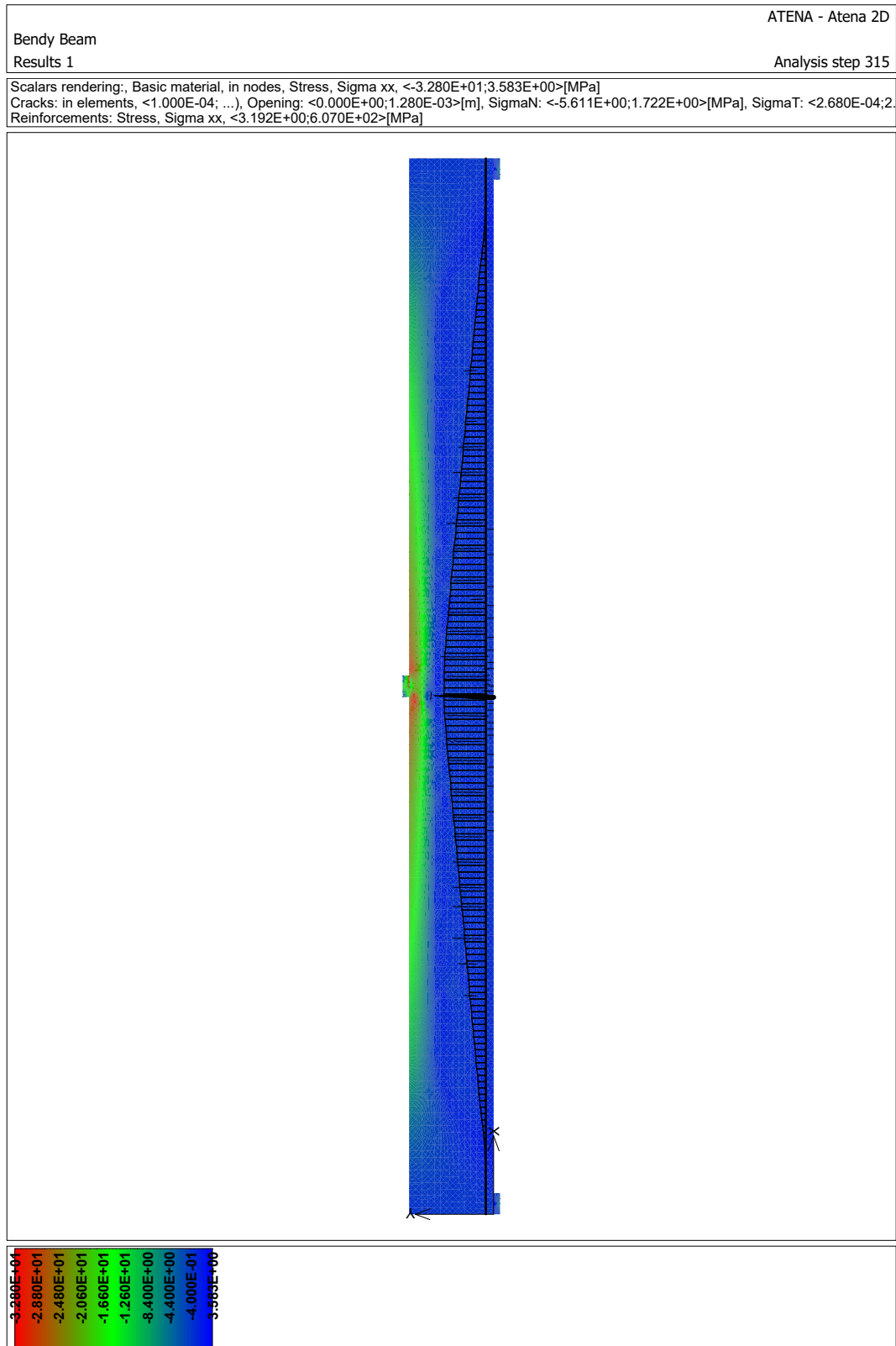


Figure B.0.10: Rectangular beam Sample no. 10.



Figure B.0.11: Rectangular beam Sample no. 11.

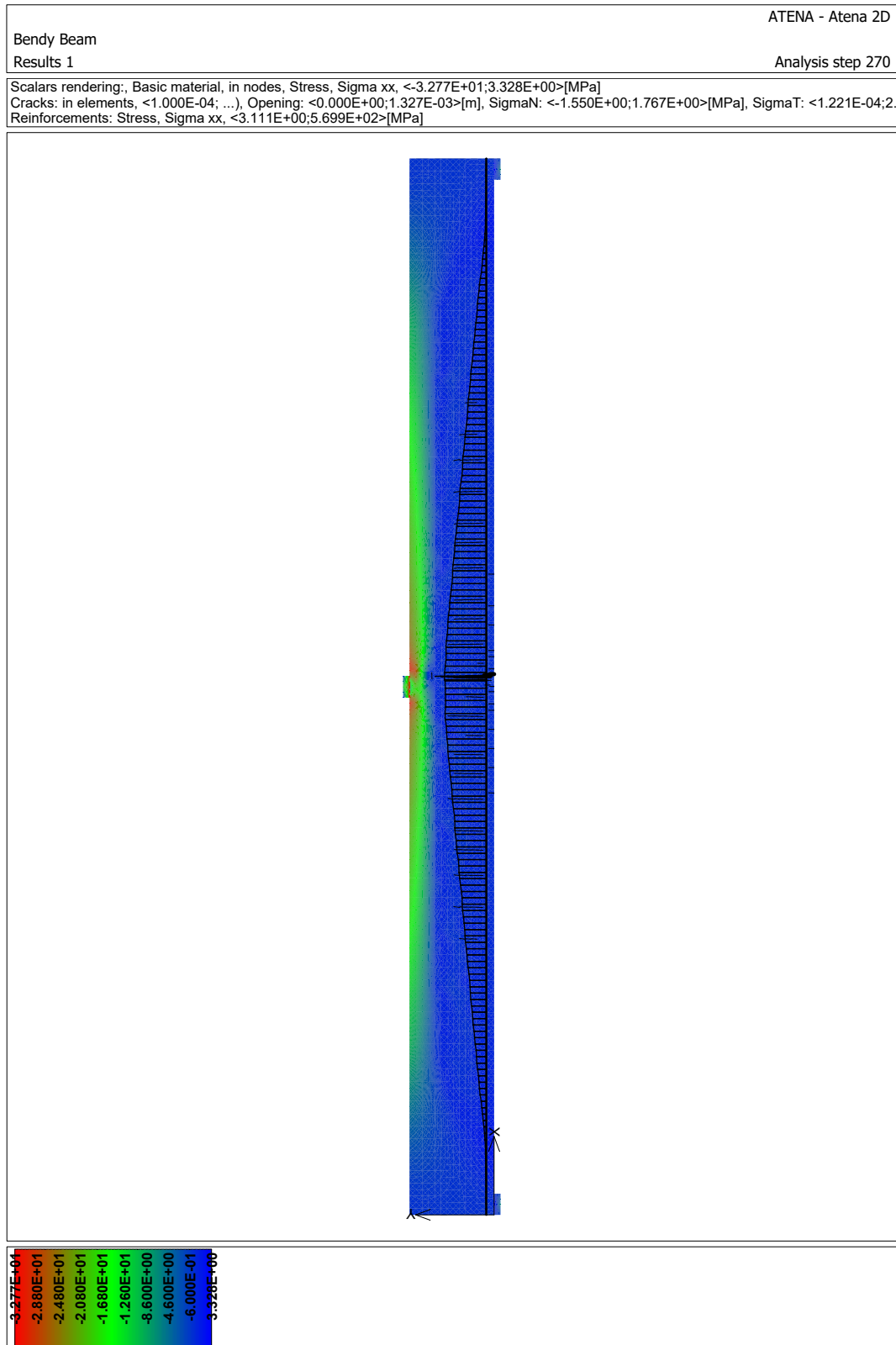


Figure B.0.12: Rectangular beam Sample no. 12.

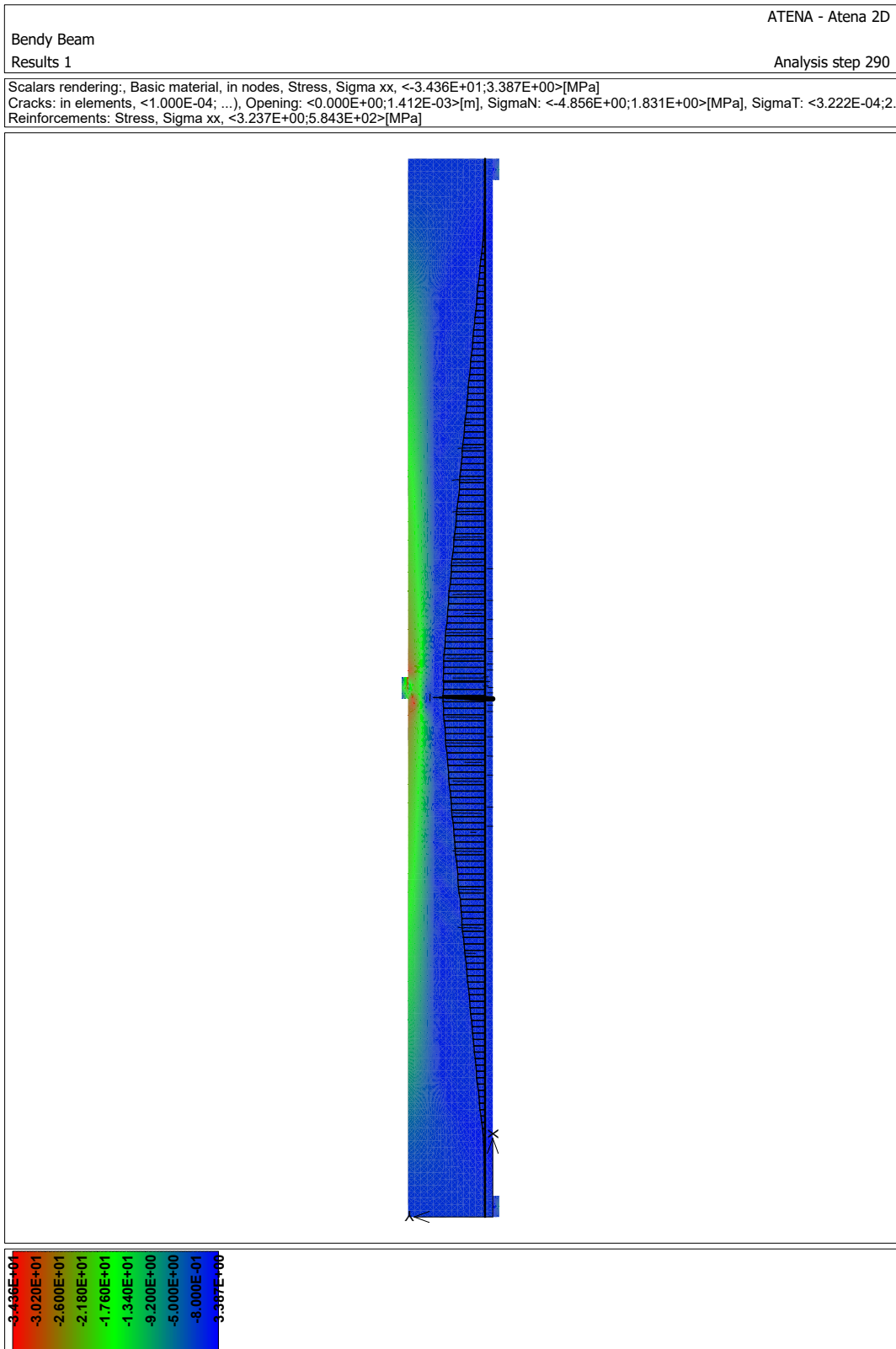


Figure B.0.13: Rectangular beam Sample no. 13.

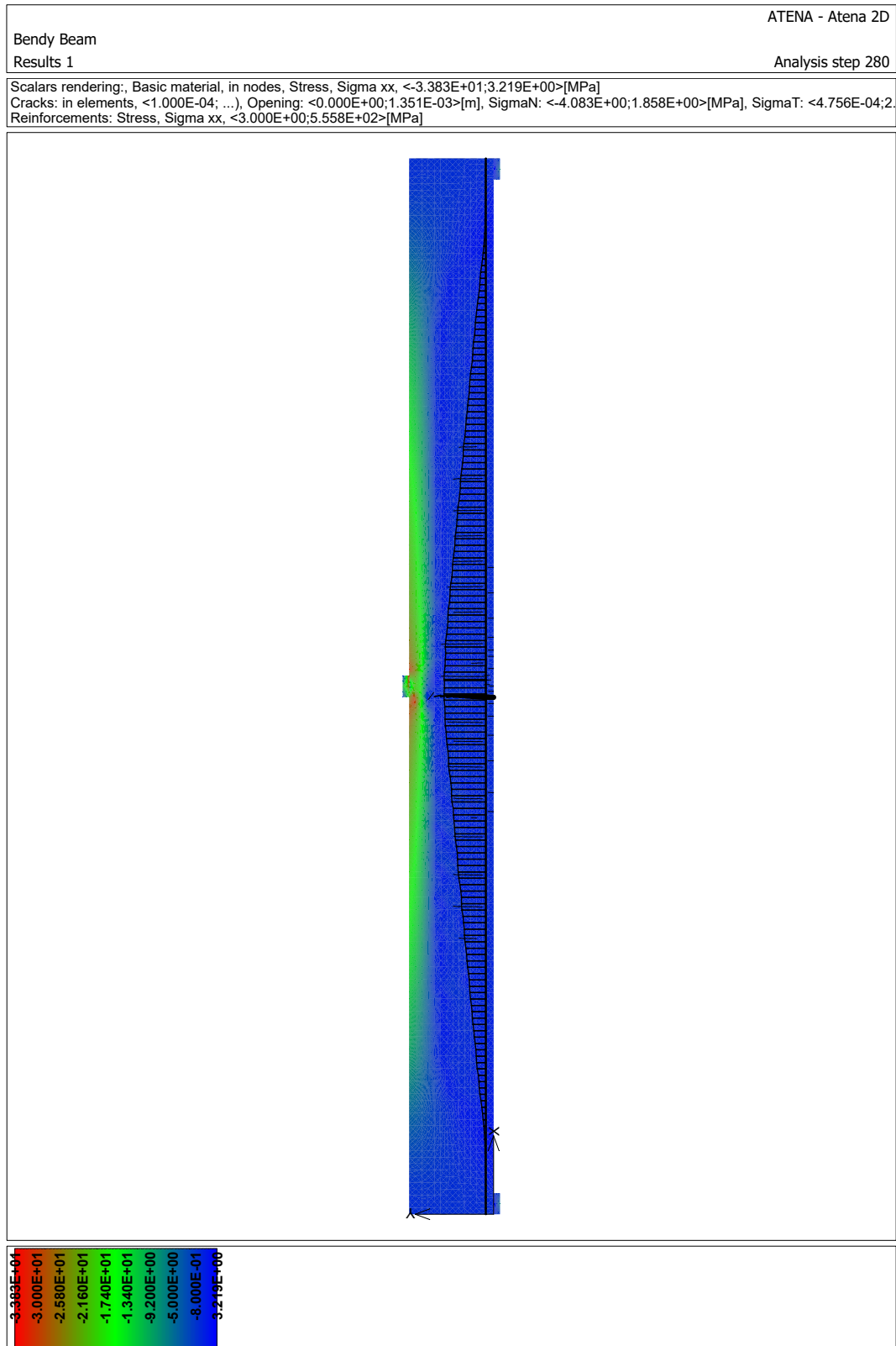


Figure B.0.14: Rectangular beam Sample no. 14.

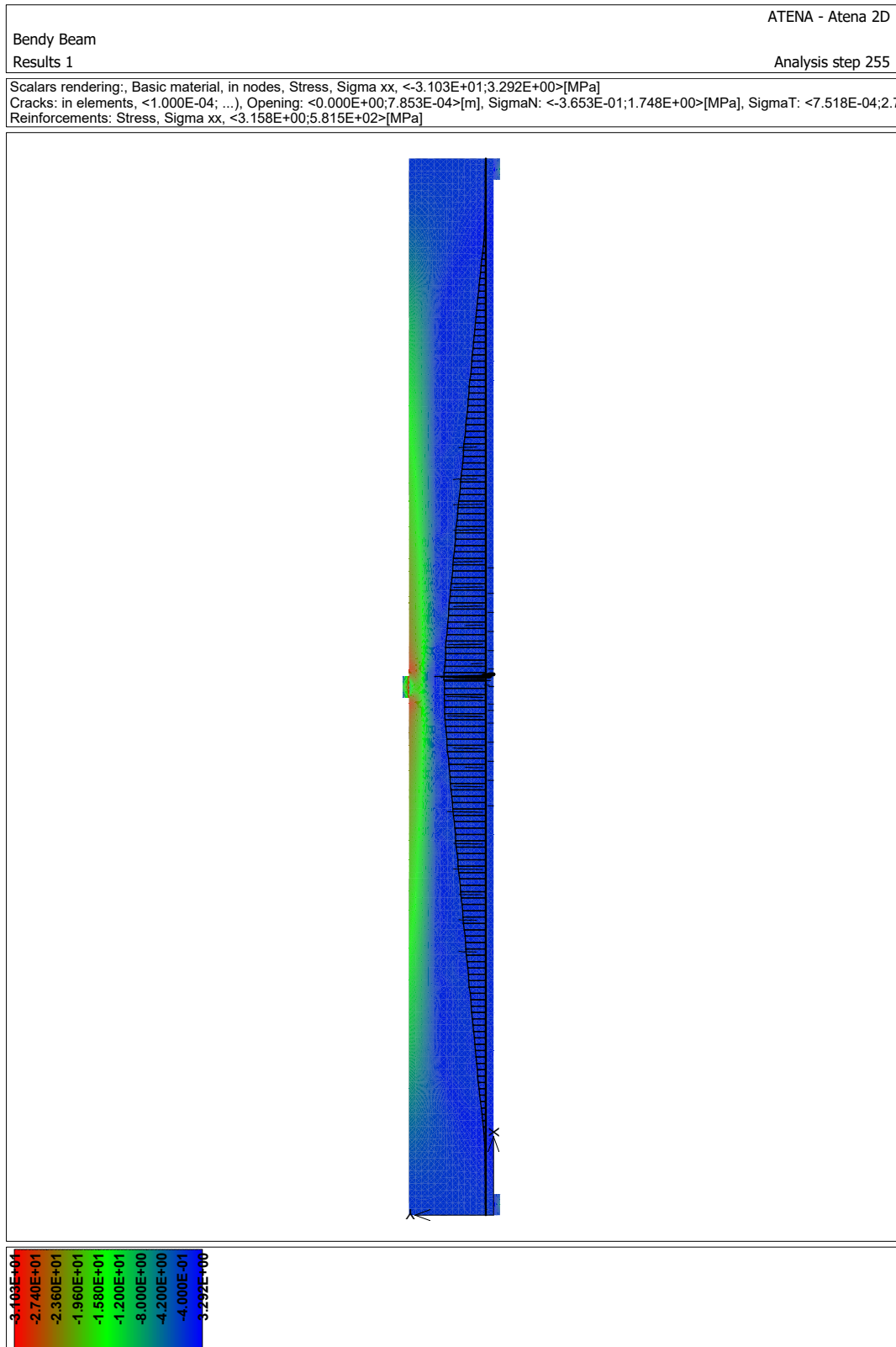


Figure B.0.15: Rectangular beam Sample no. 15.

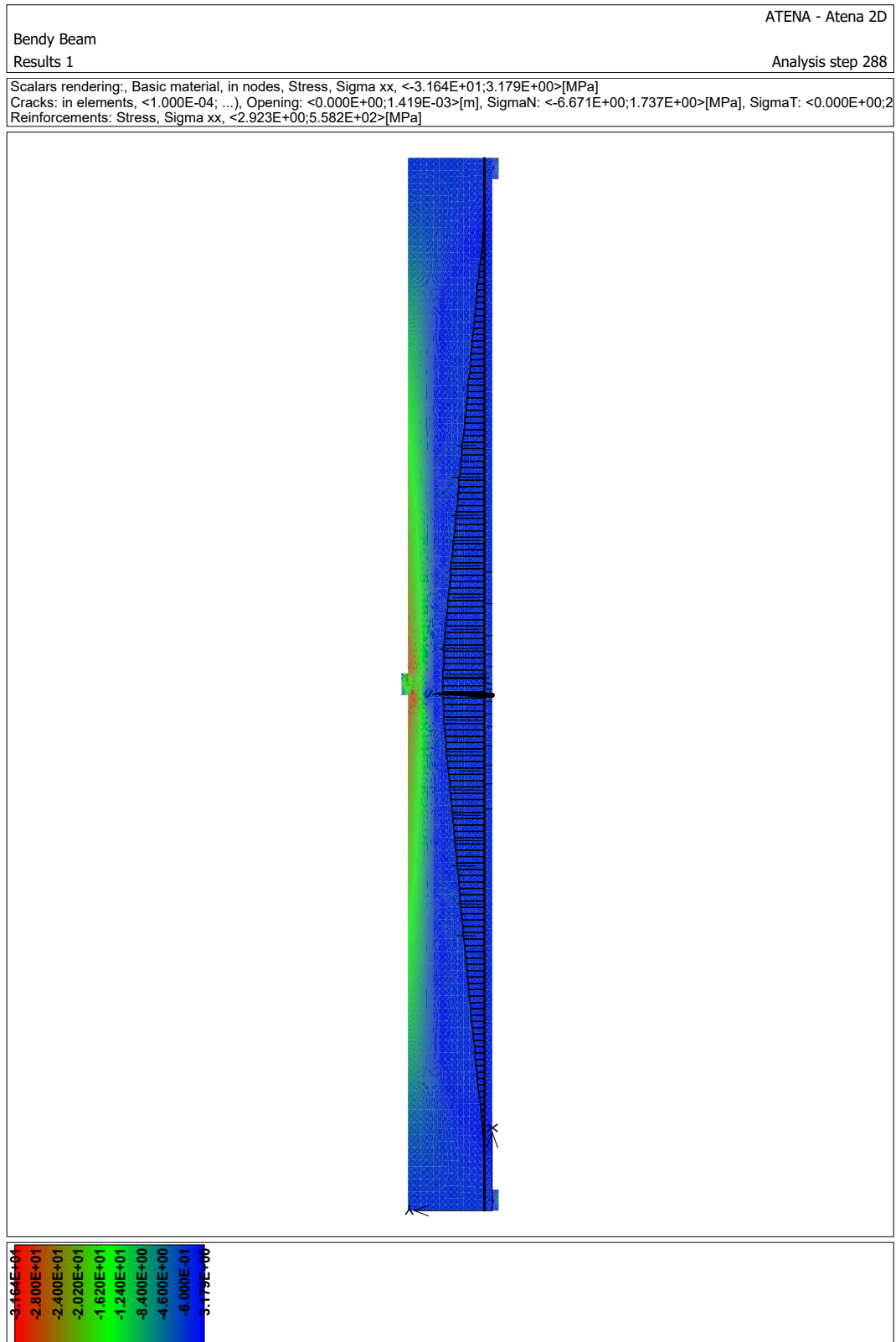


Figure B.0.16: Rectangular beam Sample no. 16.

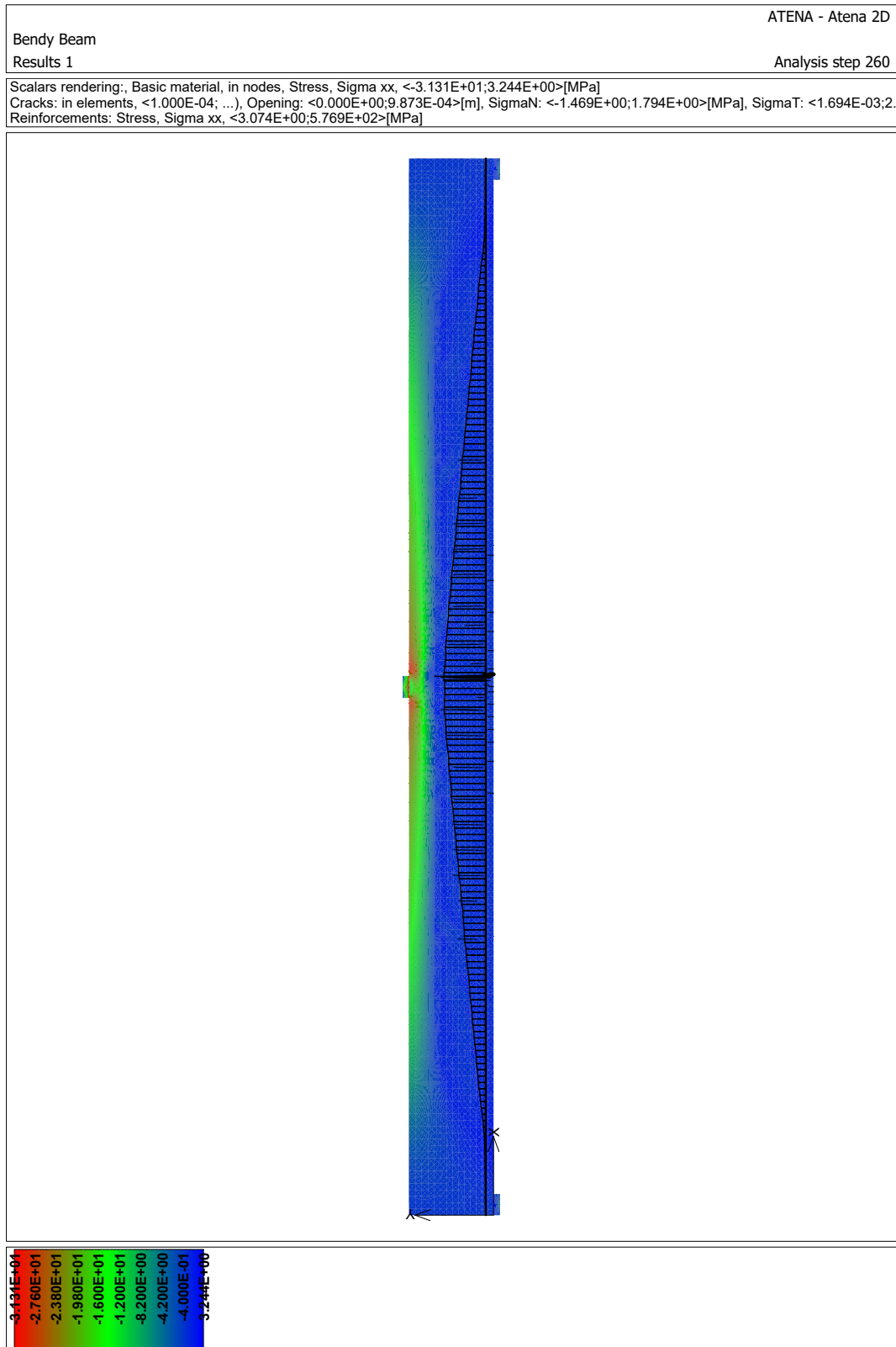


Figure B.0.17: Rectangular beam Sample no. 17.

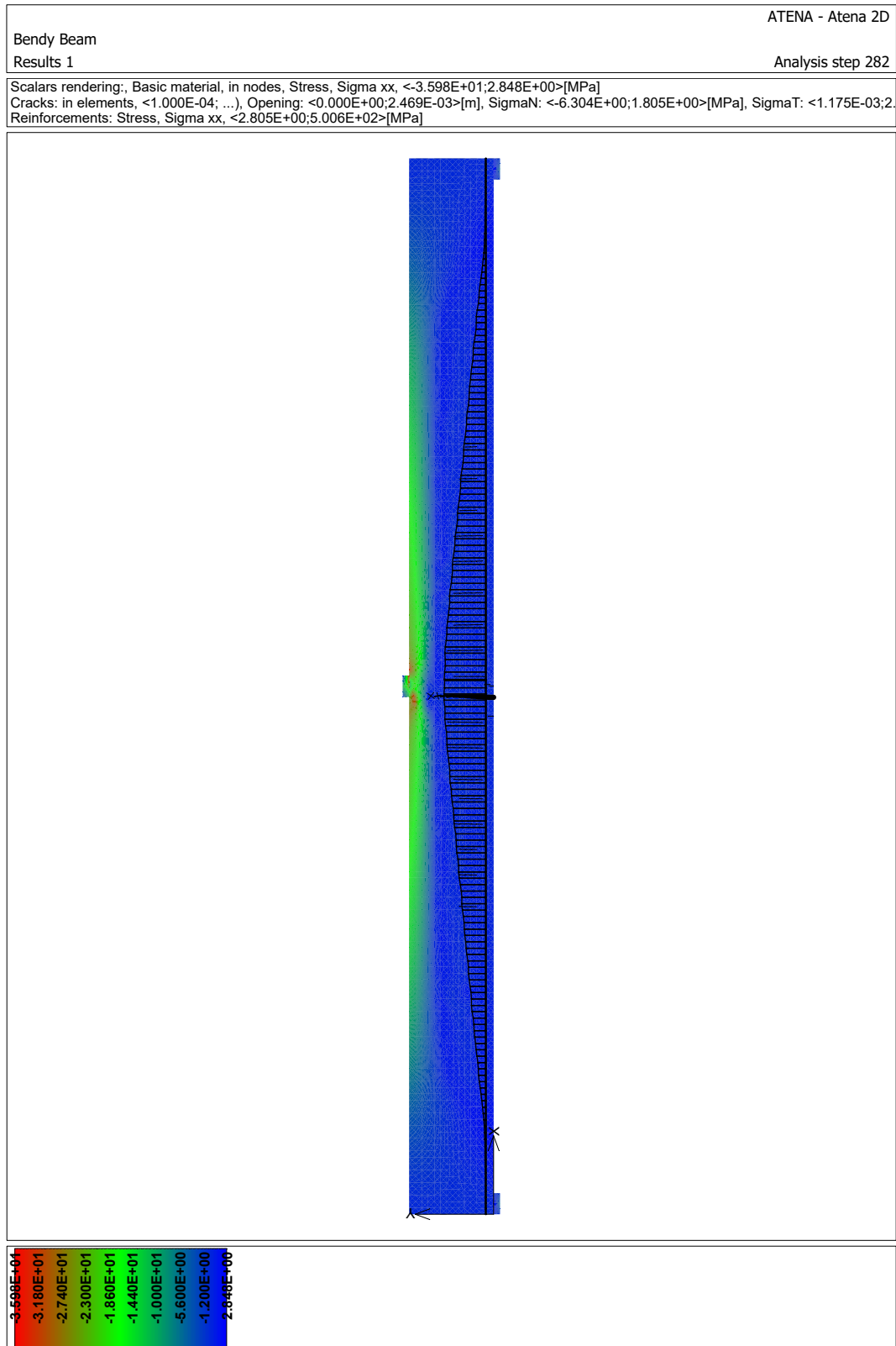


Figure B.0.18: Rectangular beam Sample no. 18.

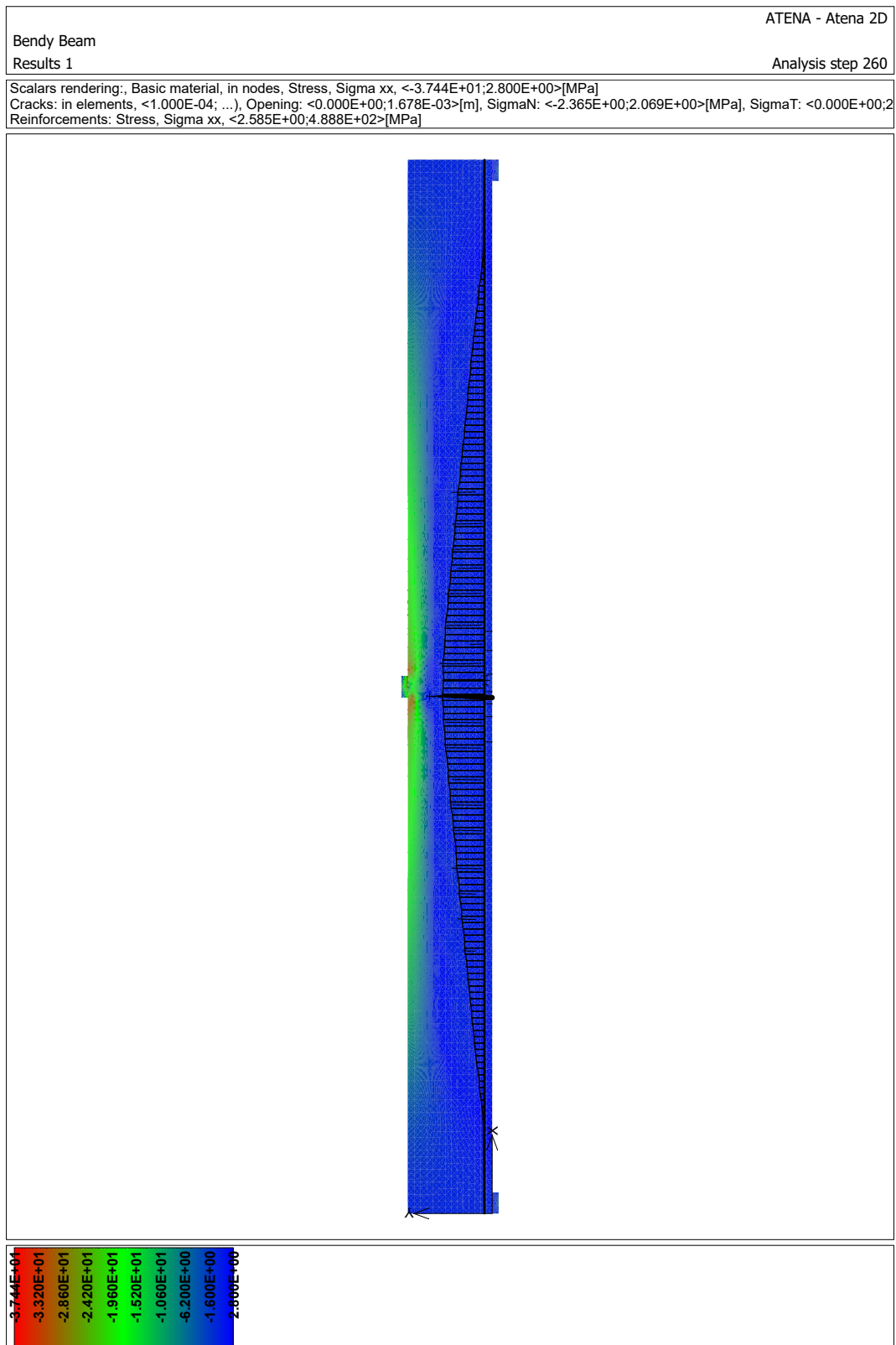


Figure B.0.19: Rectangular beam Sample no. 19.

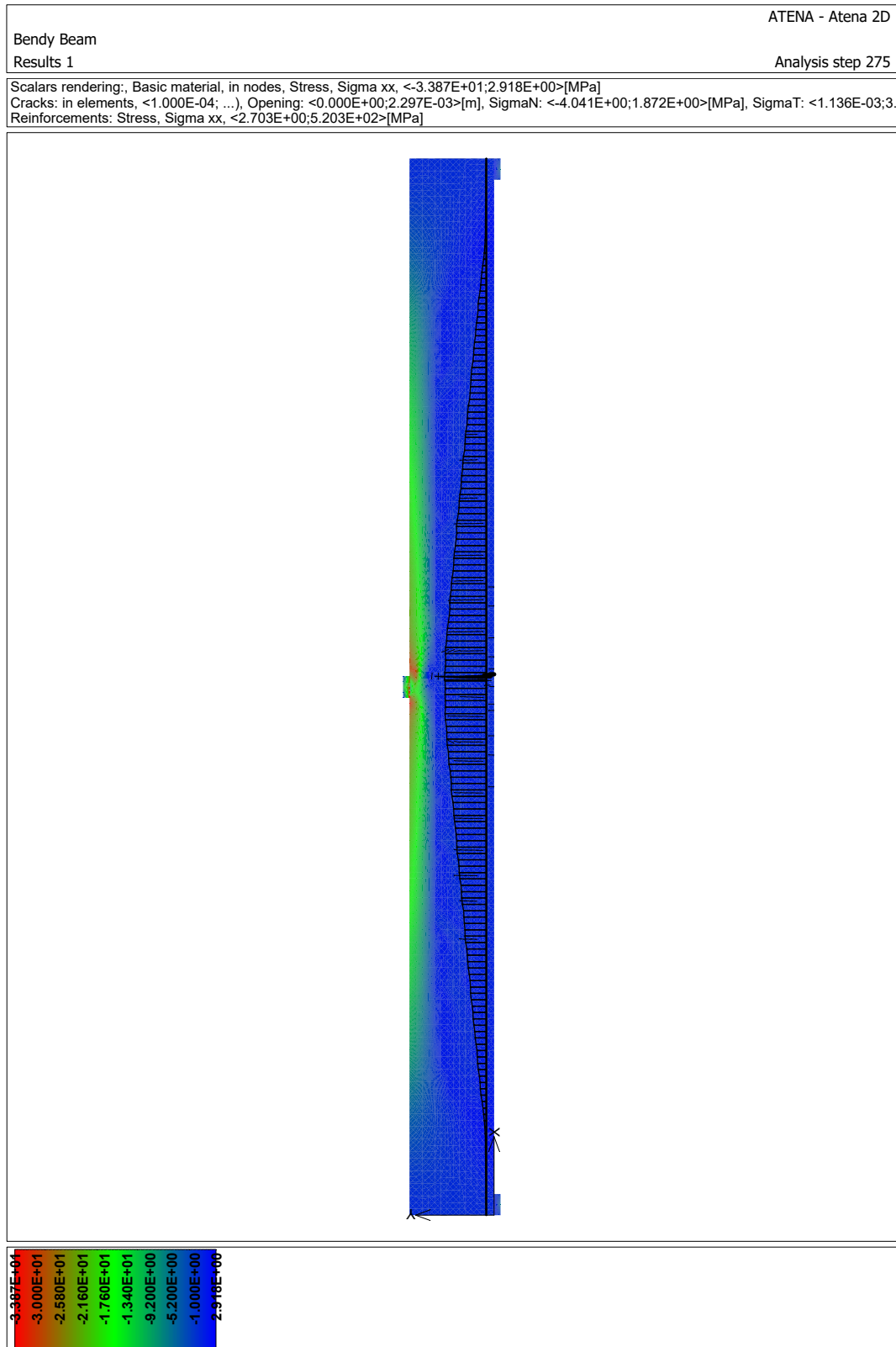


Figure B.0.20: Rectangular beam Sample no. 2o.

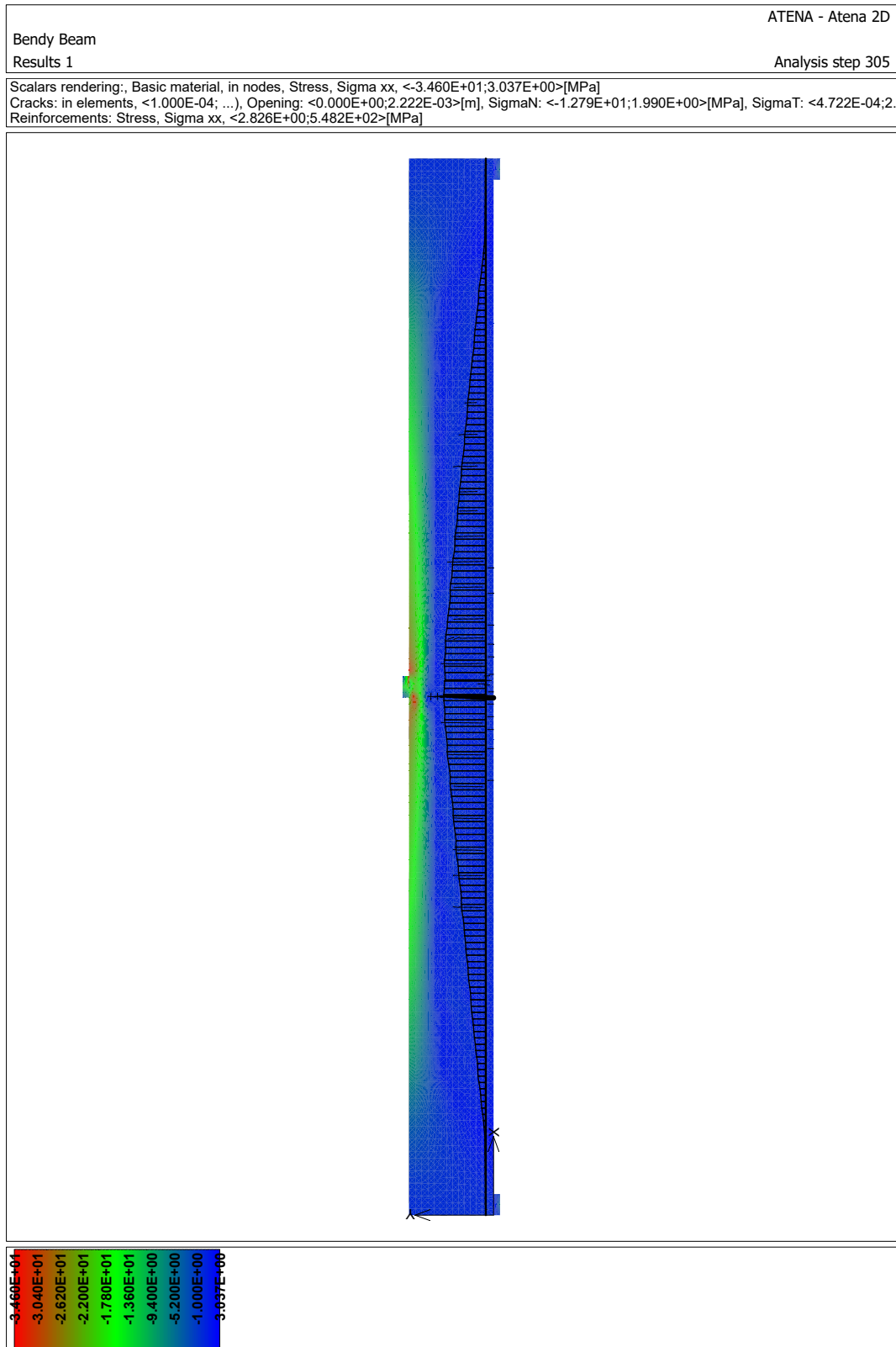


Figure B.0.21: Rectangular beam Sample no. 21.

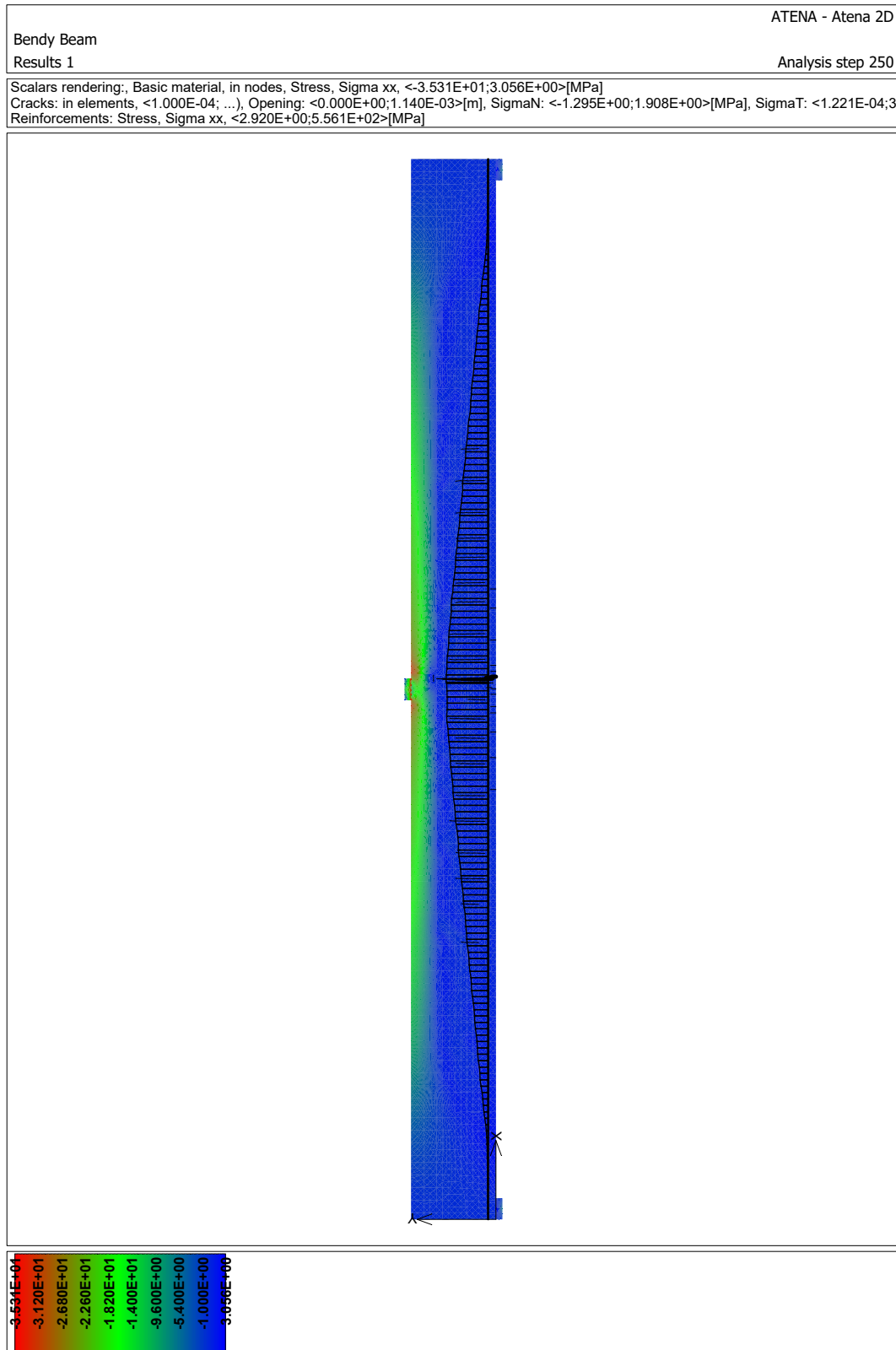


Figure B.0.22: Rectangular beam Sample no. 22.

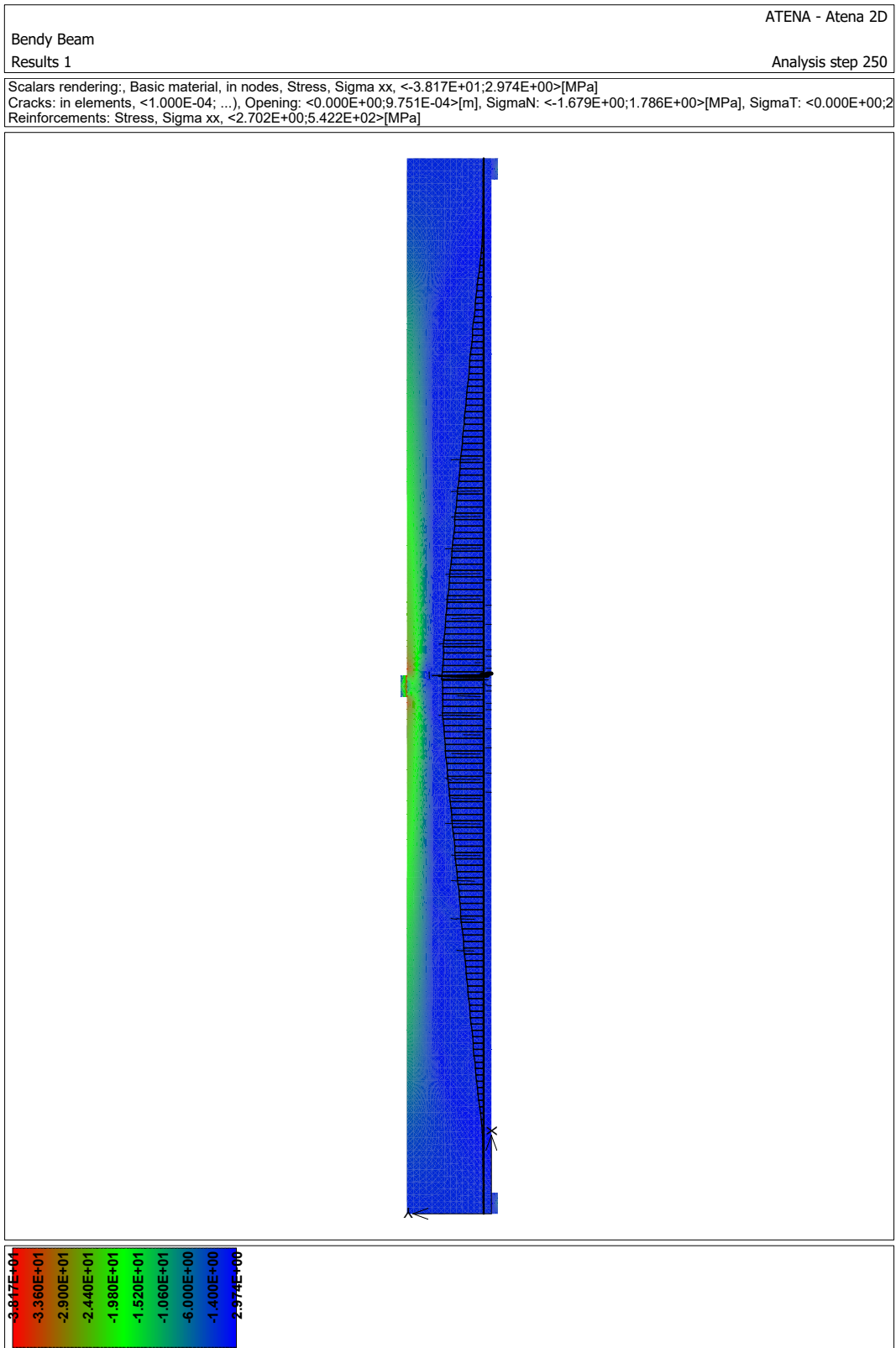


Figure B.0.23: Rectangular beam Sample no. 23.

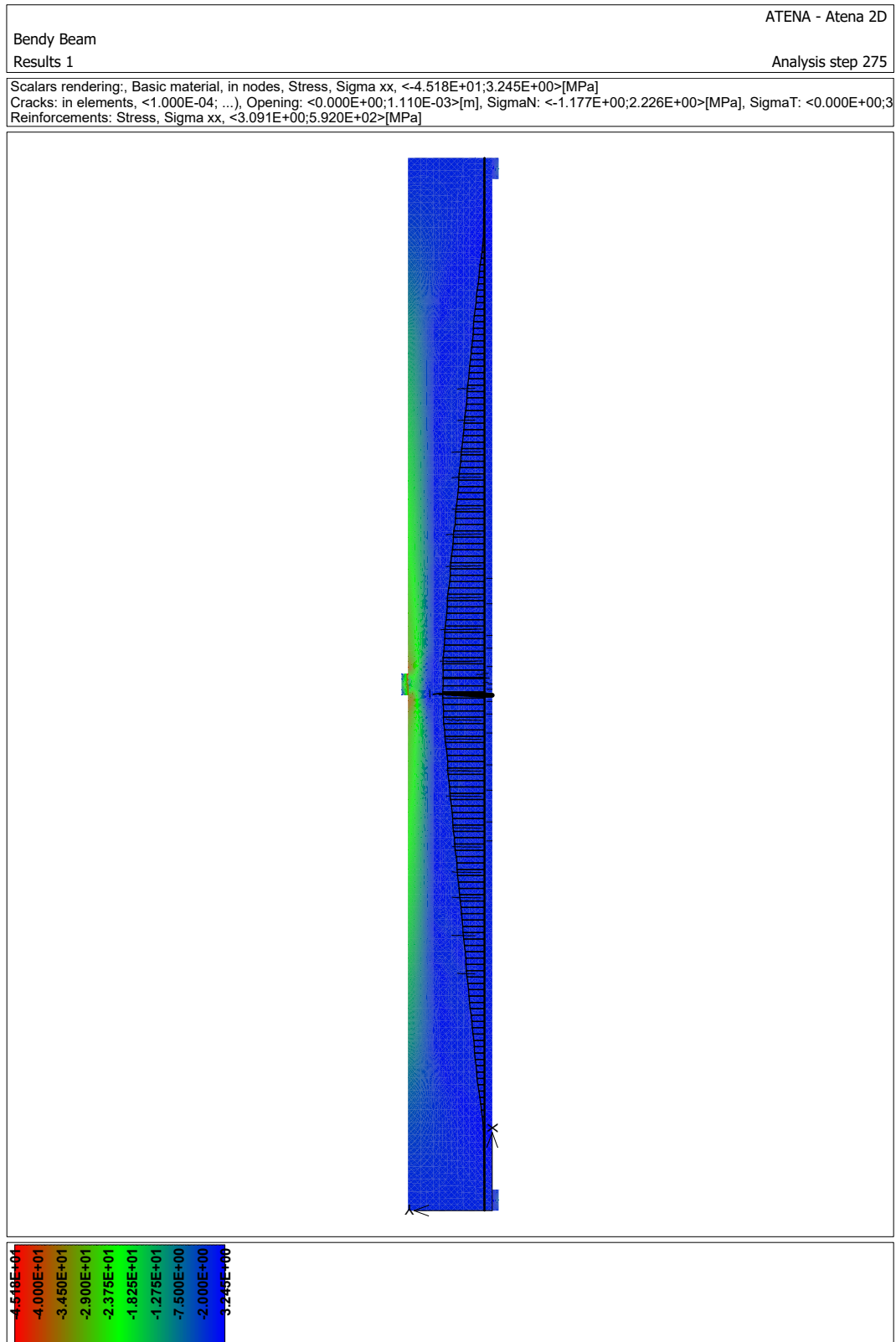


Figure B.0.24: Rectangular beam Sample no. 24.

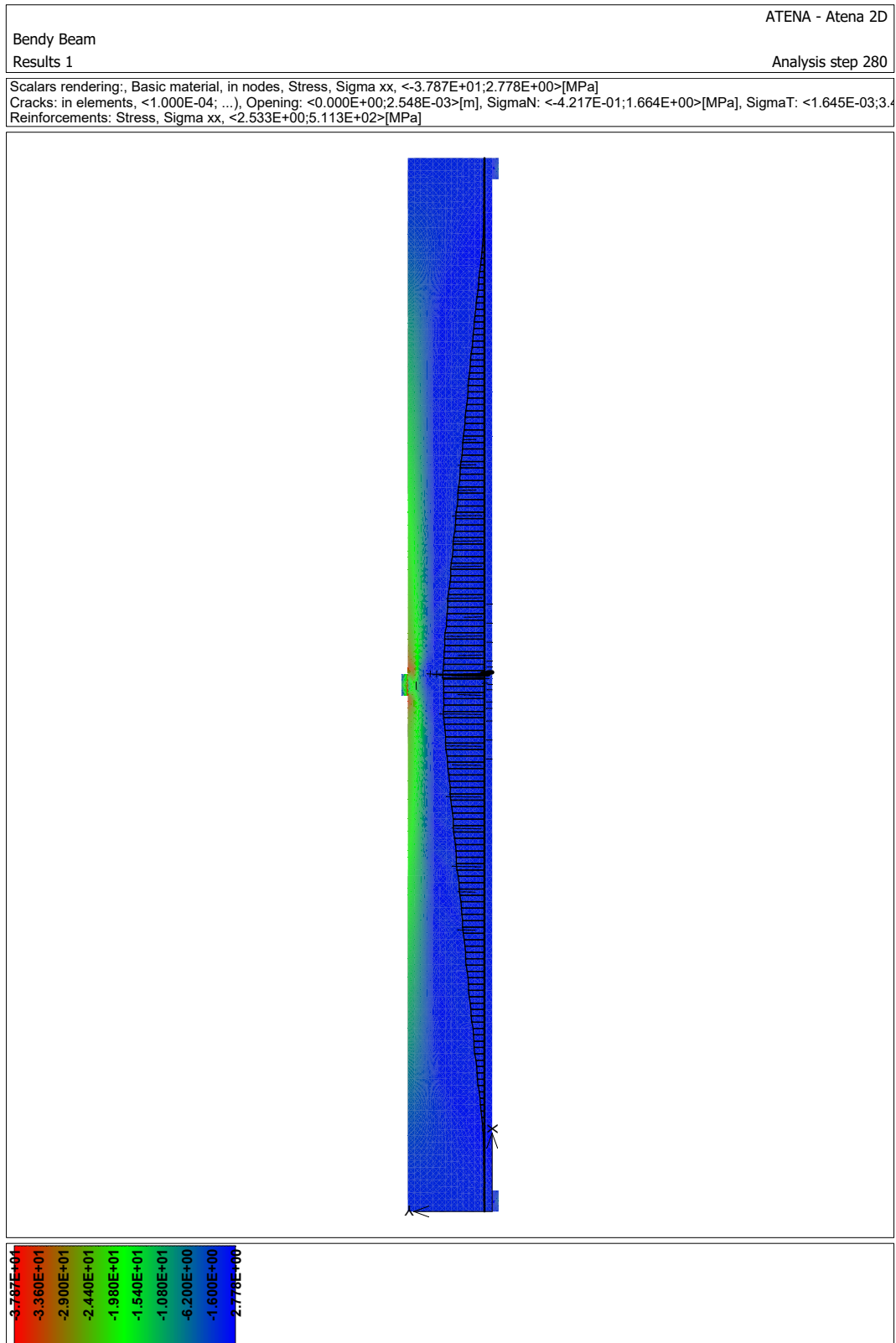


Figure B.0.25: Rectangular beam Sample no. 25.

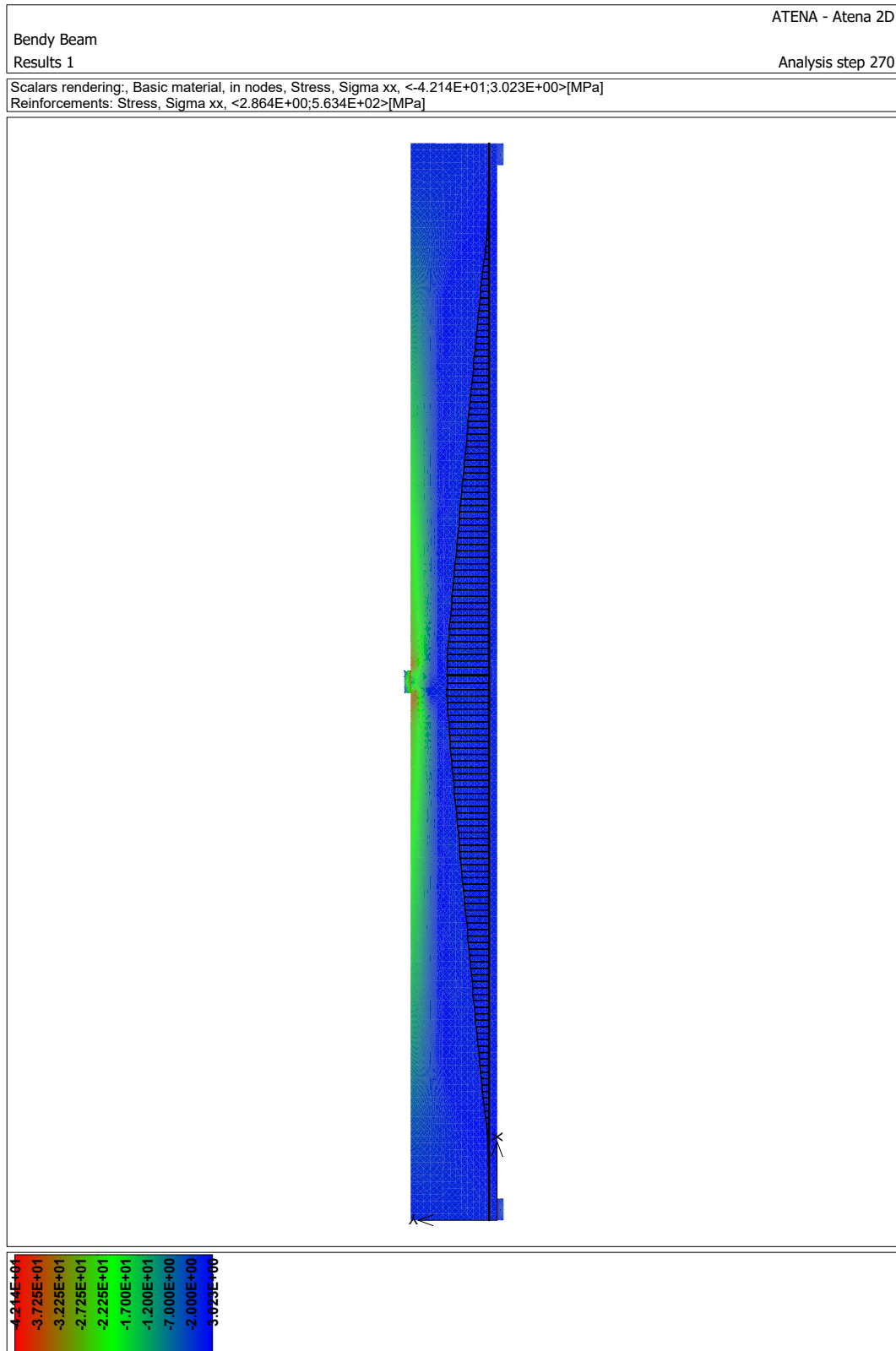


Figure B.0.26: Rectangular beam Sample no. 26.

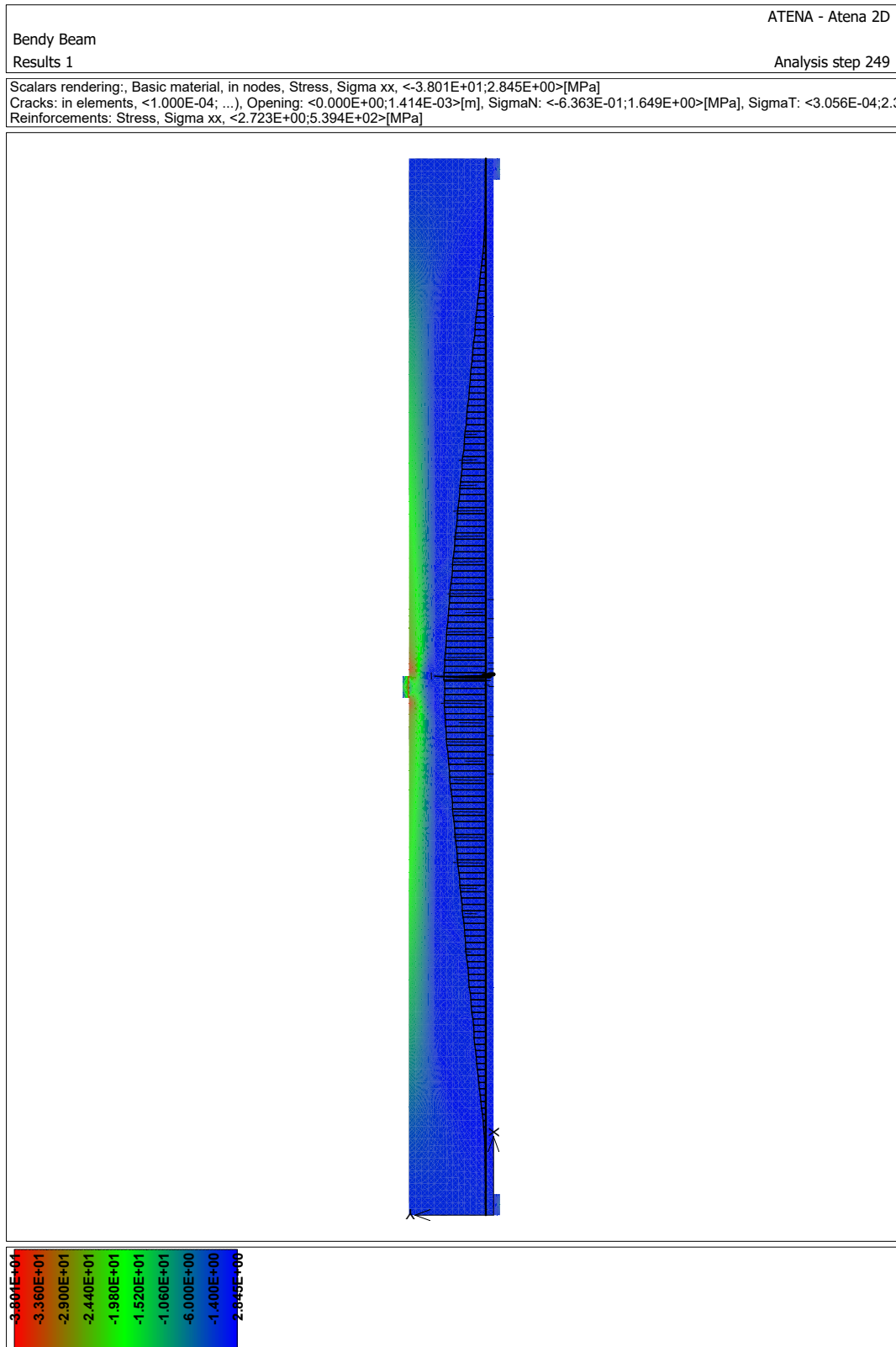


Figure B.0.27: Rectangular beam Sample no. 27.

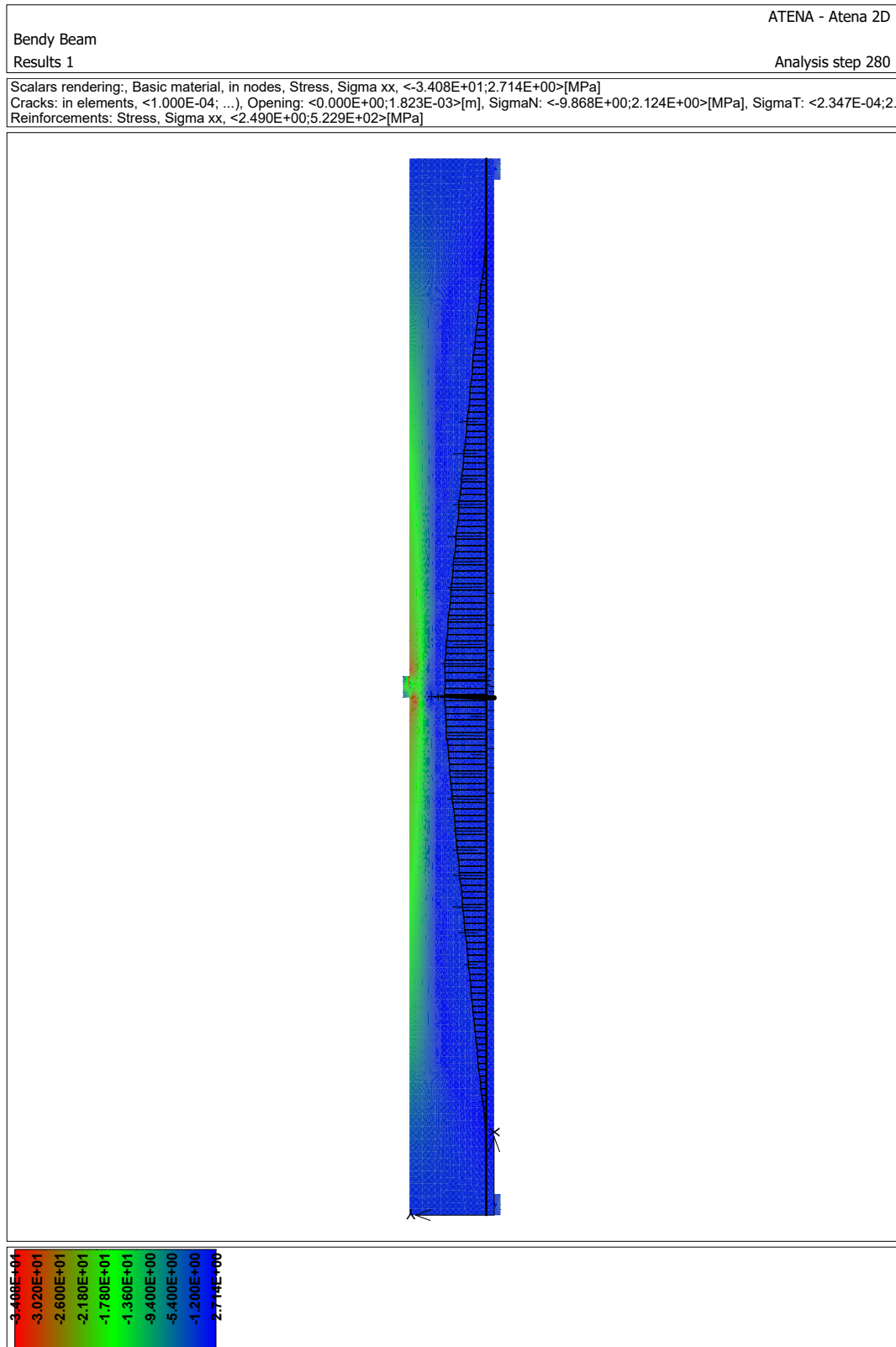


Figure B.0.28: Rectangular beam Sample no. 28.

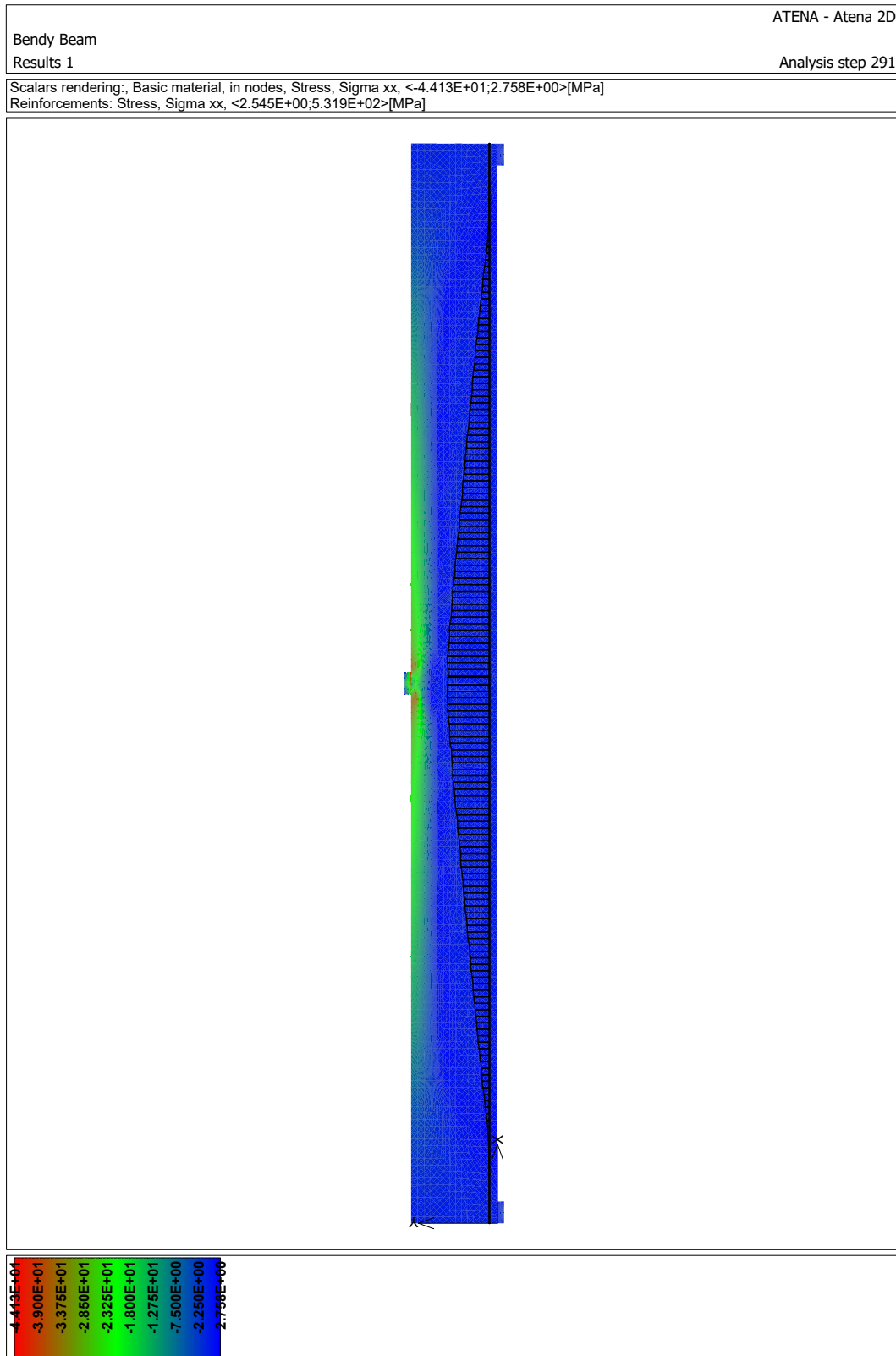


Figure B.0.29: Rectangular beam Sample no. 29.

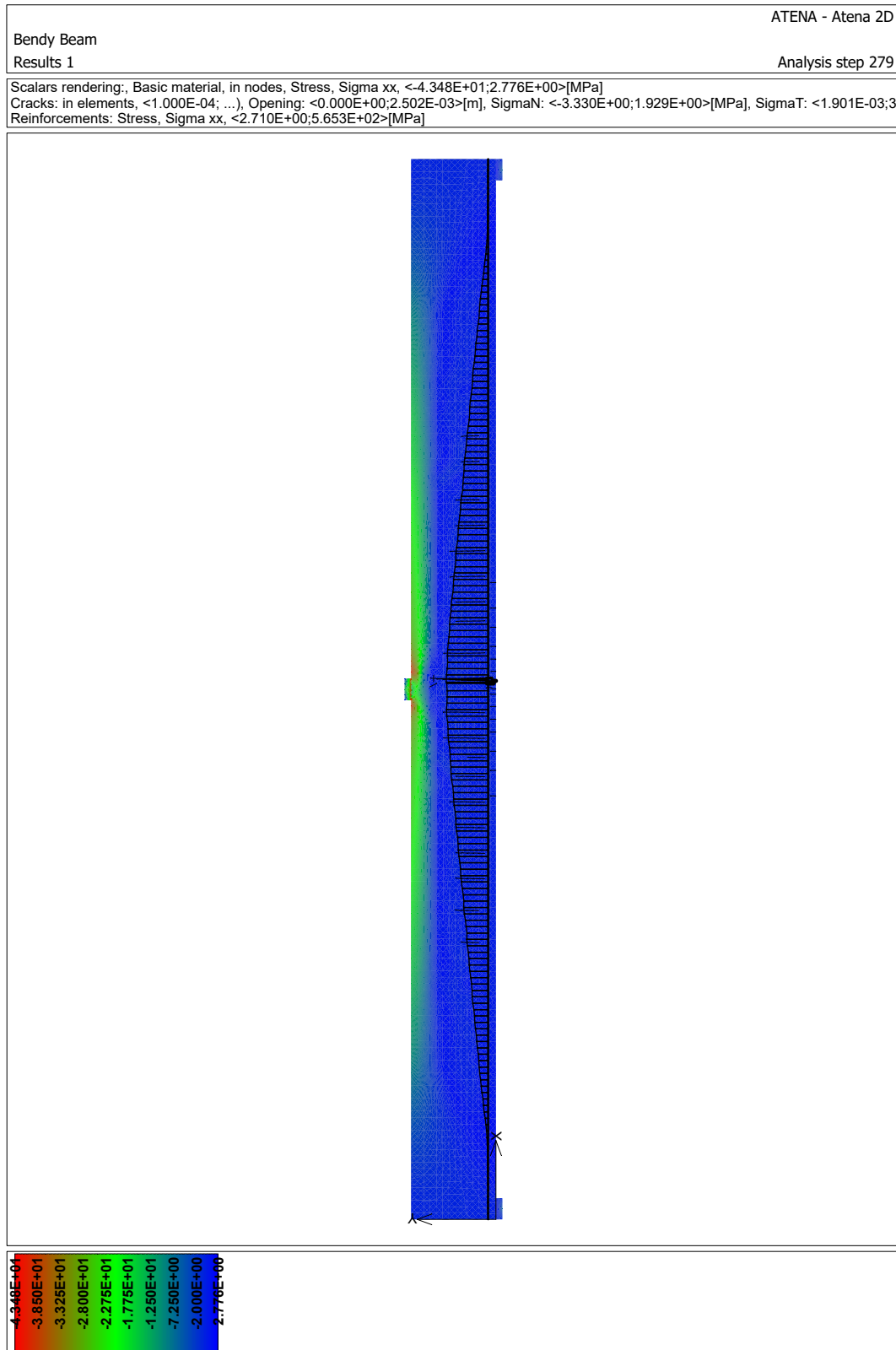


Figure B.0.30: Rectangular beam Sample no. 30.



Figure B.0.31: T-beam Sample no. 1.

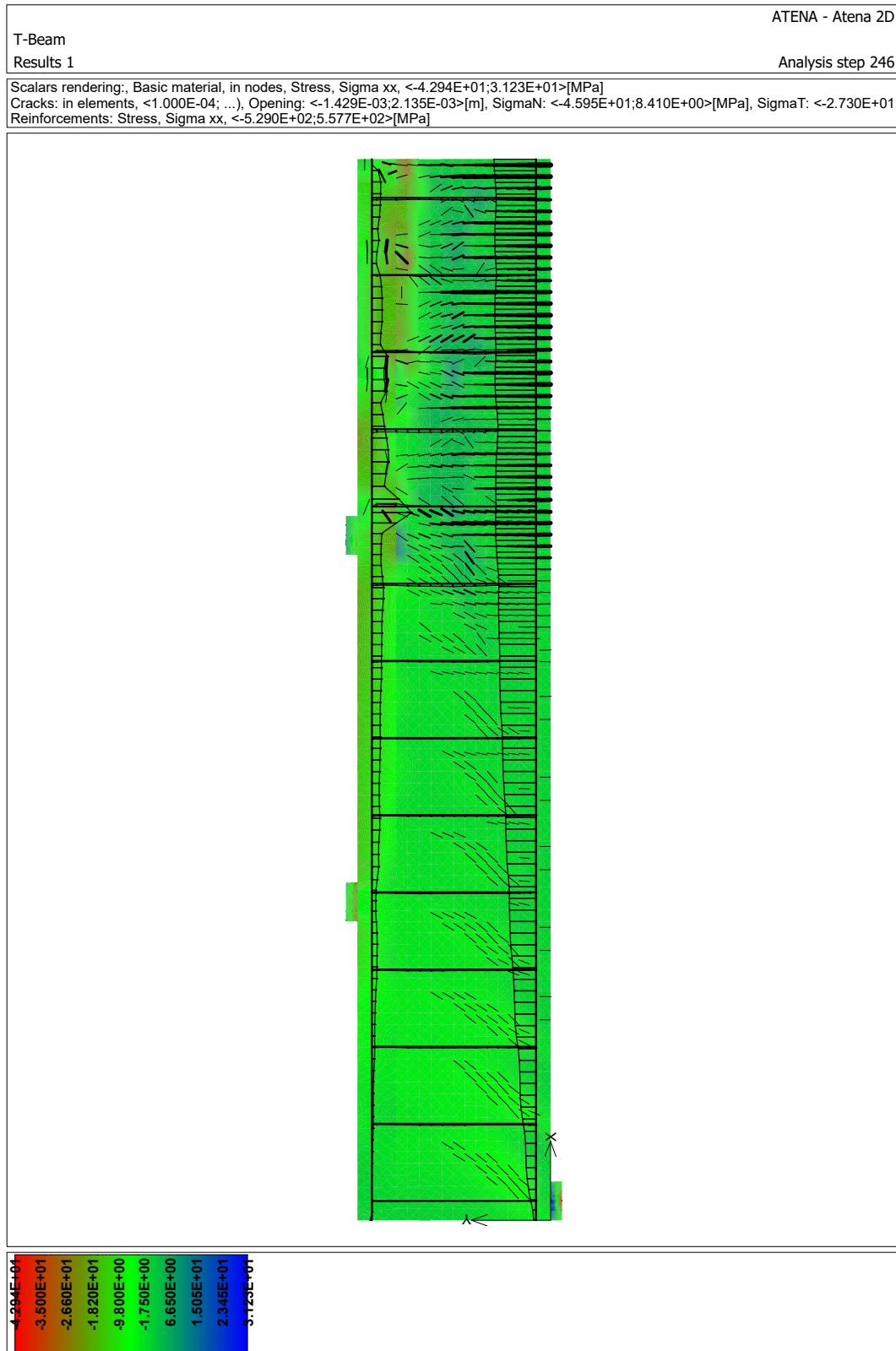


Figure B.0.32: T-beam Sample no. 2.



Figure B.0.33: T-beam Sample no. 3.

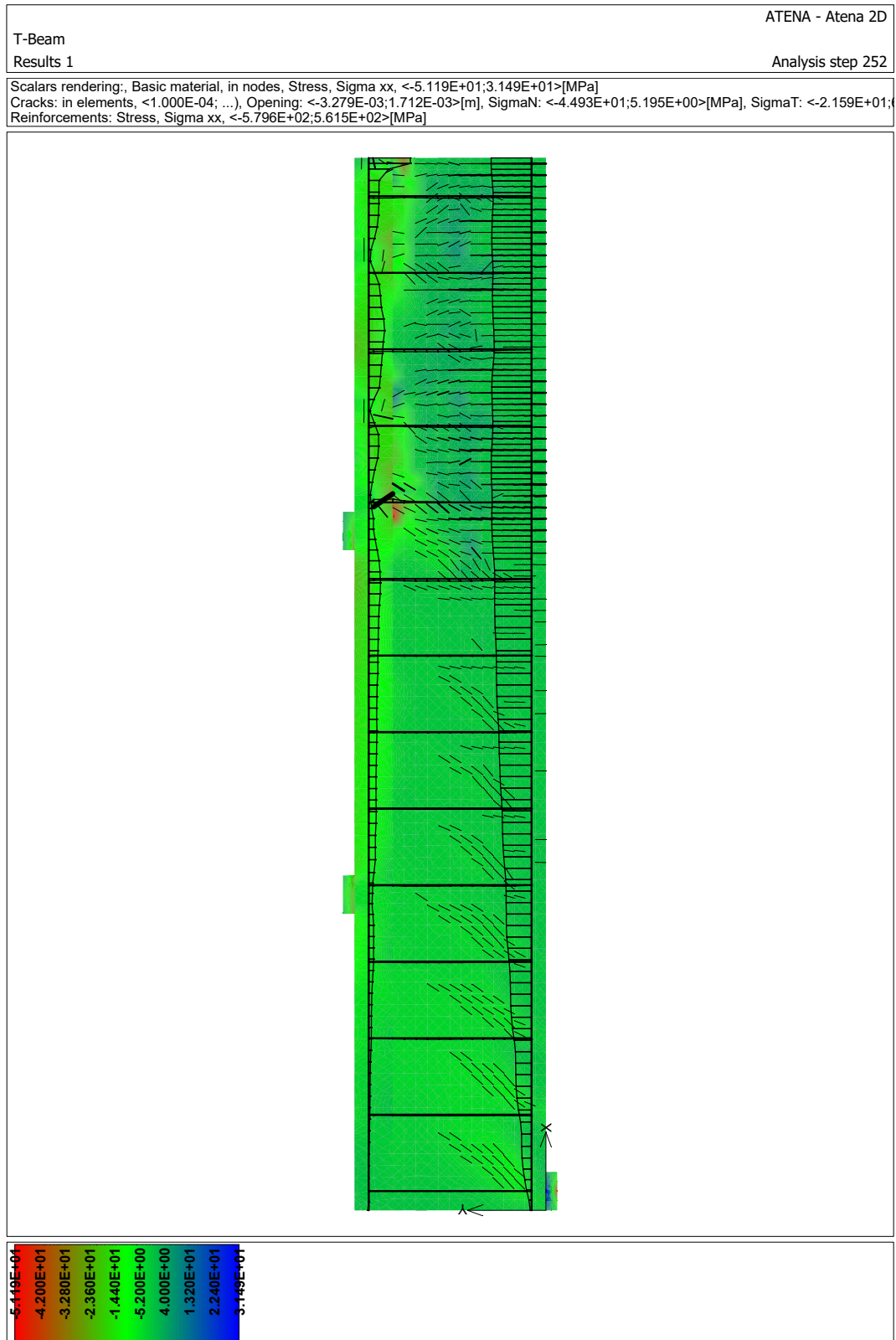


Figure B.0.34: T-beam Sample no. 4.

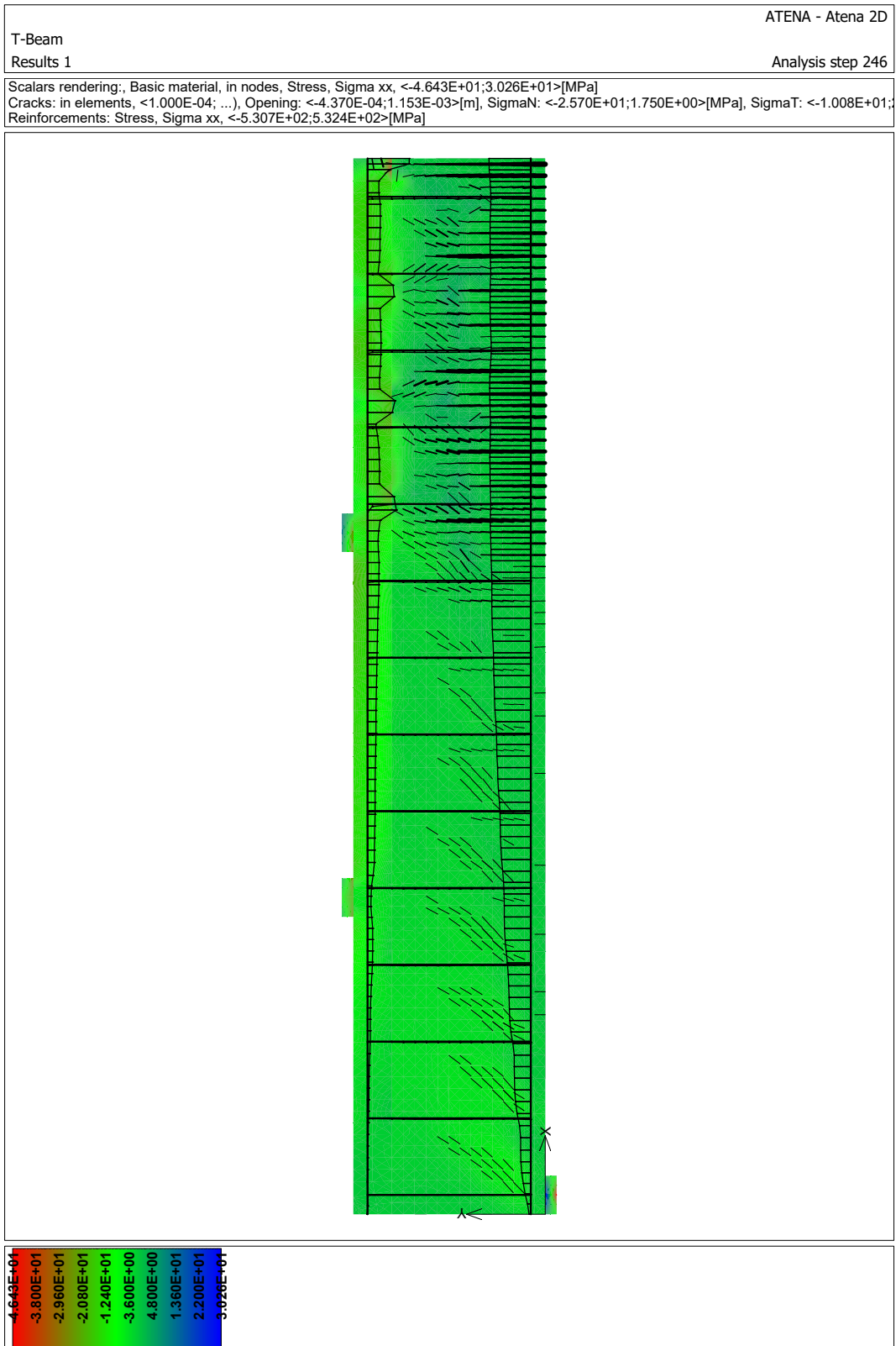


Figure B.0.35: T-beam Sample no. 5.

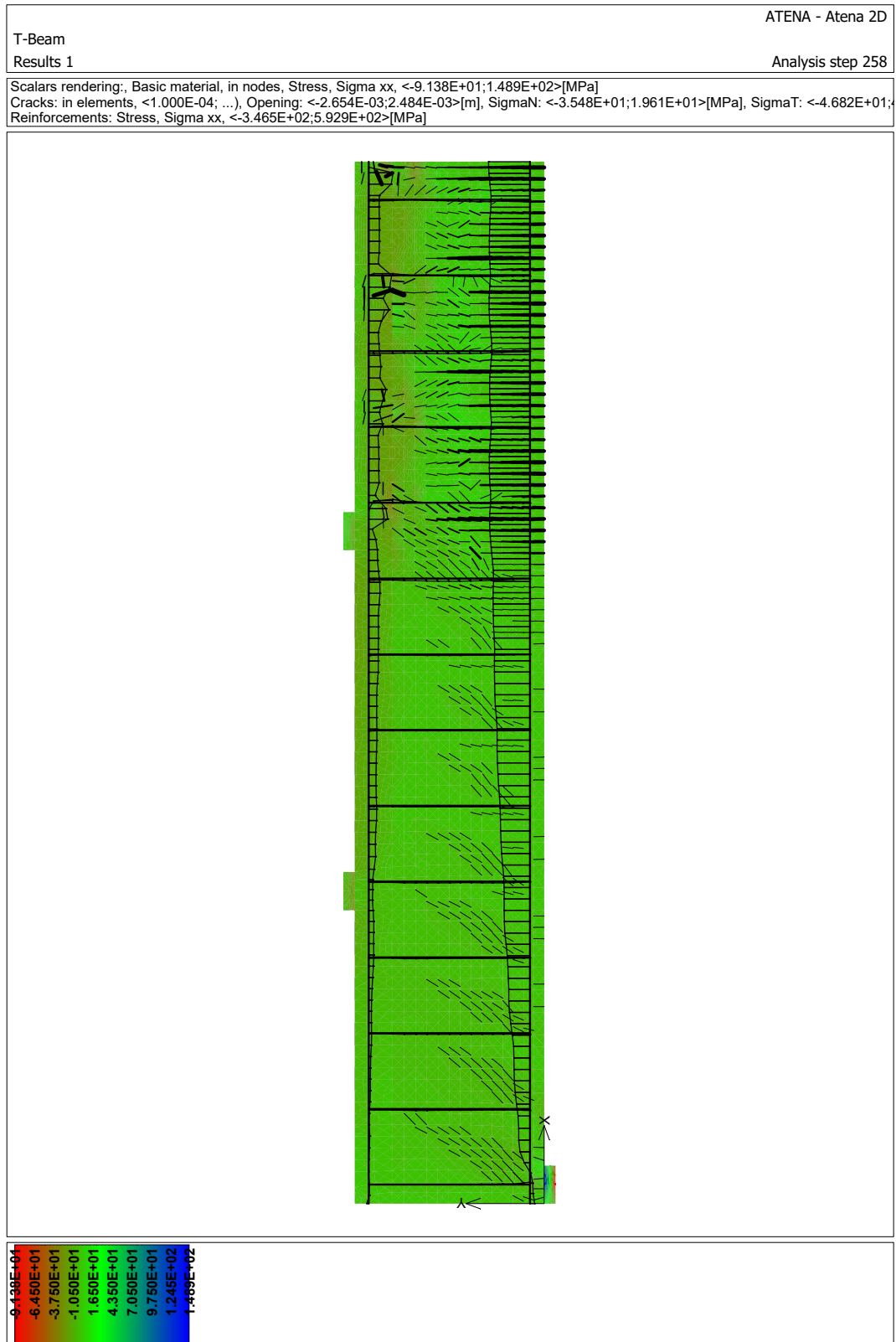


Figure B.0.36: T-beam Sample no. 6.

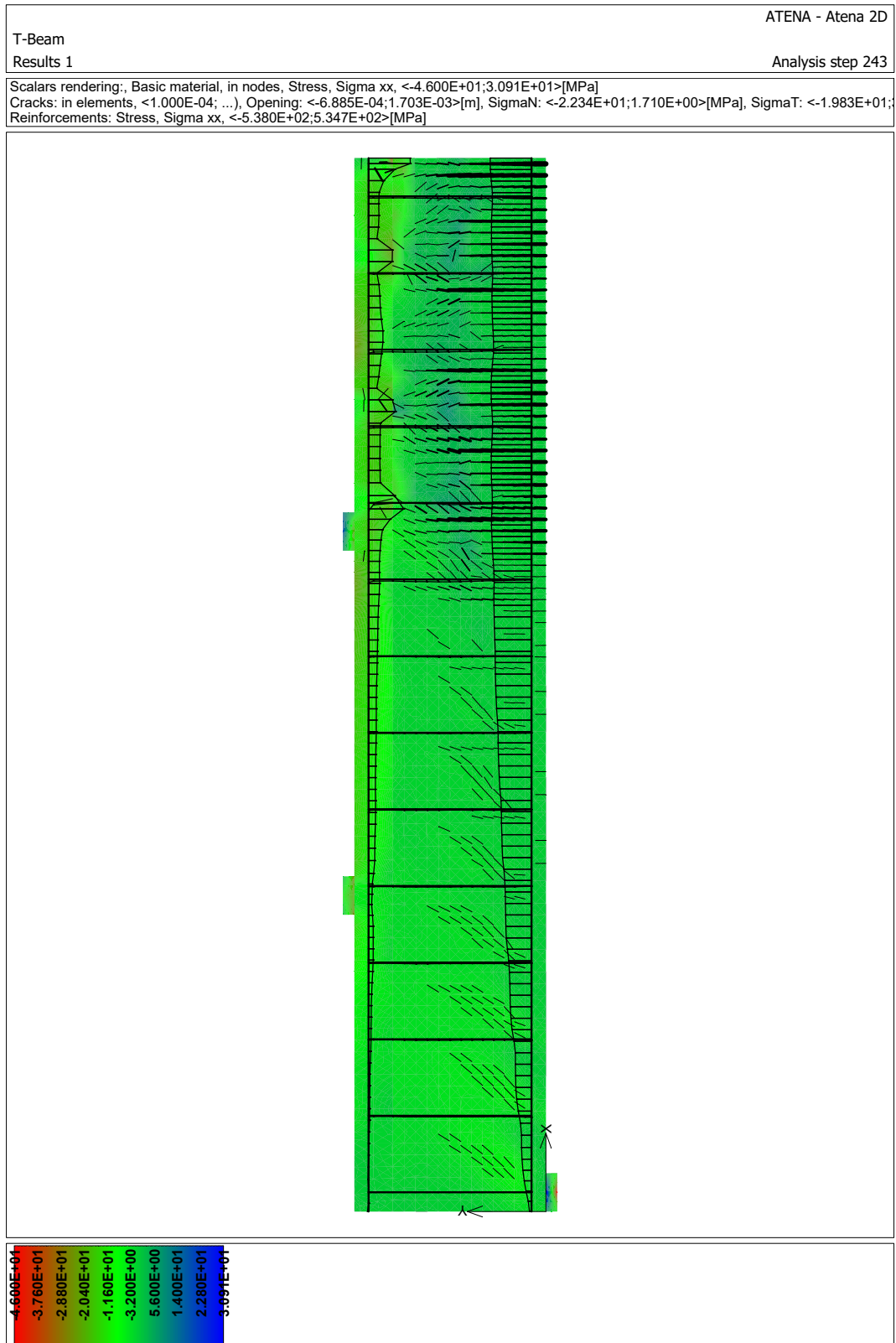


Figure B.0.37: T-beam Sample no. 7.

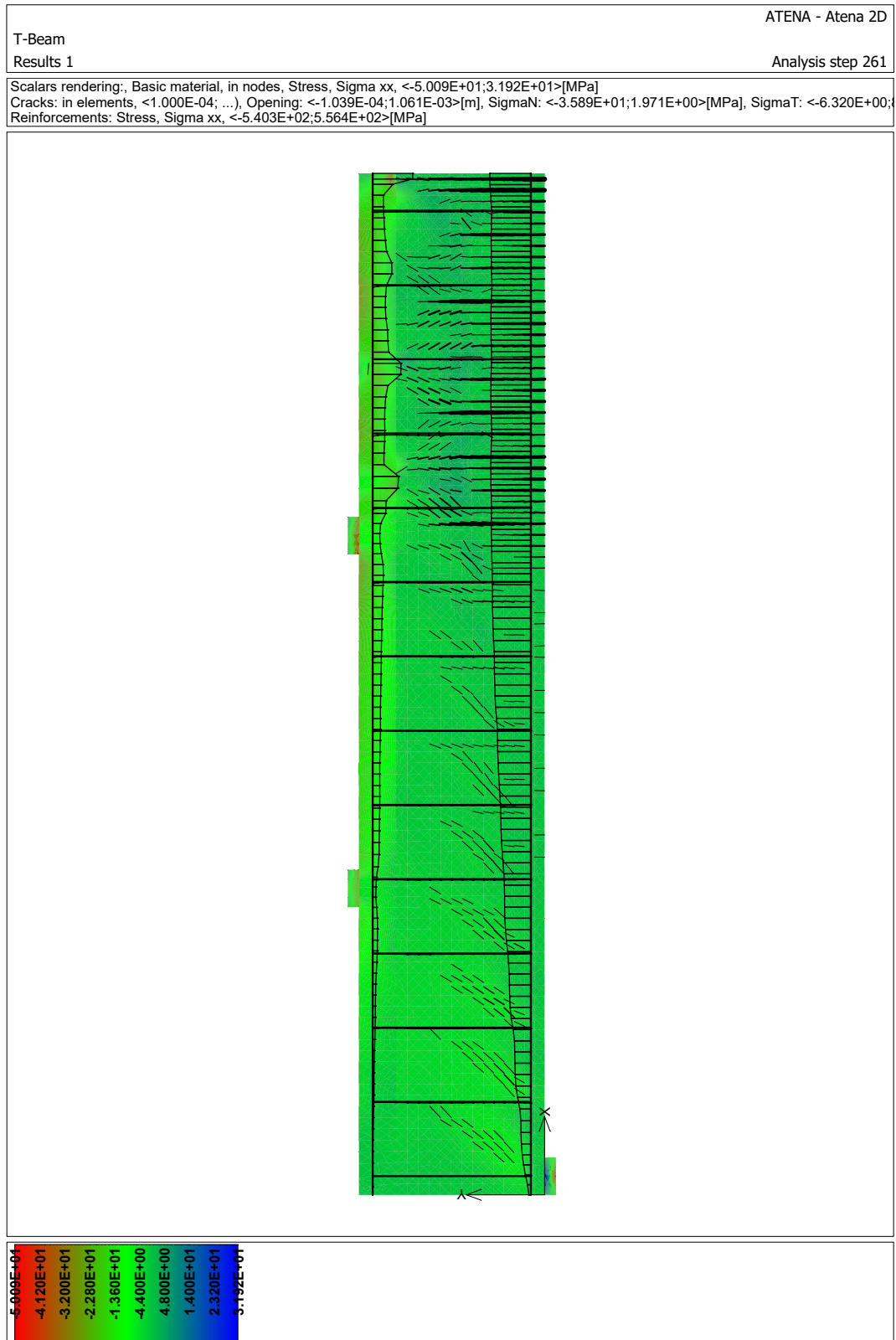


Figure B.0.38: T-beam Sample no. 8.



Figure B.0.39: T-beam Sample no. 9.

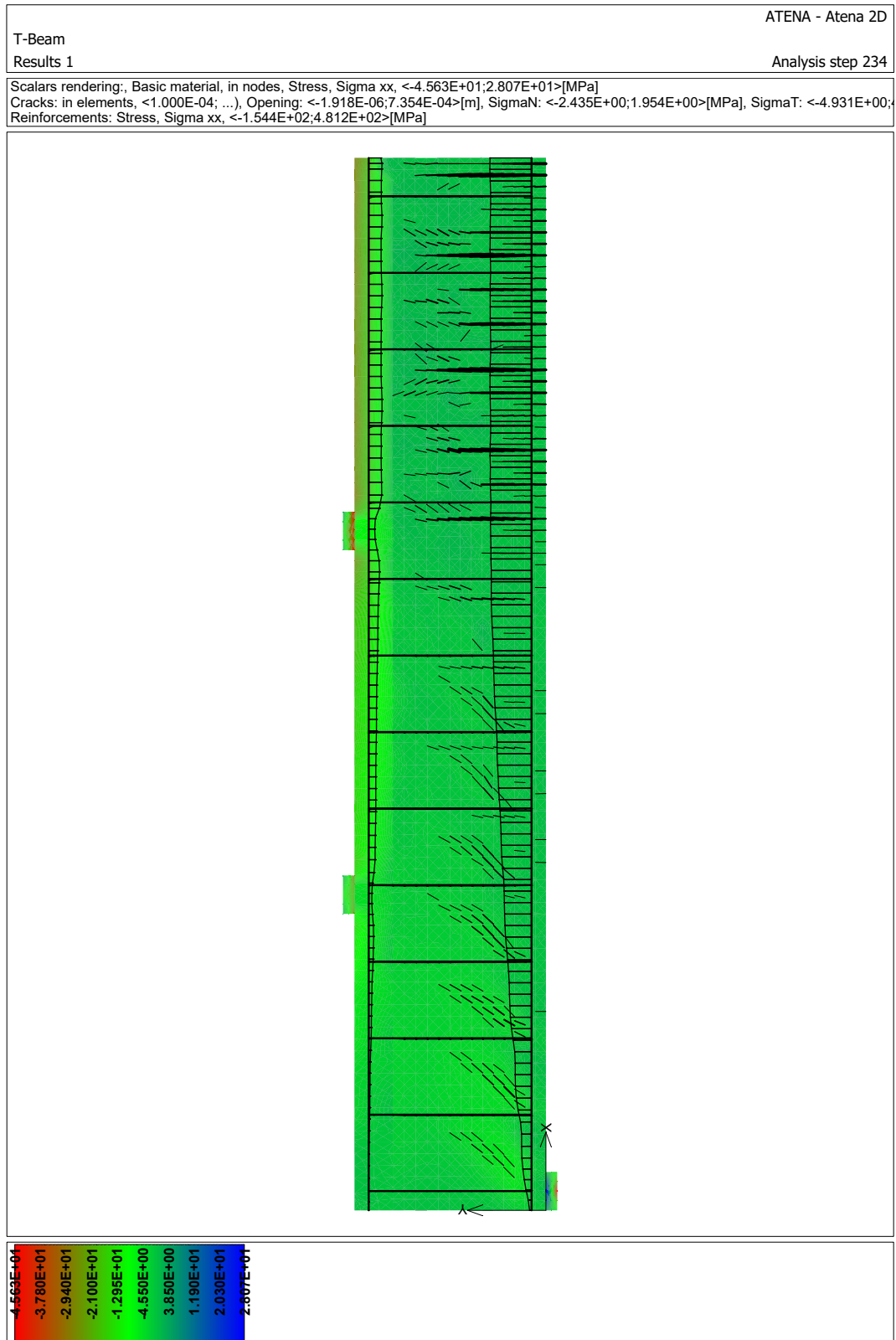


Figure B.0.40: T-beam Sample no. 10.

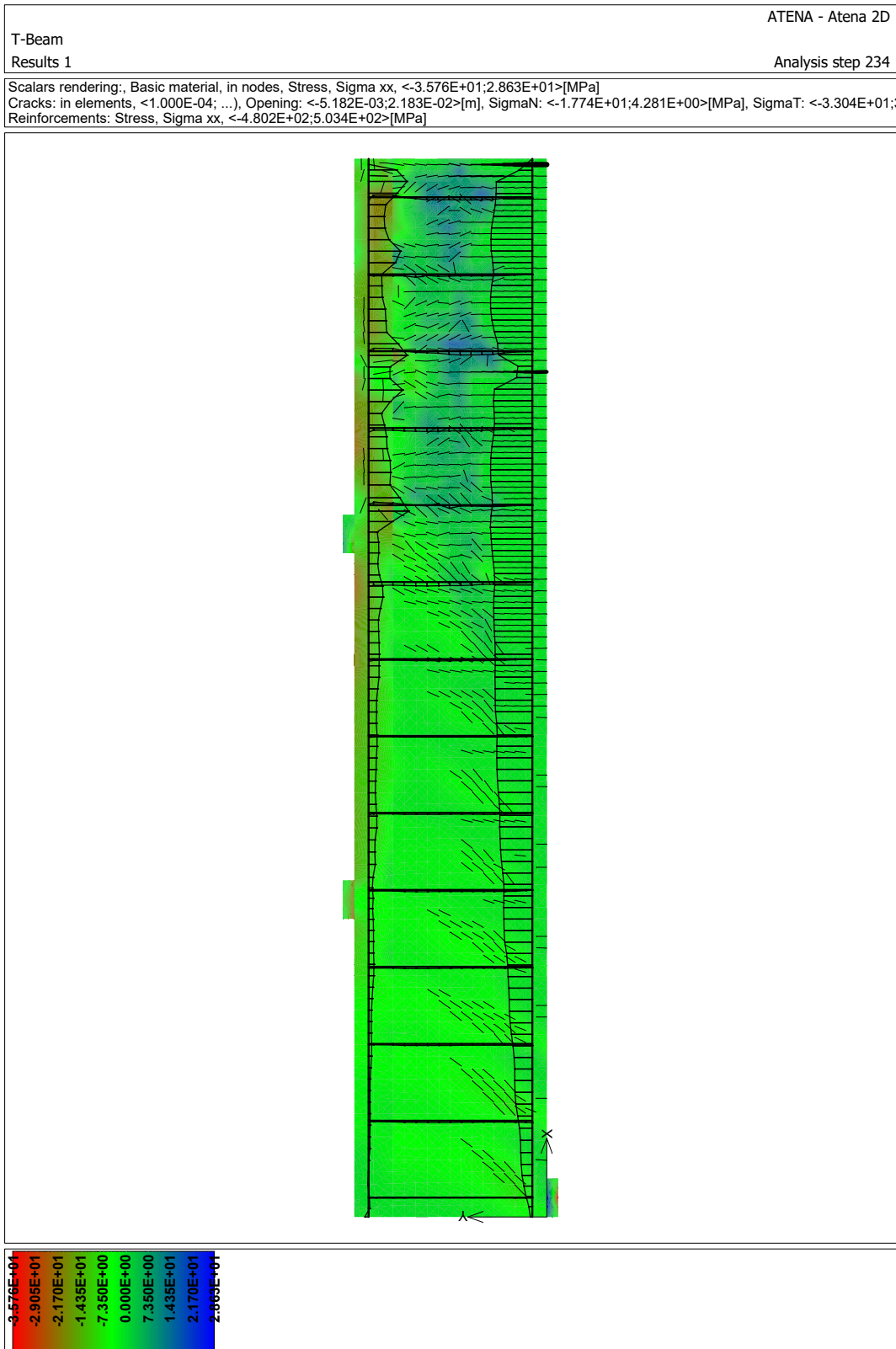


Figure B.0.41: T-beam Sample no. 11.

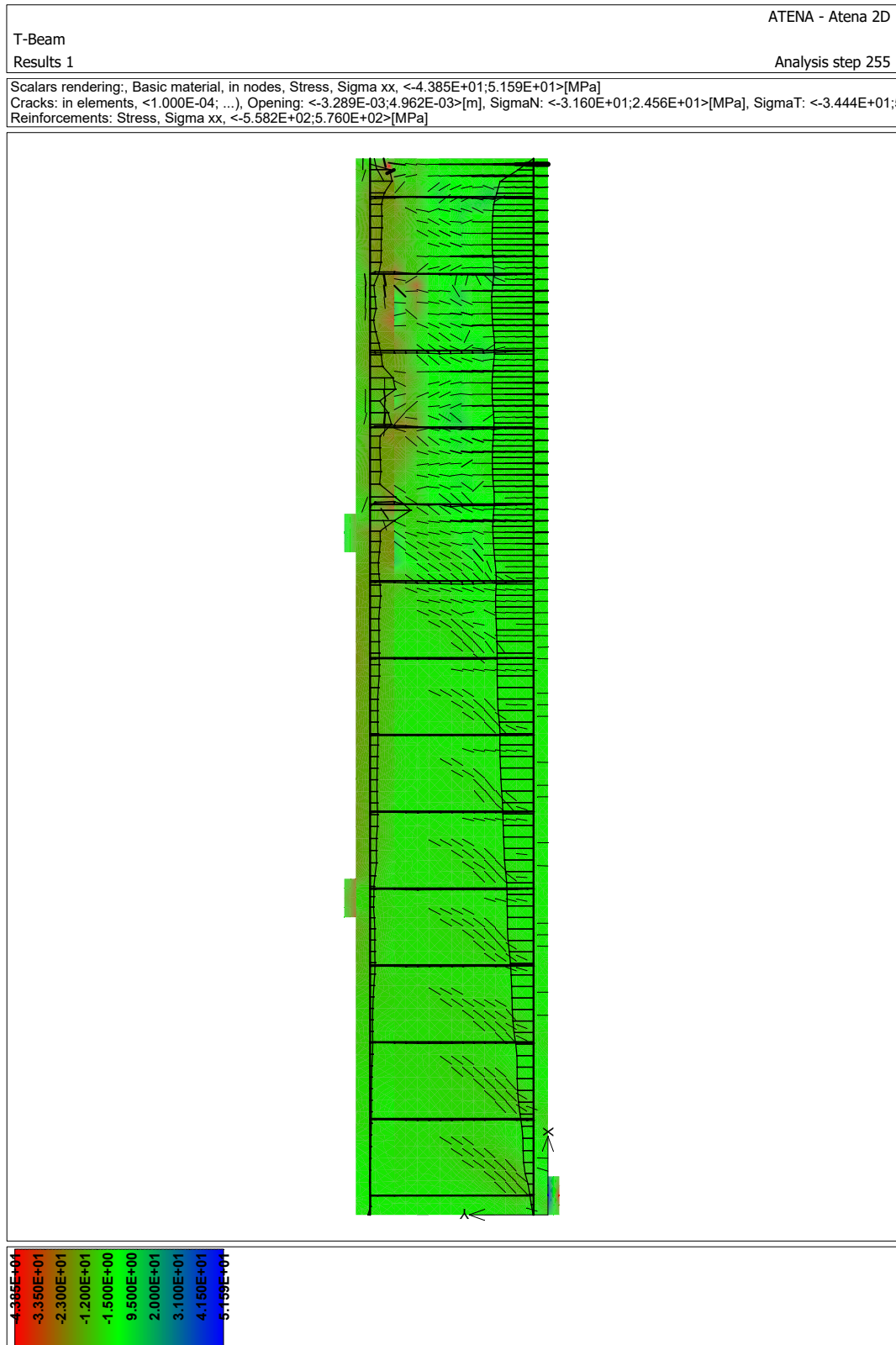


Figure B.0.42: T-beam Sample no. 12.

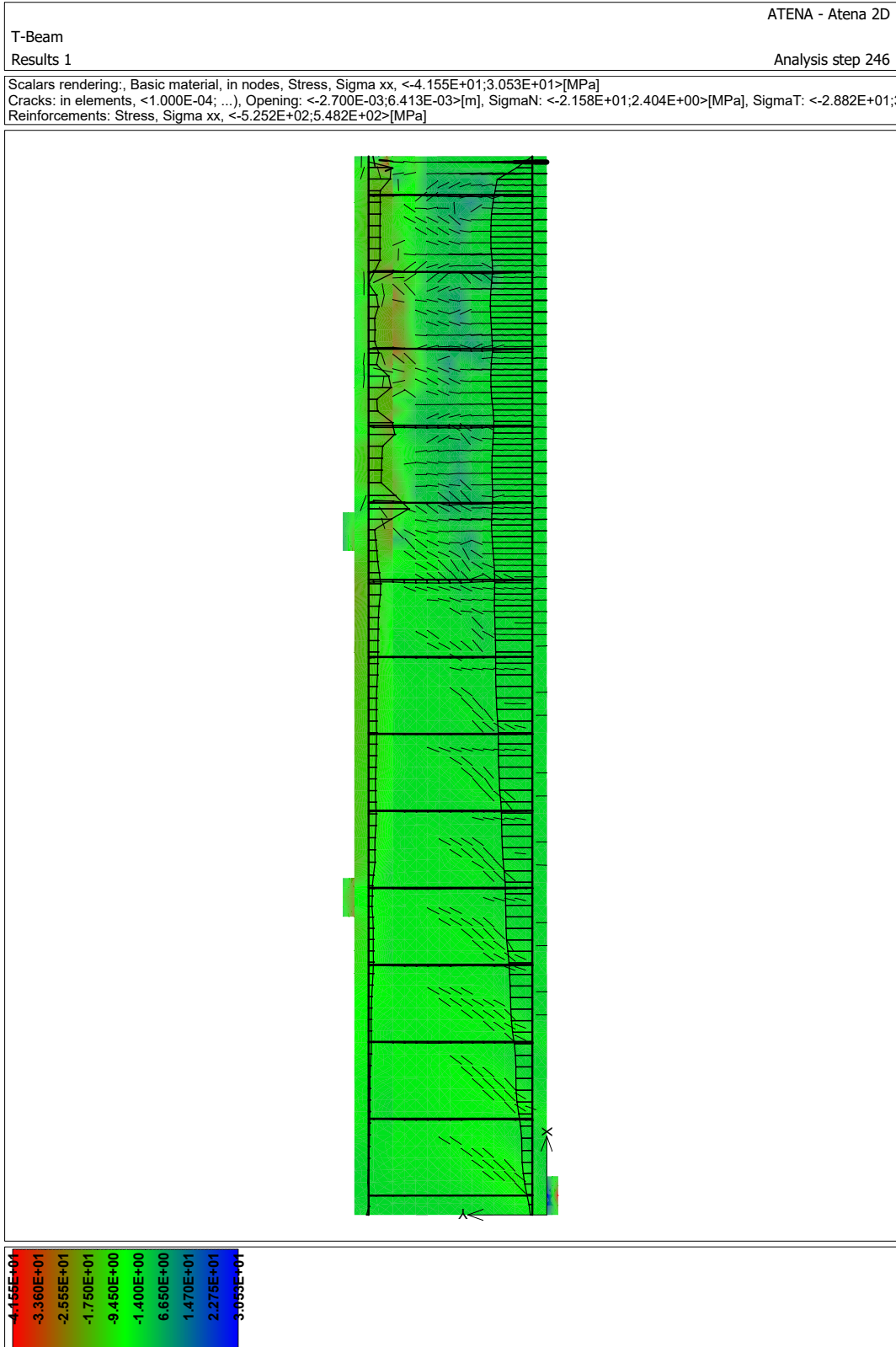


Figure B.0.43: T-beam Sample no. 13.

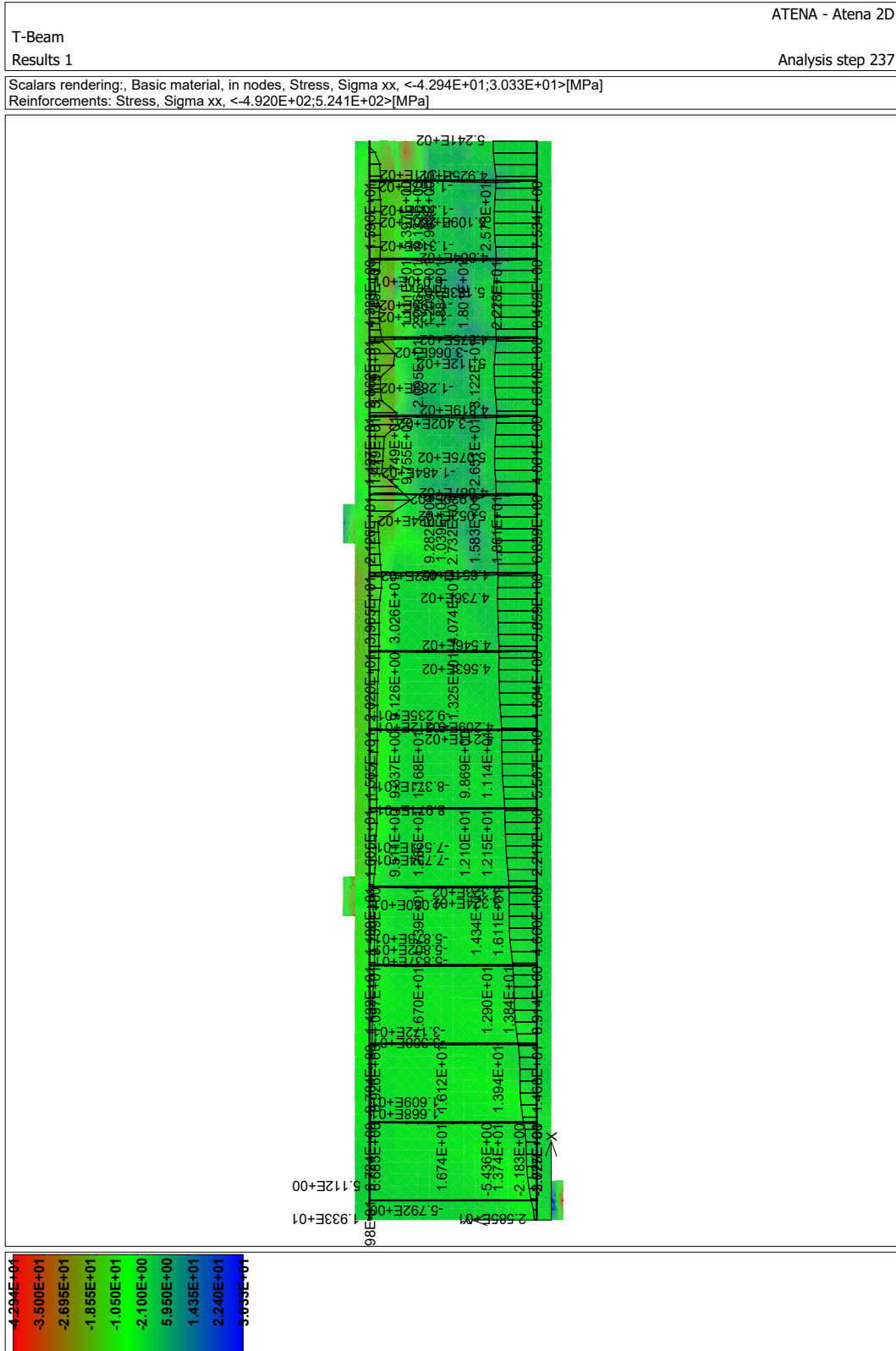


Figure B.0.44: T-beam Sample no. 14.

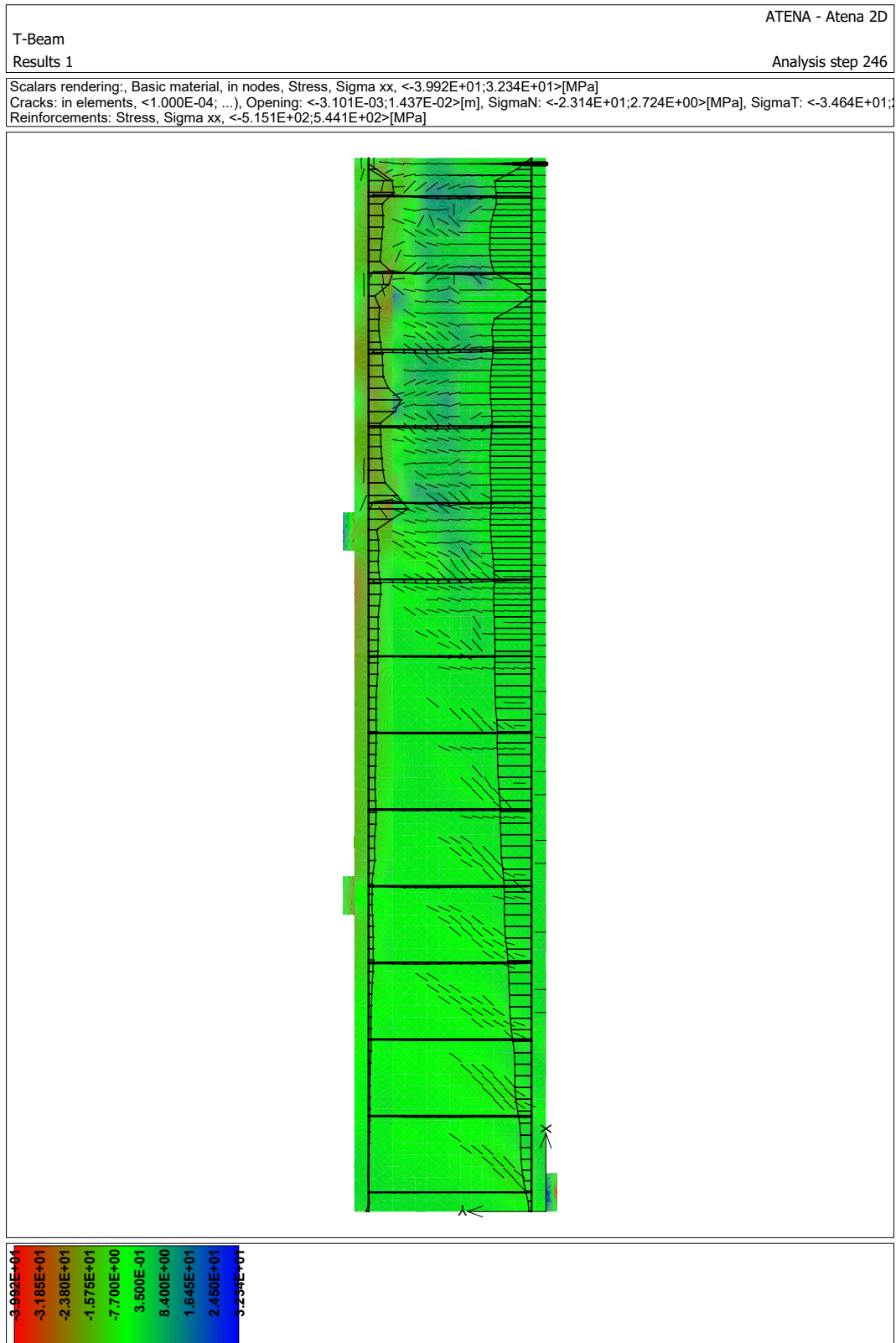


Figure B.045: T-beam Sample no. 15.

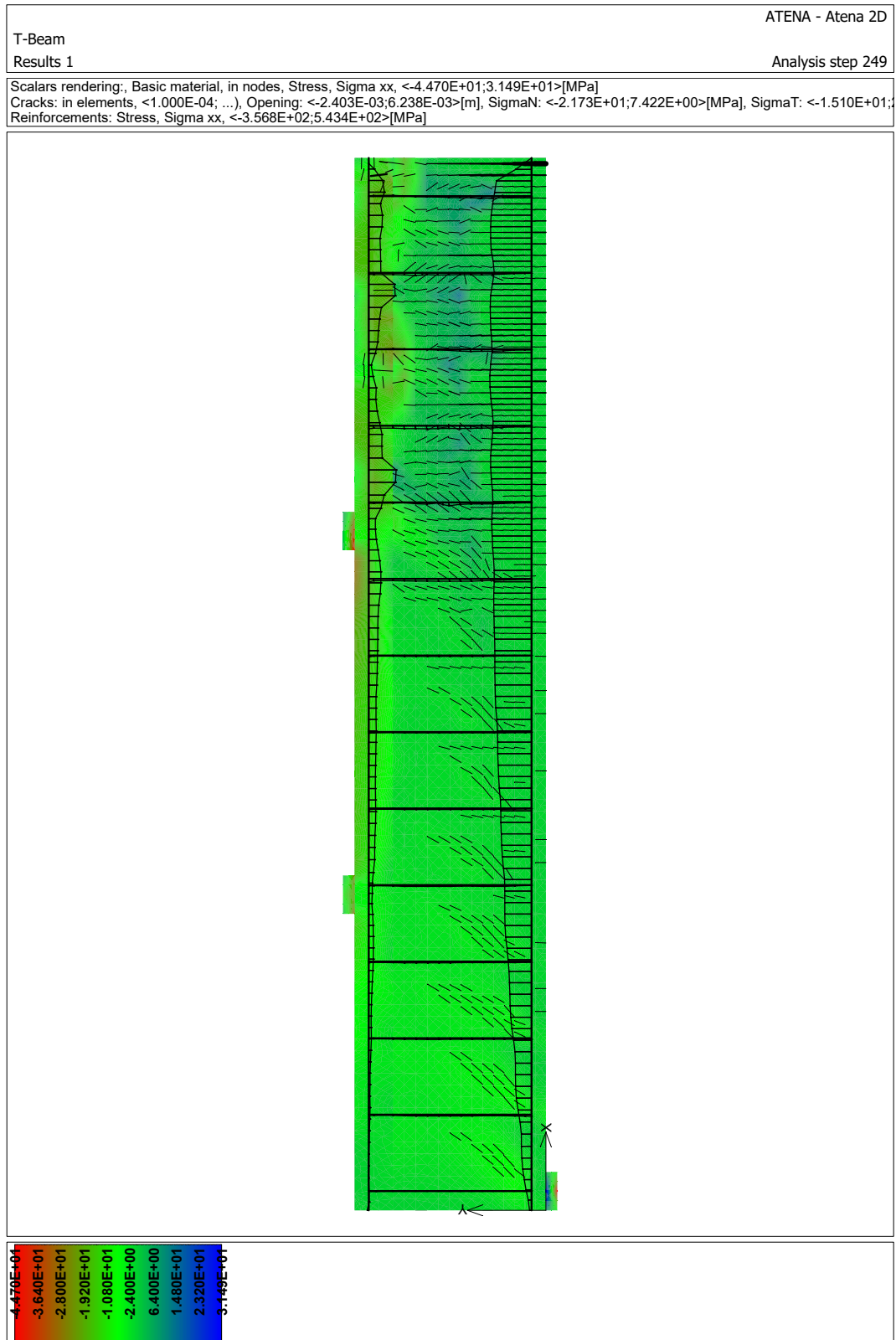


Figure B.0.46: T-beam Sample no. 16.

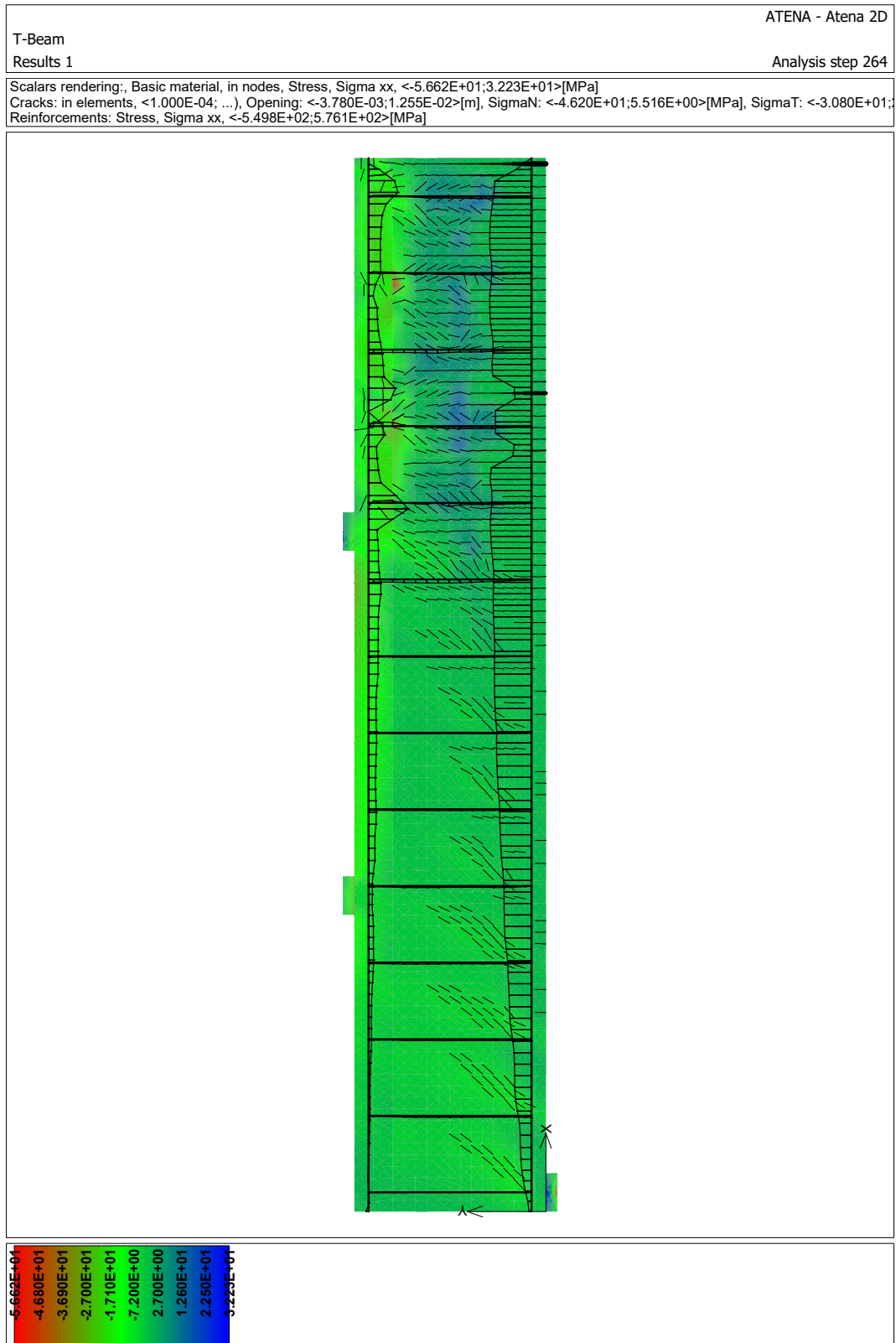


Figure B.0.47: T-beam Sample no. 17.



Figure B.0.48: T-beam Sample no. 18.

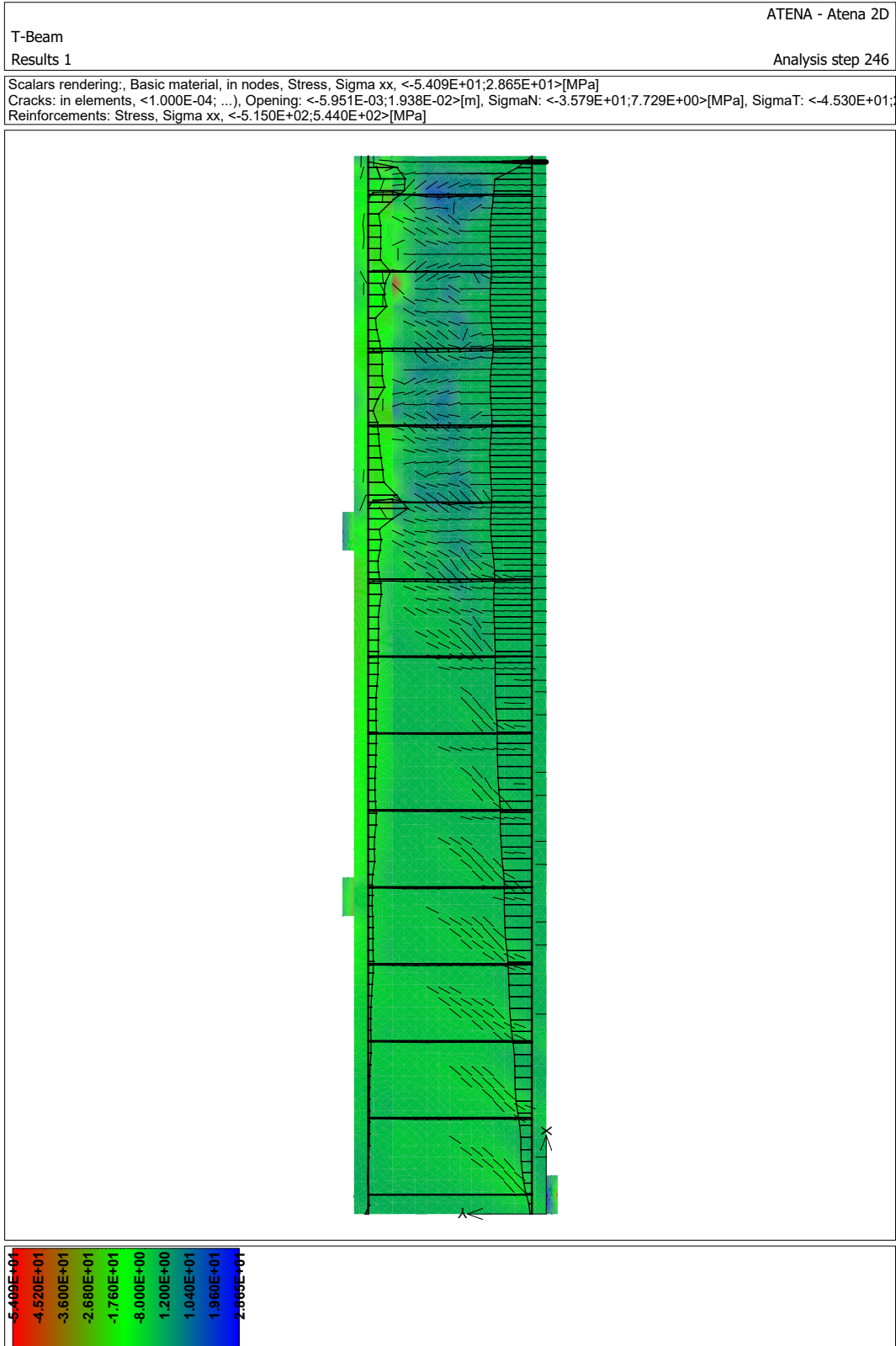


Figure B.0.49: T-beam Sample no. 19.

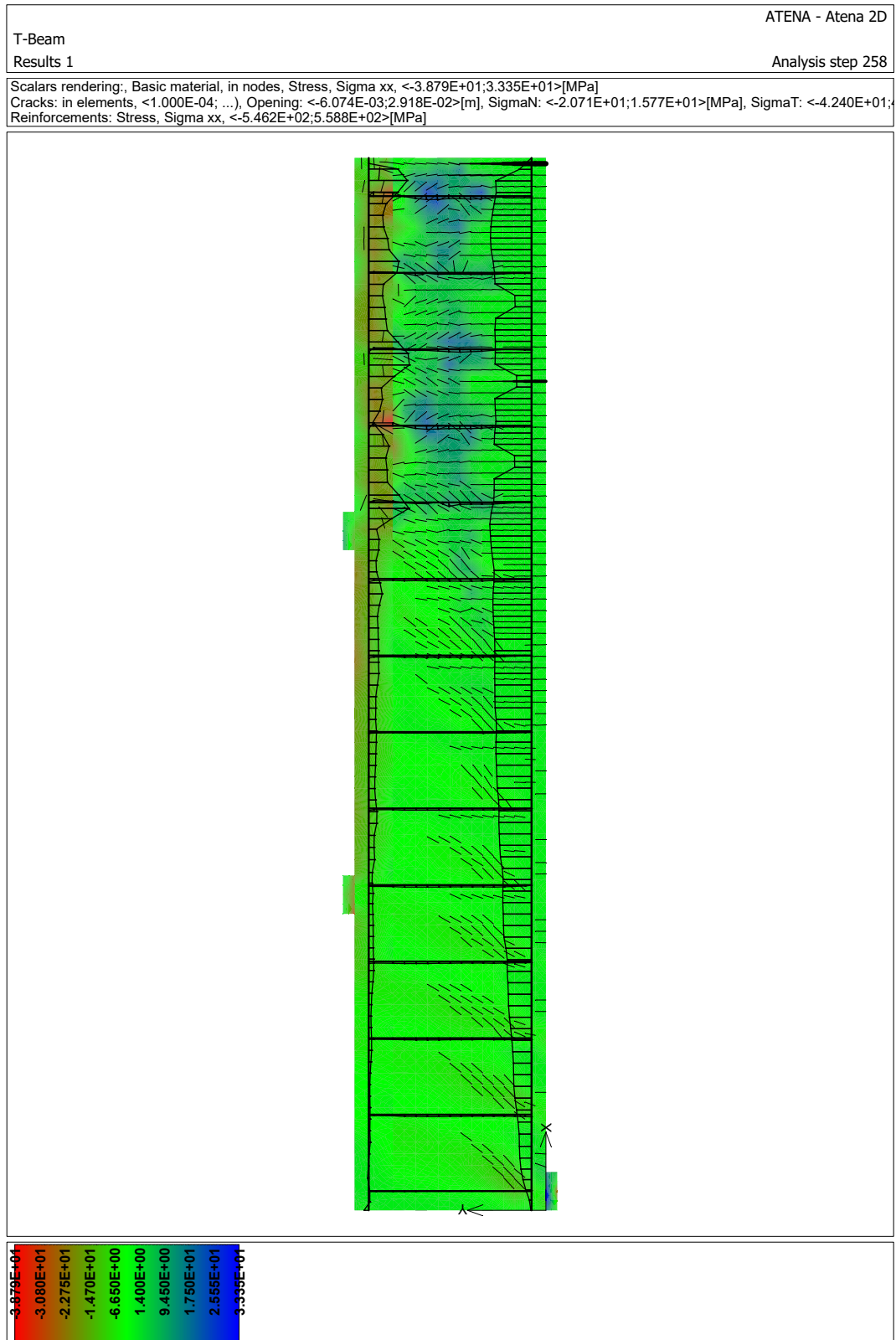


Figure B.0.50: T-beam Sample no. 2o.



Figure B.0.51: T-beam Sample no. 21.

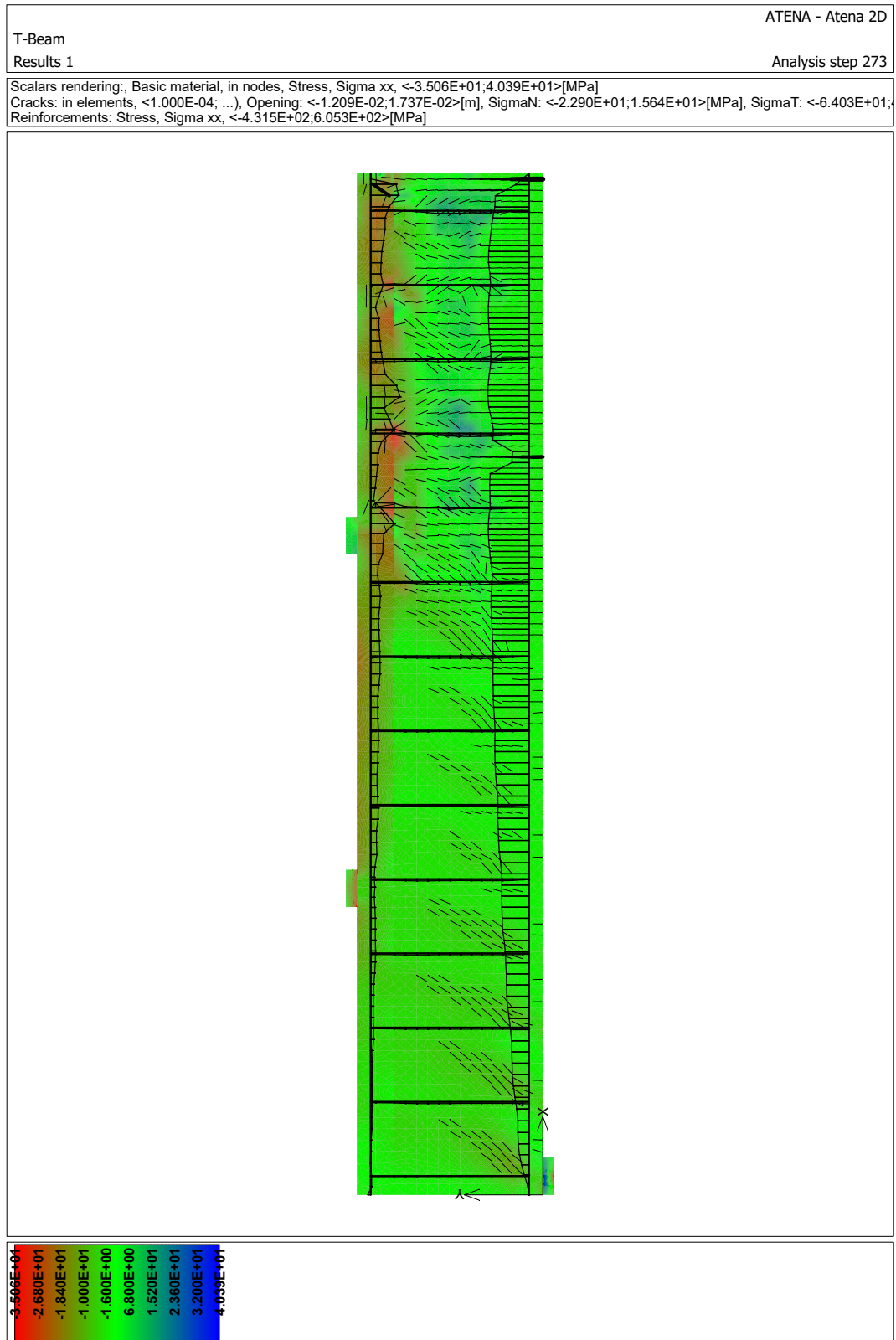


Figure B.0.52: T-beam Sample no. 22.

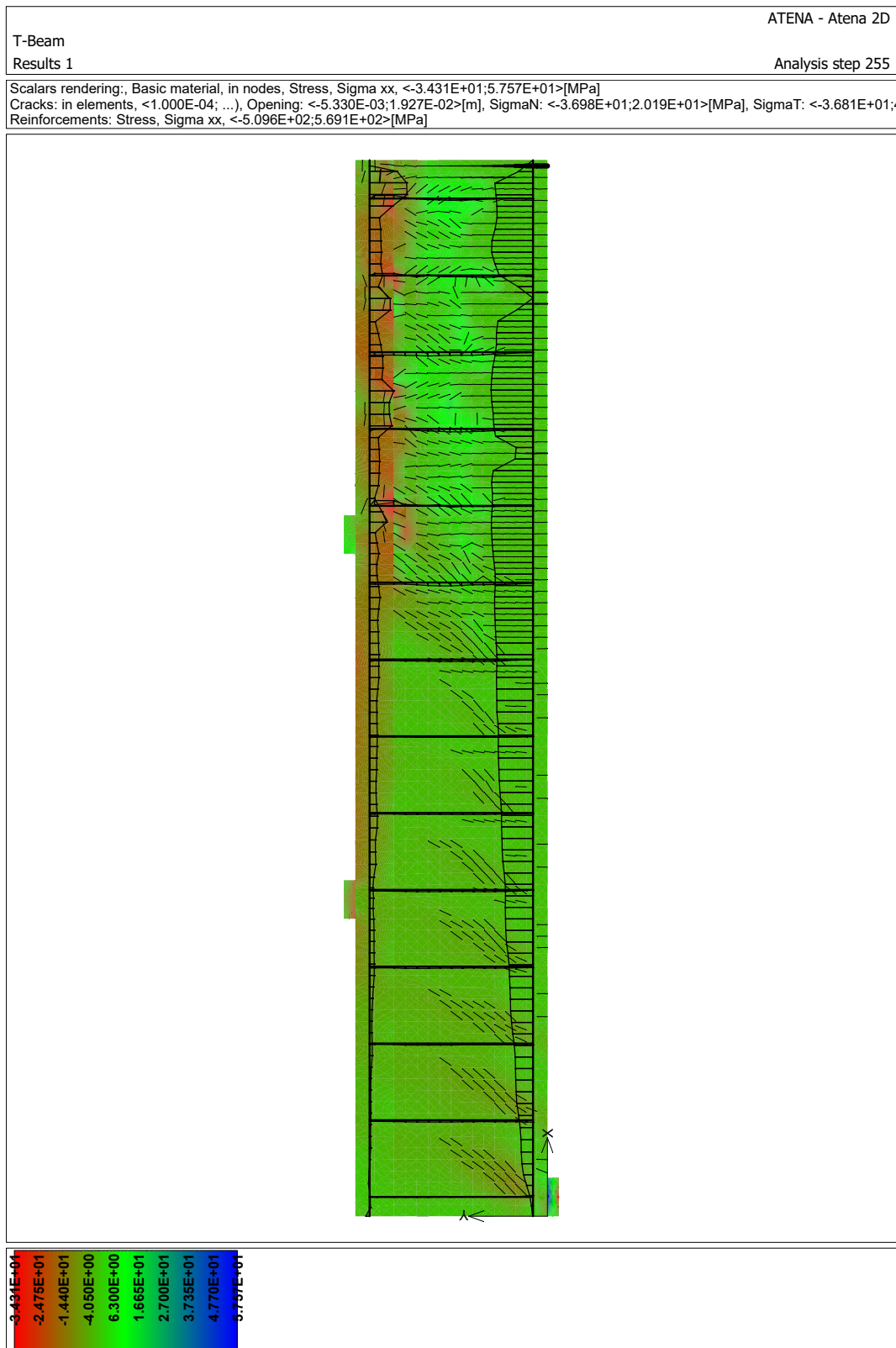


Figure B.0.53: T-beam Sample no. 23.

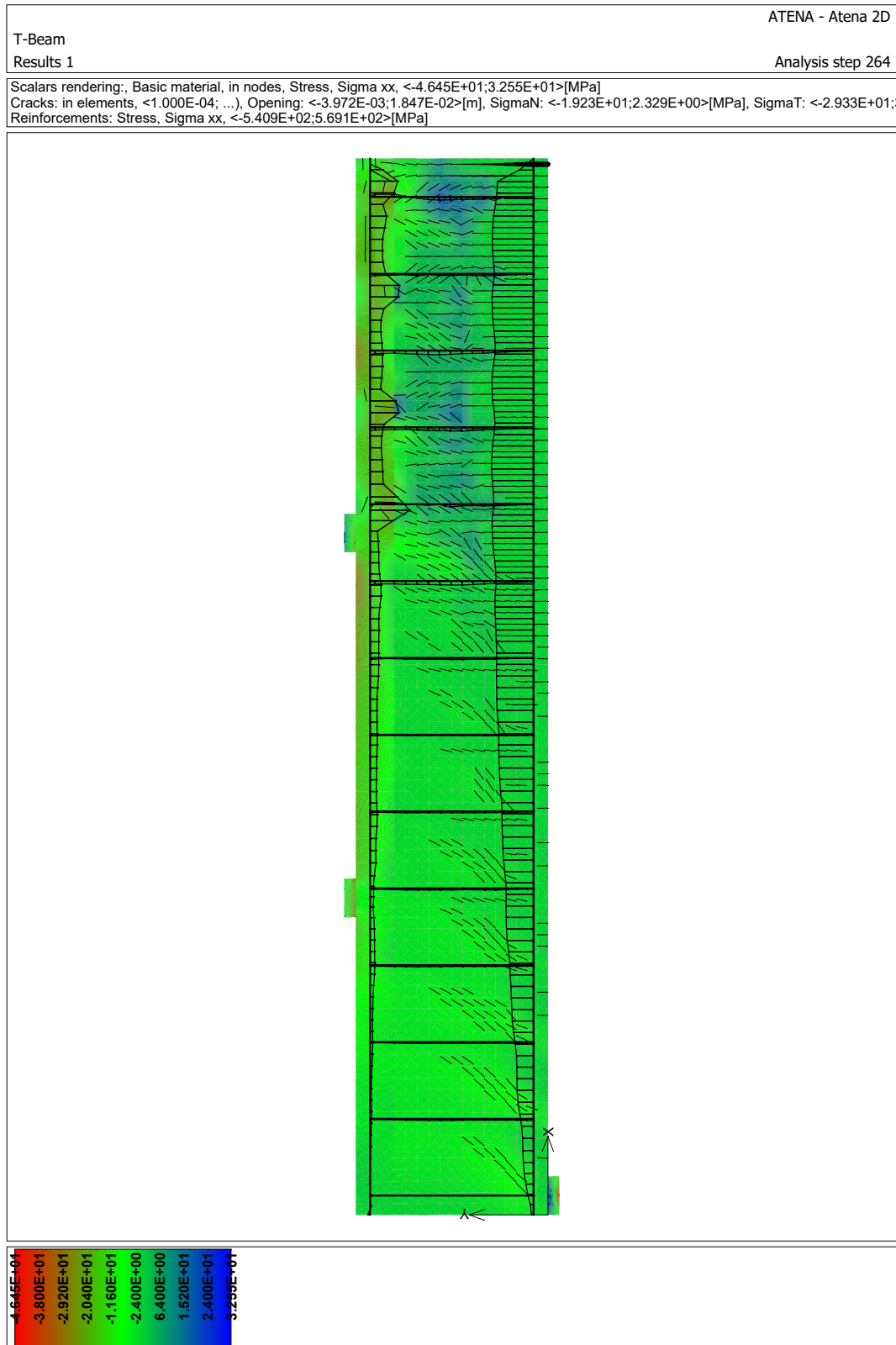


Figure B.0.54: T-beam Sample no. 24.

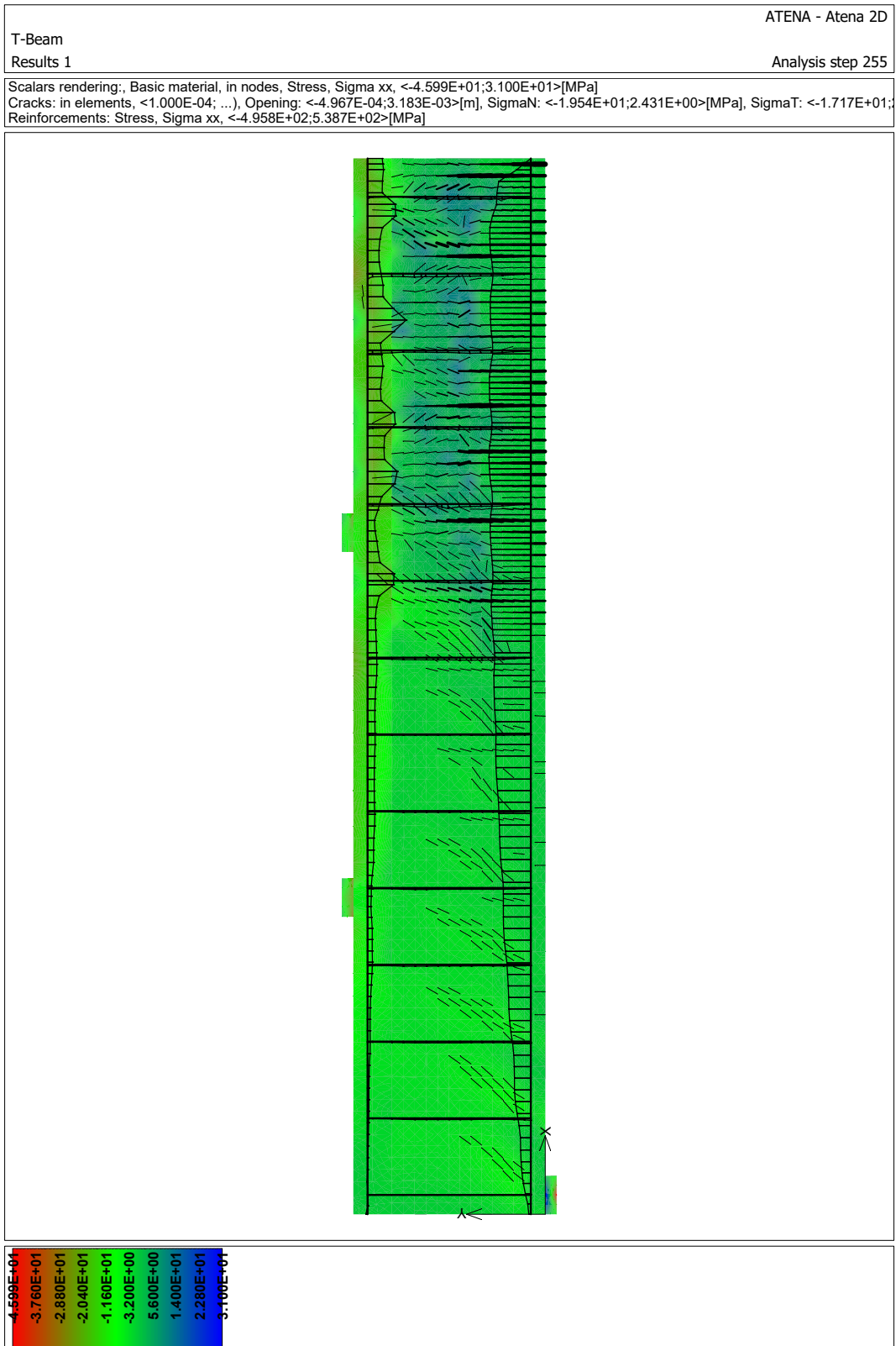


Figure B.055: T-beam Sample no. 25.

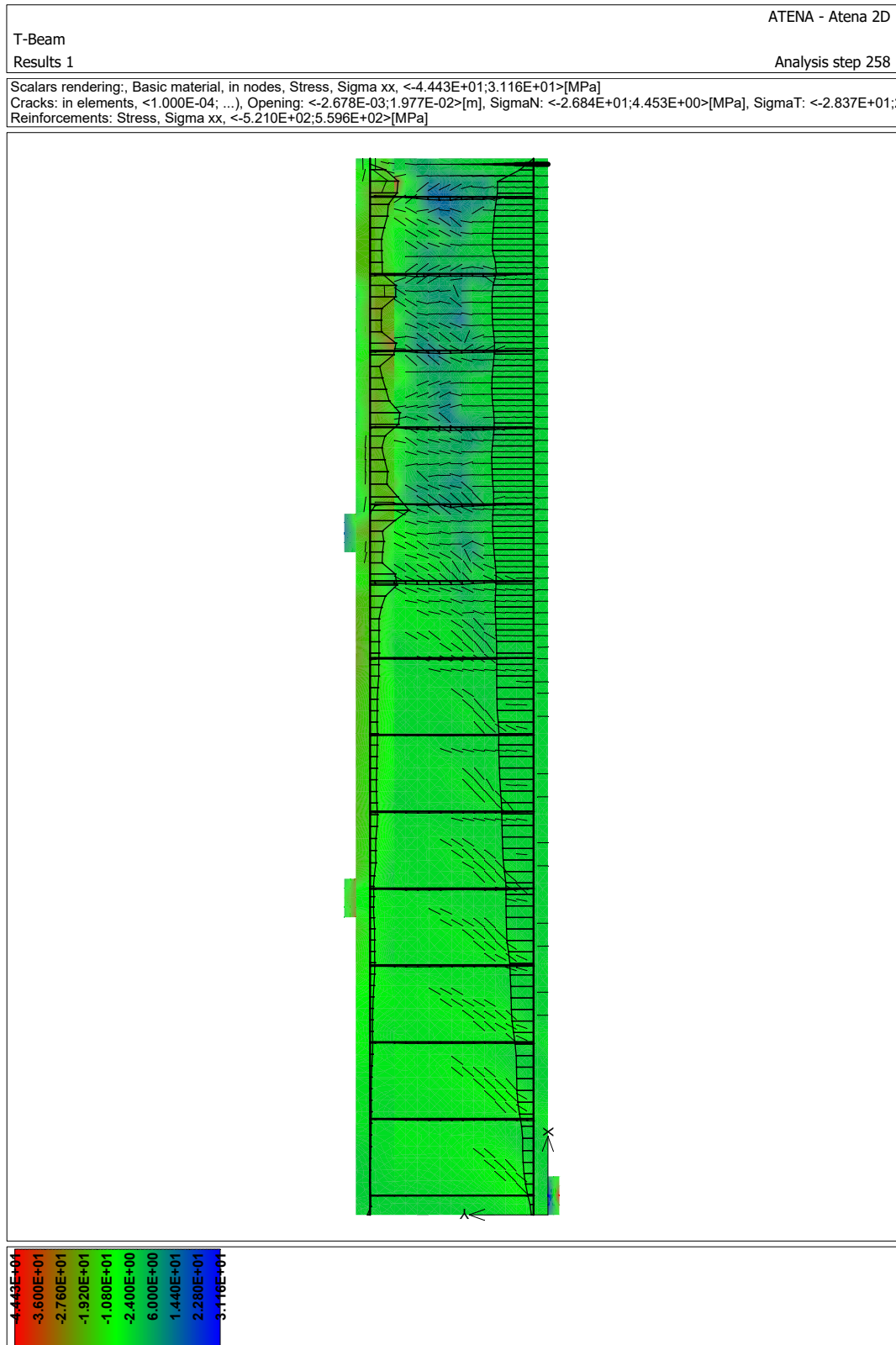


Figure B.0.56: T-beam Sample no. 26.

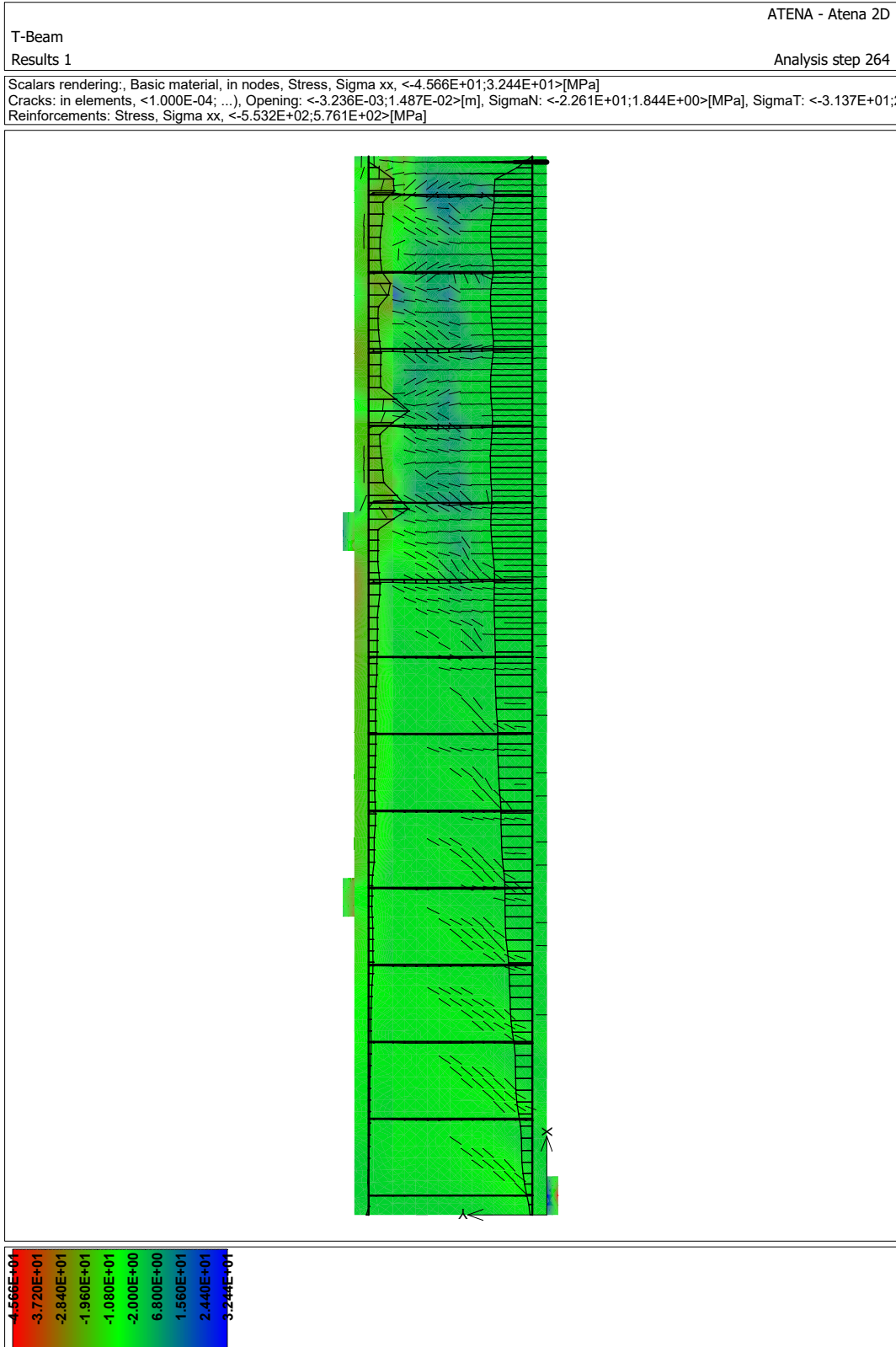


Figure B.0.57: T-beam Sample no. 27.

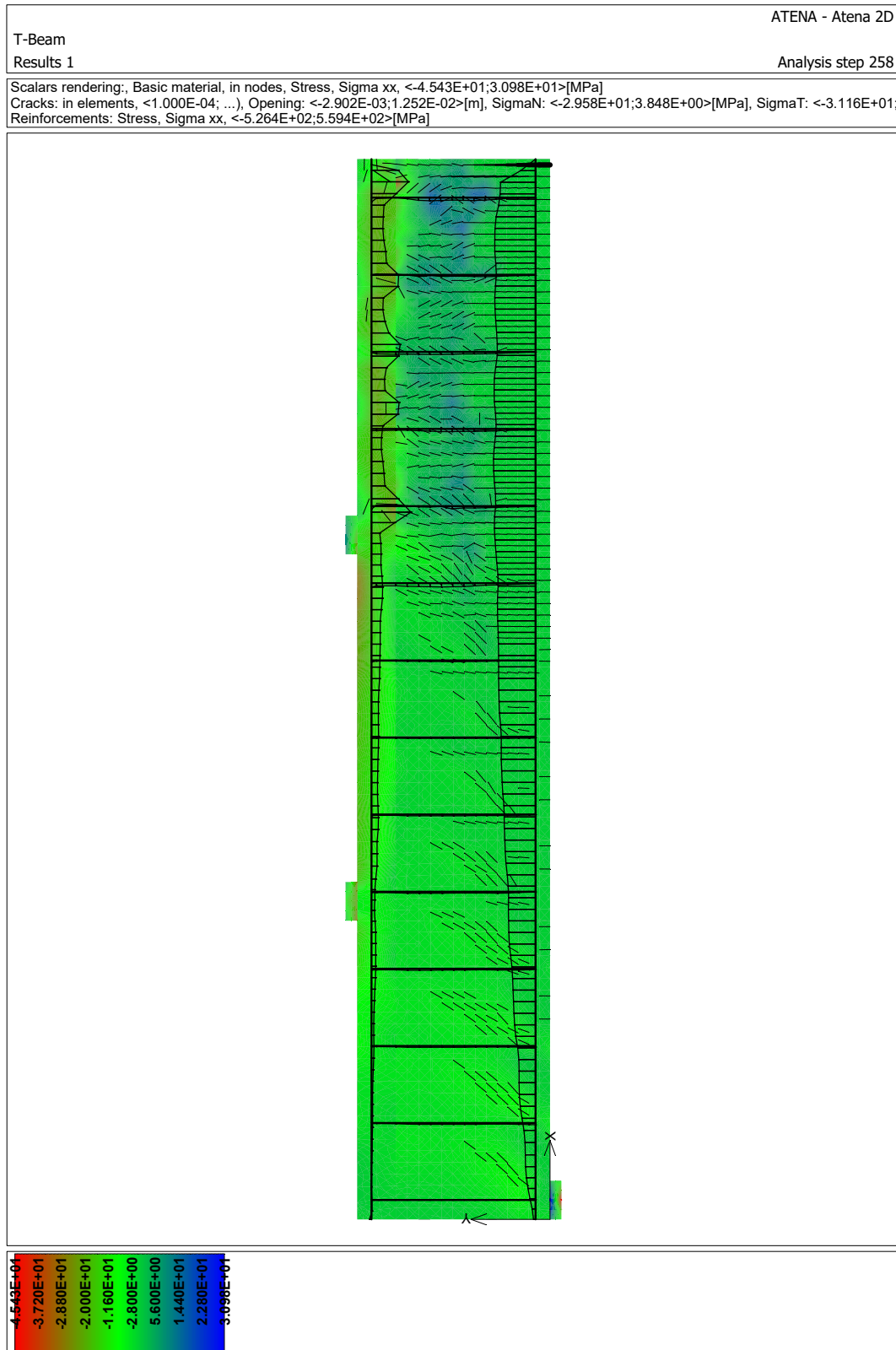


Figure B.0.58: T-beam Sample no. 28.

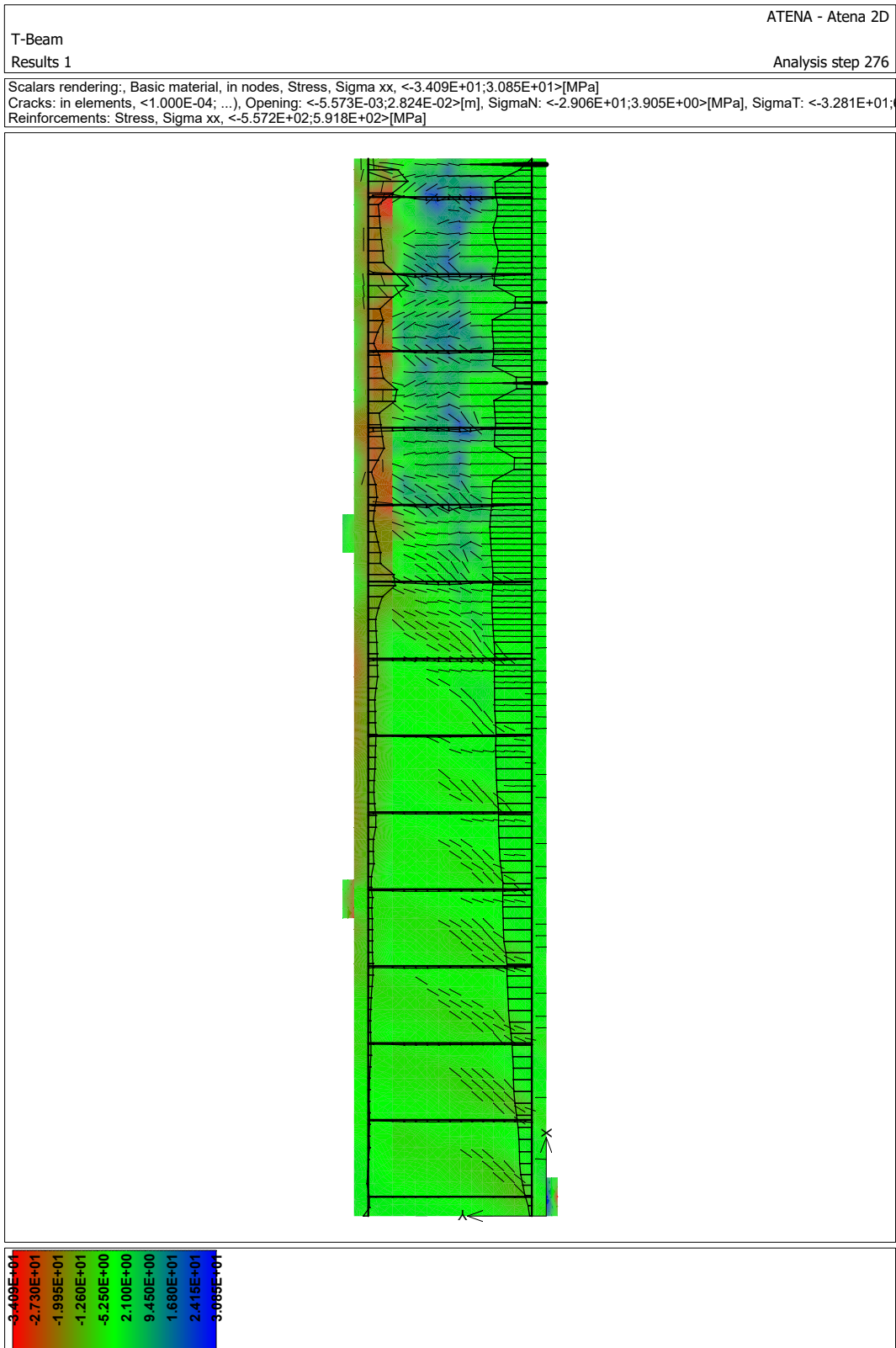


Figure B.0.59: T-beam Sample no. 29.

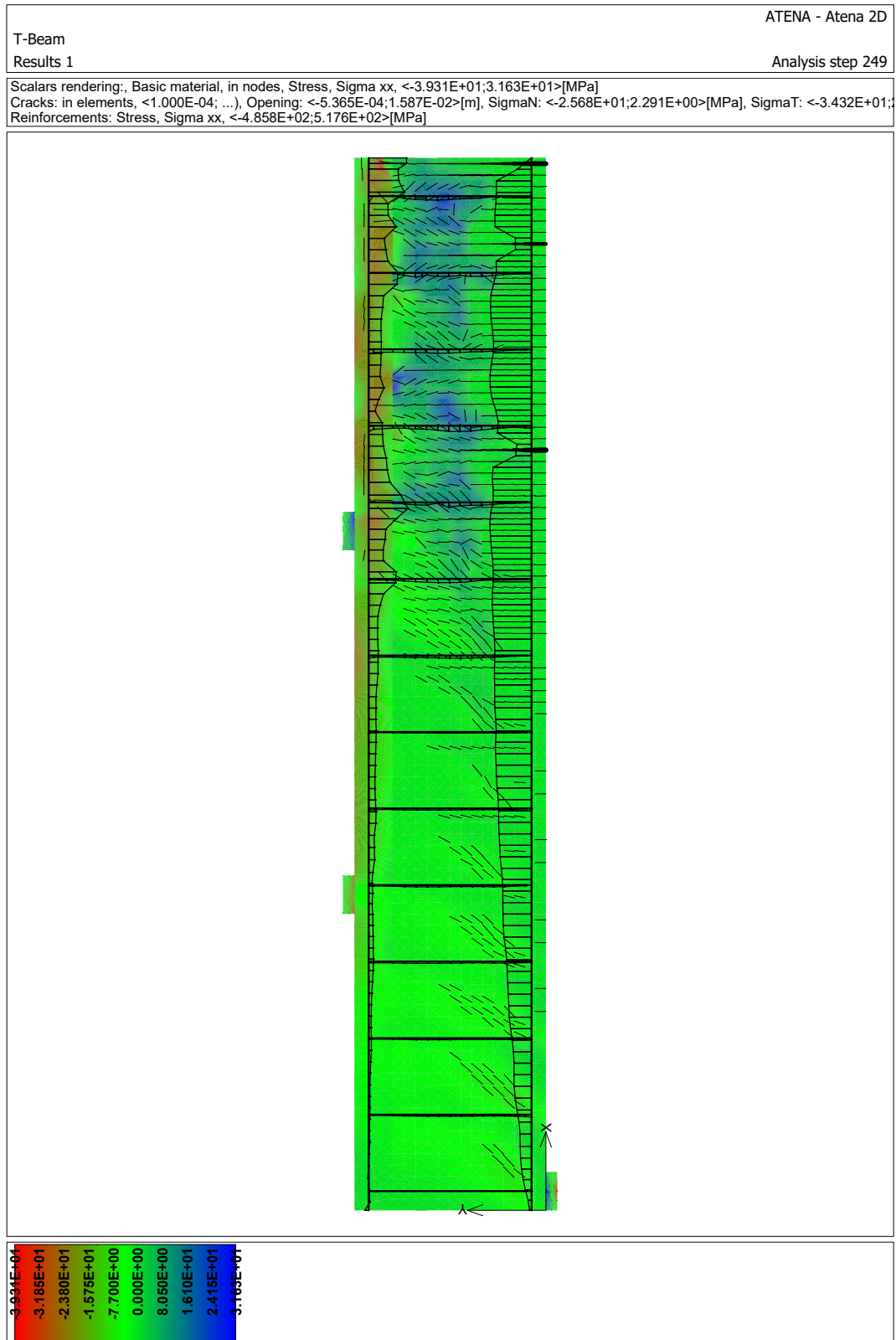


Figure B.0.60: T-beam Sample no. 30.